MIGUEL ANGEL GRIMALDO LOPEZ

MECHANISMS OF SPORICIDAL ACTIVITY INDUCED BY IONIZED HYDROGEN PEROXIDE IN THE INACTIVATION OF SPORES OF *Bacillus atrophaeus* AND *Geobacillus stearothermophilus*

Tese apresentada à Universidade Federal de Viçosa, como parte das exigências do Programa de Pós-Graduação em Bioquímica Aplicada, para obtenção do título de *Doctor Scientiae.*

Orientador: Cláudio Lisias Mafra de Siqueira

VIÇOSA - MINAS GERAIS

2020

Ficha catalográfica preparada pela Biblioteca Central da Universidade Federal de Viçosa – Campus Viçosa

T
G861m
2020

Grimaldo López, Miguel Angel, 1961-
Mechanisms of sporicidal activity induced by ionized hydrogen peroxide in the inactivation of spores of *Bacillus atrophaeus* and *Geobacillus stearothermophilus* / Miguel Angel Grimaldo López. – Viçosa, MG, 2020.
105 f. : il. (algumas color.) ; 29cm.

Orientador: Cláudio Lísias Mafra de Siqueira.
Tese (doutorado) – Universidade Federal de Viçosa.
Inclui bibliografia.

1. Peróxido de hidrogênio. 2. DNA. 3. Dano. 4. Esporos de bactérias. 5. Inativação. 6. *Bacillus atrophaeus*. 7. *Geobacillus stearothermophilus*. I. Universidade Federal de Viçosa. Departamento de Bioquímica e Biologia Molecular. Programa de Pós-Graduação em Bioquímica Aplicada. II. Título.

CDD 22. Ed. 572.86

MIGUEL ANGEL GRIMALDO LOPEZ

MECHANISMS OF SPORICIDAL ACTIVITY INDUCED BY IONIZED HYDROGEN PEROXIDE IN THE INACTIVATION OF SPORES OF *Bacillus atrophaeus* AND *Geobacillus stearothermophilus*

Tese apresentada à Universidade Federal de Viçosa, como parte das exigências do Programa de Pós-Graduação em Bioquímica Aplicada, para obtenção do título de *Doctor Scientiae*.

APROVADA: 26 de junho de 2020.

Assentimento:

Miguel Angel Grimaldo López
Autor

Cláudio Lisias Mafra de Siqueira
Orientador

AGRADECIMIENTOS

A Dios por guiarme diariamente en el camino de la búsqueda hacia la excelencia.

A mi esposa Melissa y a mis hijos Miguel Angel y Maria Teresa, por el amor que me brindan y el apoyo incondicional de siempre.

A mis padres Michelin y Coqui, por haberme dado la vida y por su apoyo en mi formación académica inicial y a mi tío, Padre Fernando Guardia, S.J., por haberme introducido al camino de la búsqueda de la sabiduría.

To Dr. Michael Laposata, Chair of the Department of Pathology at UTMB, for the encouragement given to me five years ago to begin pursuing my Doctoral Degree.

To my advisors Prof. Dr. Claudio Mafra & Prof. Dr. Donald Bouyer, for trusting me and allowing me to reach a goal that I had pending in my professional career.

To my "pro-tempore" advisors at UTMB, Nathen, and Nicole, for their valuable input during the development of the research project.

To John, Chris, and Mark at UTMB for their unconditional support on my day to day activities while away in class or doing research and to Edu, Marcos, Elisa, and Humberto for their academic and administrative support in UFV.

To my Brazilian friends Claudio & Simone, Ricardo & Luciana, Otto, Marcos y Andre, thanks for offering to me and Melissa your friendship and for sharing with us your beautiful country.

To the Universidade Federal de Viçosa and the Department of Biochemistry and Molecular Biology for the opportunity to achieve my Doctoral Degree.

O presente trabalho foi realizado com apoio da Coordenação de Aperfeiçoamento de Pessoal de Nível Superior – Brasil (CAPES) – Código de Financiamento 001.

“Alcance a excelência e compartilhe-a”.

(San Ignacio de Loyola)

RESUMO

GRIMALDO, Miguel Angel, D.Sc., Universidade Federal de Viçosa, junho de 2020. **Mecanismos de atividade esporicida induzida por peróxido de hidrogênio ionizado na inativação de esporos de *Bacillus atropheaus* e *Geobacillus sterothermophilus*.** Orientador: Cláudio Lísias Mafra de Siqueira.

O peróxido de hidrogênio ionizado (iHP) é uma nova tecnologia usada para a descontaminação de superfícies ou áreas de laboratório. Trata-se de uma baixa concentração de peróxido de hidrogênio (H_2O_2) misturada com o ar e ionizada através de um arco de plasma frio. Essa tecnologia gera espécies reativas de oxigênio (ERO) que atuarão em processos de descontaminação. Embora a tecnologia tenha demonstrado eficácia na inativação de esporos de indicadores biológicos como *Bacillus atrophaeus* e *Geobacillus stearothermophilus*, seu mecanismo exato permanece desconhecido. Portanto, o objetivo deste estudo foi determinar o mecanismo de inativação utilizado por iHP. A hipótese desse trabalho é que o mecanismo da atividade esporicida induzida por peróxido de hidrogênio ionizado em esporos de *B. atrophaeus* e *G. stearothermophilus* era induzido por lesões no DNA genômico ou em fatores germinativos essenciais na ativação da cascata de germinação de esporos e estes afetariam o processo de crescimento vegetativo. Para determinar o mecanismo exato, investigamos duas vias de inativação. Para responder a estes questionamentos, primeiro a verificação visual foi realizada com o uso de um microscópio eletrônico de transmissão para identificação os efeitos do iHP na estrutura dos esporos, e a segunda forma foi a verificação do impacto através da análise dos danos ao DNA dos esporos pelo uso de uma reação em cadeia da polimerase quantitativa (qPCR) baseada em fluorescência verde SYBR. A inativação uniforme de *B. atrophaeus* e *G. stearothermophilus* e a redução da atividade residual da adenilato quinase termoestável (tAK) dos indicadores de enzimas mostram que o iHP tem um efeito de difusão semelhante a gás. Também observamos danos bioquímicos diretos no DNA genômico pelos resultados da análise visual e quantitativa.

Em conclusão, o iHP inativa os esporos tanto pelos danos físicos da estrutura dos esporos quanto pelos danos subsequentes ao DNA.

Palavras-chave: Peróxido de hidrogênio ionizado. Dano ao ADN. Inativação de esporos. *Bacillus atrophaeus. Geobacillus stearothermophilus.*

ABSTRACT

GRIMALDO, Miguel Angel, D.Sc., Universidade Federal de Viçosa, June 2020. **Mechanisms of Sporicidal Activity induced by Ionized Hydrogen Peroxide in the Inactivation of Spores of *Bacillus atrophaeus* and *Geobacillus stearothermophilus*.** Adviser: Cláudio Lísias Mafra de Siqueira.

Ionized Hydrogen Peroxide (iHP) is a new technology used for the decontamination of surfaces or laboratory areas. It utilizes a low concentration of hydrogen peroxide (H_2O_2) mixed with air and ionized through a cold plasma arc. This technology generates reactive oxygen species (ROS) as a means of decontamination. Although the technology has shown effectiveness in the inactivation of spores of biological indicators of *Bacillus atrophaeus* and *Geobacillus stearothermophilus,* its exact mechanism remains unknown. Therefore the purpose of this study was to determine the mechanism of inactivation utilized by iHP. The hypothesis of this research project was that the mechanism of sporicidal activity induced by ionized hydrogen peroxide was that it inactivates spores of *B. atrophaeus* and *G. stearothermophilus* by direct biochemical damage to the genomic DNA or by damage to essential germination factors that trigger the initiation of the spore germination and outgrowth process. To determine the exact mechanism, two pathways of inactivation were investigated. First, it was the visual verification with the use of a transmission electron microscope of the effects to the structure of the spores, and the second pathway was the verification of the impact by analyzing damages to the DNA of the spores by use of a SYBR green fluorescence-based quantitative polymerase chain reaction (qPCR). The uniform inactivation of *B. atrophaeus* and *G. stearothermophilus* and the reduction of the residual thermostable adenylate kinase (tAK) activity of enzyme indicators shows that iHP has a gas-like diffusion effect. Also direct biochemical damage to the genomic DNA was observed by the results of the visual and quantitative analysis. In conclusion, iHP inactivates spores by both physical damages of the spore structure and subsequent damage to the DNA.

Keywords: Ionized Hydrogen Peroxide. DNA Damage. Inactivation of Spores. *Bacillus atrophaeus*. *Geobacillus stearothermophilus*.

LISTA DE ILUSTRAÇÕES

REVISÃO BIBLIOGRÁFICA

CAPÍTULO 1

CAPÍTULO 2

LISTA DE TABELAS

CAPÍTULO 1

CAPÍTULO 2

LISTA DE ABREVIATURAS E SIGLAS

BLASTn	Nucleotide Basic Local Alignment Search Tool
BLASTx	Basic Local Alignment Search Tool for translated nucleotide query
bp	Bases pair
CNPq	Conselho Nacional de Desenvolvimento Científico e Tecnológico
CAPES	Coordenação de Aperfeiçoamento de Pessoal de Nível Superior
DBB/UFV	Departamento de Bioquímica e Biologia Molecular – UFV
DNA	Ácido desoxirribonucleico
iHP	Peroxido de Hidrogeno Ionizado
NIH	National Institute Health
PCR	Polymerase Chain Reaction
pH	Potential of Hydrogen
qPCR	Real Time Polymerase Chain Rreaction Quantitative
rcf	Relative Centrifugal Force
ROS	Reactive Oxygen Species
SeqID	Idential residues alignment sequence
UFV	Universidade Federal de Viçosa
UniProt	Resource Protein Universal
UTMB	University of Texas Medical Branch

LISTA DE SÍMBOLOS

α	Alfa
ß	Beta
°C	Graus Celsius
Ft	Pés
M	Molar
mL	Mililitro
µg	micrograma
µL	microlitro
µM	micromolar
µg/mL	micrograma por mililitro

SUMARIO

MECANISMOS DE ATIVIDADE ESPORICIDA INDUZIDA POR PERÓXIDO DE HIDROGÊNIO IONIZADO NA INATIVAÇÃO DE ESPOROS DE *Bacillus atropheaus* E *Geobacillus stearothermophilus*.

1. Introdução

As instalações de saúde, os laboratórios de diagnóstico e pesquisa e as instalações de produção de vacinas geralmente encontram problemas com a contaminação da superfície ou do espaço (ambiental) por patógenos fúngicos, bacterianos ou virais. Dependendo do grau ou tipo de contaminação, a desinfecção tópica com desinfetantes é adequada. No entanto, se a contaminação for muito forte ou dependendo do patógeno, poderá ser necessária descontaminação daquele ambiente. Desde o final da década de 1880, o formaldeído tem sido usado como desinfetante (LACH, 1990), sendo há muito tempo considerado como padrão ouro para a descontaminação (ALBINA *et al.*, 2011). No entanto, desde 1983, o formaldeído é conhecido por causar câncer em camundongos e ratos por exposição prolongada à inalação (KERNS *et al.*, 1983). Em junho de 2004, um grupo de trabalho interdisciplinar de cientistas especialistas se reuniu na Agência Internacional de Pesquisa em Câncer (IARC) para desenvolver as Monografias da IARC sobre a Avaliação do Risco Carcinogênico de Produtos Químicos para Humanos. Estes autores concluíram que o formaldeído é cancerígeno para os seres humanos, com base em evidências suficientes em seres humanos e em animais experimentais (COGLIANO *et al.*, 2005). Desde esta declaração, vários países, incluindo a União Europeia, estabeleceram regulamentos para o controle e, ou, proibição do uso deste produto, como a regra recentemente publicada pela Agência de Proteção Ambiental para a regulamentação do formaldeído em produtos de madeira (Padrões de emissão de formaldeído para compostos) Produtos de madeira (RIN 2070-AJ44, 2016). Assim, novas tecnologias de desinfecção, como vapor de peróxido de hidrogênio (HPV), gás dióxido de cloro (ClO_2) e peróxido de hidrogênio ionizado (iHP) surgiram como possíveis opções para substituição ao uso de gás formaldeído no ambiente de laboratório. No entanto, sua ação completa de inativação de esporos usados como indicadores biológicos nas provas de validação destes agentes não é totalmente compreendida. Neste sentido, compreender como agentes e tecnologias de descontaminação induzem a inativação de esporos permitirá a seleção de uma tecnologia de descontaminação de substituição para o gás formaldeído, com essas informações podendo fornecer mais dados quanto a eficácia de tecnologia com o menor efeito

negativo em superfícies ou dificuldades em sua aplicação. Dentre estas tecnologias de descontaminação, a mais nova é o peróxido de hidrogênio ionizado (iHP), até o momento sem documentação quanto aos seus problemas de eficácia, aplicação e incompatibilidade. Em estudos anteriores (Comunicação pessoal), o sistema de peróxido de hidrogênio ionizado apresentou padrões de difusão como um sistema gasoso, não apresentando danos a componentes eletrônicos.

2. Hipótese

O peróxido de hidrogênio ionizado inativa os esporos de *Bacillus atrophaeus* e *Geobacillus stearothermophilus* por lesões diretas no DNA genômico ou por inativação de fatores germinativos essenciais que desencadeiam o início do processo de germinação e crescimento vegetativo da bactéria.

3. Revisão Bibliográfica

3.1. Indicadores biológicos e esporos de referência

Os esporos de *Bacillus atrophaeus* anteriormente conhecido como *Bacillus subtilis* var. niger e *Geobacillus stearothermophilus* são os indicadores biológicos mais comumente utilizados para validar os processos de descontaminação/ esterilização. Para avaliar sua eficácia, faz-se essencial entender como a tecnologia de descontaminação afeta a estrutura dos esporos.

As células vegetativas de Bacillus atrophaeus são em forma de bastonete, com 0,5 a 1,0 μm de largura por 2,0 a 4,0 μm de comprimento (conforme determinado por microscopia de fase) e ocorrem isoladamente e em cadeias curtas. Motile. Gram-positivo com temperatura de crescimento ideal varia de 28 a 30 ° C, a temperatura máxima de crescimento varia de 50 a 55 ° C e a temperatura mínima de crescimento varia de 5 a 10 ° C. Bacillus atrophaeus cresce a pH 5,6 ou 5,7 e na presença de 7% de NaC1, e seu crescimento é inibido por 0,001% de lisozima. (NAKAMURA, 1989)

As células vegetativas de *G. stearothermophilus* apresentam-se na forma de bastonete, ocorrendo isoladamente ou em cadeias curtas. Móveis, utilizando flagelos peritríqueo ou sem motilidade, são Gram-positivos com a reação à coloração de Gram podendo variar entre positivo e negativo. Sua estrutura de parede celular é elipsóide ou cilíndrica, estando os endosporos localizados terminal ou sub-terminalmente em esporângios levemente

inchados ou não inchados. Aeróbios ou anaeróbios facultativos, são obrigatoriamente termofílicos, apresentando faixa de temperatura para crescimento entre 37°C a 75°C, com uma temperatura ideal entre 55°C a 65°C. Neutrofílico, apresenta crescimento em uma faixa de pH de 6,0 a 8,5, sendo ideal em pH 6,2 a 7,5 (NAZINA *et al.*, 2001).

3.2. Morfologia do esporo

3.2.1. Formação

Múltiplos sinais ambientais podem desencadear a diferenciação de células vegetativas em esporos, dentre os quais, privação de nutrientes, alta composição mineral, pH neutro, temperatura e alta densidade celular (SELLA *et al.*, 2014), com estes podendo sobreviver neste estado inativo por muitos anos ou até persistir por milhões de anos (LEGGETT *et al.*, 2012). Com a melhor compreensão quanto os fatores de estrutura e resistência em várias bactérias formadoras de esporos, temos elevado potencial de desenvolvimento de métodos químicos e físicos otimizados de inativação dessas estruturas únicas (LEGGETT *et al.*, 2012).

Conforme detalhado por Legget *et al.* (2012), Sella *et al.* (2014) e Wang & Levin (2009), a formação de esporos é dividida em sete estágios, sendo esse processo é tipicamente idêntico para todas as bactérias formadoras de esporos. O Estágio 0 no ciclo de formação de esporos, com o crescimento celular normal da célula, caracterizando-se pelo início da divisão celular, replicação cromossômica e conclusão da divisão celular. Nos Estágios I e II, a célula vegetativa sofre divisão celular assimétrica originando dois compartimentos com completa segregação do DNA, os quais, com posterior invaginação da membrana plasmática, criam um pre-esporo, separado por um septo. Durante o Estágio III, a célula mãe envolve o pré-esporo formando uma célula distinta denominada exósporo, com as membranas internas e externas cercando novo indivíduo. No Estágio IV, observa-se a síntese do córtex de esporos, composto de peptidoglicano, entre a membrana anterior e interna. A formação do revestimento de esporos se dá no Estágio V. Durante os estágios IV e V, a célula mãe sintetiza uma molécula específica, muito abundante, o ácido piridina-2,6-dicarboxílico [ácido dipicolínico (DPA)]. Essa molécula se acumula no exósporo, concomitante a uma redução no teor de água. A maturação dos esporos ocorre durante o Estágio VI, onde o material do revestimento se torna mais denso na aparência. No

Estágio VII (estágio final), vê a lise da célula mãe por ruptura com enzimas líticas e liberação da estrutura de esporos maduros (Figura 0-1). De acordo com LEGGETT *et al.* (2012), a estrutura de esporos maduros protegeria o microrganismo adormecido de influências externas até que as condições se tornem novamente favoráveis ao crescimento celular vegetativo.

Figura 0-1: Morphological changes during sporulation (Daniellemaclean144 [CC BY-SA (https://creativecommons.org/licenses/by-sa/4.0)]).

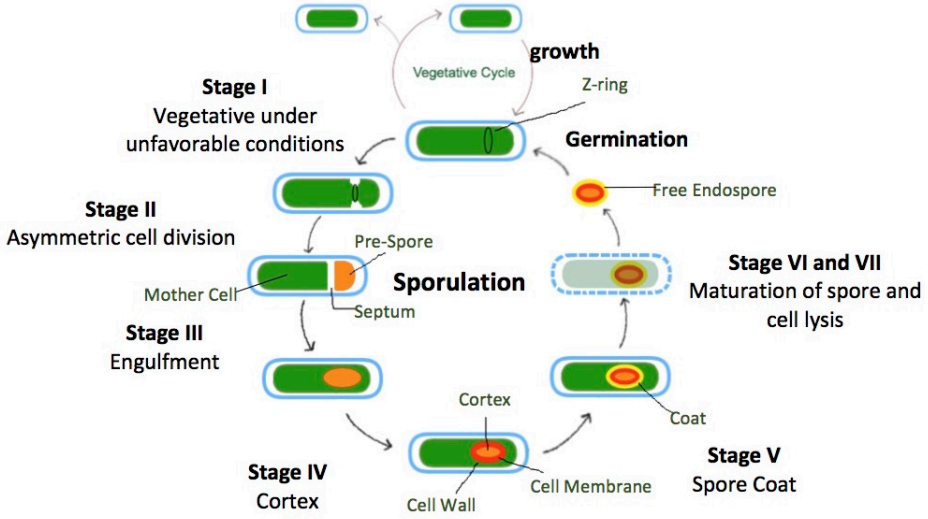

3.3. Estrutura

A estrutura do esporo bacteriano, sob muitos aspectos, é diferente da estrutura da célula vegetativa mãe. O esporo bacteriano é composto por diferentes camadas ou membranas que desempenham um papel essencial na sobrevivência do esporo. São compostos de camadas como exosporium, casacos (revestimento externo e revestimento interno), membrana externa, córtex, parede celular germinativa e membrana interna e o núcleo central (SETLOW, 2006), onde residem o material cromossômico do DNA, os ribossomos e a maioria de suas enzimas (SETLOW, 2014) (Figura 0-2).

Figura 0-2: Spore cellular structure. (Applied and Environmental Microbiology Dec 1969)

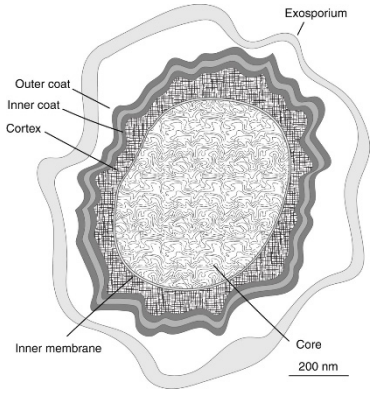

3.3.1. Exosporia

O exosporia é a estrutura mais externa da camada em muitos esporos bacterianos, podendo estar ausente em outros. Quando presente, o exoesporo é uma concha multicamada que envolve todo o esporo fora da pelagem, entretanto não conectada ao esporo ou à pelagem (DRIKS, 1999). É composto principalmente de proteínas, lipídios e carboidratos, não demonstrou fornecer ao esporo nenhuma proteção significativa contra ataque de biocidas (LEGGETT *et al.*, 2012).

3.3.2. Cobertura do esporo (Camadas interna e externa)

A camada de esporos é uma estrutura de várias camadas e, como a camada interna corando mais levemente que a camada externa, essas camadas são chamadas de camada interna e externa. Algumas espécies têm diferentes arranjos de cobertura, com uma a três camadas distintas, mas todas em contato fechado em um dado esporo, sugerindo que ligações químicas as conectam (DRIKS & EICHENBERGER, 2016). A cobertura é composta predominantemente por proteínas, mas também conténdo também componentes menores de carboidratos (LEGGETT *et al.*, 2012). Nos esporos de *B. subtilis*, a camada é composta por pelo menos 80 proteínas diferentes (DRIKS & EICHENBERGER, 2016). O revestimento de esporos desempenha algum papel na resistência dos esporos, especialmente na prevenção do acesso de enzimas peptidoglicanas ao córtex de esporos, provavelmente também desempenhando um papel na resistência dos esporos a alguns produtos químicos, como peróxido de hidrogênio (NICHOLSON *et al.*, 2000). A principal função conhecida do revestimento é proteger o esporo, com as duas camadas, o revestimento interno e externo, desempenhando um papel crítico nessa proteção. As camadas de esporos agem como uma peneira molecular, excluindo enzimas, entratanto permitindo a passagem de

moléculas pequenas, como germinantes. Driks (1999) estudou a capacidade desta camada atuar como uma barreira que mede a capacidade de proteger o córtex dos danos da lisozima.

3.3.3. Membrana externa

A membrana externa é encontrada sob o revestimento interno dos esporos. Conforme descrito por SETLOW (2006), sua função precisa não é clara, embora seja uma estrutura essencial na formação de esporos, não sendo, no entanto, uma barreira significativa à permeabilidade. Sua presença é, às vezes, questionada devido à falta de evidências morfológicas, apesar de existirem evidências funcionais e bioquímicas para apoiá-la (LEGGETT *et al.*, 2012).

3.3.4. Cortex

O córtex do esporo é composto por peptidoglicanos (LEGGETT *et al.*, 2012), participando da manutenção de seu estado desidratado. Sua propriedade de resistência ao calor depende do estado desidratado do núcleo do esporo, o qual, por sua vez, depende da manutenção da desidratação do córtex (DRIKS, 1999).

3.3.5. Parede da célula germinativa

A parede das células germinativas está localizada sob o córtex, sendo também composta por peptidoglicano. Sua estrutura provavelmente é idêntica à camada peptidoglicana de uma célula vegetativa. A parede das células germinativas provavelmente não desempenha nenhum papel na resistência dos esporos, mas se torna a parede celular do esporo que cresce em excess (SETLOW, 2006).

3.3.6. Membrana interna

Localizado sob a parede celular germinativa, é onde residem os Receptores Germinantes (RG) e onde a maioria das principais proteínas envolvidas na germinação de esporos está presente ou adjacente a ela (SETLOW, 2014).

3.3.7. Núcleo

O núcleo central é onde reside o material cromossômico do DNA, os ribossomos e a maioria das enzimas dos esporos. O baixo teor de água deste ambiente impede a mobilidade das proteínas nos esporos adormecidos e germinados no Estágio I, podendo também impedir a ação enzimática por não fornecer água suficiente para a função enzimática (COWAN *et al.*, 2003). O núcleo apresenta um baixo teor de água de peso úmido (entre 25% a 50%) e uma quantidade considerável de ácido piridina-

2,6-dicarboxílico da molécula específica de esporos (ácido dipicolínico [DPA] em um quelato 1:1 com cátions divalentes, predominantemente Ca2+(CaDPA), contando com cerca de 10% do peso seco total dos esporos (SETLOW, 2014).

3.4. Germination

Uma vez que uma bactéria vegetativa se torna um esporo, ela pode sobreviver por anos em seu estado adormecido, mesmo por 25 a 40 milhões de anos (CANO & BORUCKI, 1995). No entanto, se dadas as condições ambientais adequadas, como nutrientes, pH, temperatura e umidade, os esporos podem perder rapidamente sua dormência, incluindo suas propriedades de resistência, as quais podem ser afetadas durante a germinação. No entanto, esse compromisso de germinação também pode ser revertido se as condições não forem adequadas. Uma vez iniciado o processo de germinação, segue-se o crescimento que converte o esporo germinado em uma célula viável (SETLOW, 2014). Moléculas germinantes de nutrientes incluem aminoácidos, açúcares, nucleosídeos de purina, sais inorgânicos ou combinações deles. Esses nutrientes não precisam ser metabolizados ou entrar no núcleo dos esporos; outras moléculas como o ácido Ca2+-dipicolínico (CaDPA) ou dodecilamina são denominadas germinantes não nutricionais. Além disso, o aminoácido L-alanina e seus análogos são freqüentemente eficazes como germinantes únicos ou em combinação com outros (MOIR & COOPER, 2015; KOCHAN *et al.*, 2018). A estrutura especializada do esporo que os ajuda a manter suas propriedades de dormência e resistência oferece uma oportunidade para ampla dispersão de esporos no ambiente e para sua sobrevivência em condições desfavoráveis ao crescimento. Embora os esporos estejam inativos e desafiando condições ambientais adversas, o esporo permanece sensível a indicações de que as condições são favoráveis ao crescimento vegetativo. (MOIR & COOPER, 2015; KOCHAN *et al.*, 2018). O processo de germinação tem vários estágios. Para iniciar o processo de germinação, as primeiras moléculas de nutrientes ou não nutrientes devem atravessar as camadas externas do esporo para acessar os receptores de nutrientes localizados na membrana ou adjacentes à membrana interna (*Figura 0-3*).

Figura 0-3: Schematic outline of nutrient germination of spores of Bacillus species (SETLOW, 2014).

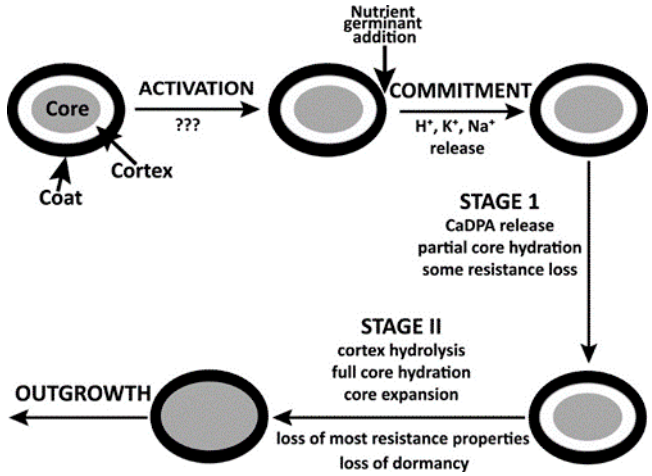

3.4.1. Estágio I da Germinação

Uma vez que o esporo se compromete a germinar, os receptores na membrana interna do esporo detectam as moléculas germinantes específicas. Este sinal é transduzido, resultando na ativação de proteínas que permitem o movimento de pequenas moléculas através da membrana e desconstroem as camadas protetoras, restaurando a hidratação normal e o metabolismo ativo (MOIR & COOPER, 2015).

3.4.2. Estágio II da Germinação

No estágio II da germinação, as enzimas líticas do córtex são ativadas pela liberação de CaDPA do núcleo, clivando o peptidoglicano contendo δ-lactama murâmico, deixando intacta a parede celular (MOIR & COOPER, 2015; KOCHAN *et al.*, 2018). O gene *yaaH* (SleL) codifica a proteína YaaH (SleL), uma N-acetilglucosaminidase, como uma enzima do córtex lítico para apoiar a hidrólise do córtex.

3.4.3. Degradação do Revestimento de Esporos

A degradação do revestimento de esporos começa quase ao mesmo tempo a hidrólise do córtex, iniciada pelo sinal de germinação e transduzida para ativar a quebra parcial do revestimento de esporos. Alguma camada de esporos permanece mesmo após a germinação (MOIR & COOPER, 2015; SANTO &DOI, 1974) (Figura *0-4*).

3.4.4. Crescimento

O esporo germinado retoma o metabolismo e o crescimento em uma célula vegetativa (MOIR & COOPER, 2015), atuando na estrutura morfológica do esporo,

levando a mudanças progressivas na estrutura do córtex, revestimento externo do esporo e revestimento interno do esporo durante o processo de germinação (SANTO & DOI, 1974) (Figura *0-4*).

Figura 0-4: Micrografias eletrônicas de seções delgadas de esporos adormecidos, em germinação e crescentes. a) Esporos dormentes; (b) 10 min; (c) 20 min, setas indicam cortes; (d) 30 min, as setas indicam cortes; (e) 40 min; (f) 50 min; (g) 60 min; (h) 90 min. As barras representam 0,1 µm nas figuras a a g. Na figura h, representa 1,0 µm. CX, córtex; OSC, revestimento externo de esporos; ISC, revestimento interno de esporos; M, mesossomo (SANTO & DOI, 1974)

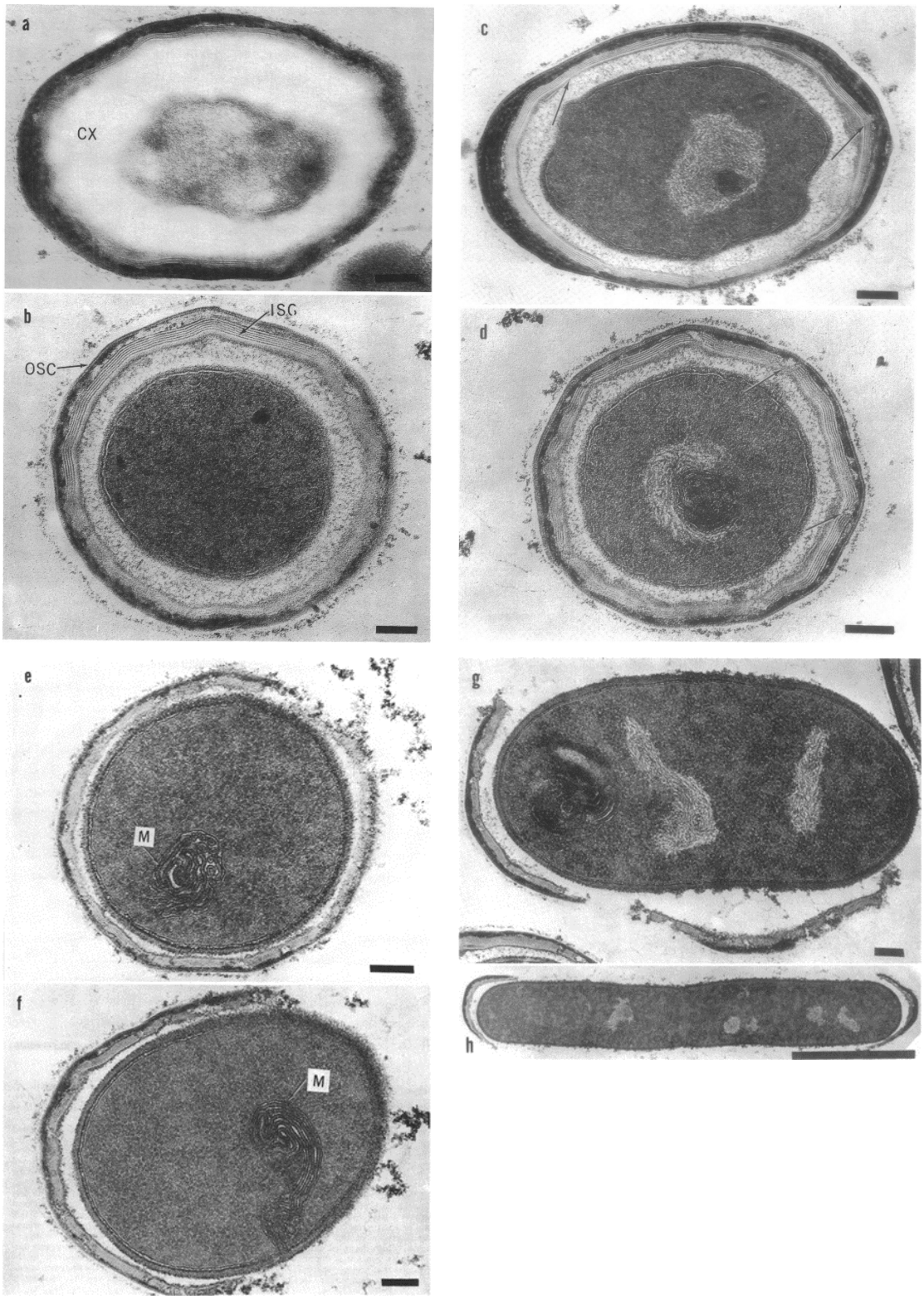

O modelo de indução da germinação por L-alanina, Figura 0-5 para *B. anthracis* (KOCHAN *et al.*, 2018), este modelo pode ser representativo do processo semelhante a outras bactérias do gênero.

Figura 0-5: Modelo de germinação de L-alanina de Bacillus anthracis. Os nutrientes entram no esporo através do complexo GerPABCDEF (A), que facilita o movimento da L-alanina através do revestimento esporático e da membrana externa para a membrana interna do esporo, onde se liga aos receptores de germinação GerK e / ou GerL (B). Essas interações receptor-germinante levam a uma leve reidratação do núcleo (C) e à liberação de Ca-DPA do núcleo do esporo (D). O Ca-DPA viaja através do córtex (ou pode ser adicionado exogenamente) e liga-se a CwlJ (E). Essa ligação ativa a CwlJ, iniciando a hidrólise do peptidoglicano do córtex (F). Isso leva à reidratação total do núcleo e ao crescimento de esporos. (KOCHAN et al., 2018).

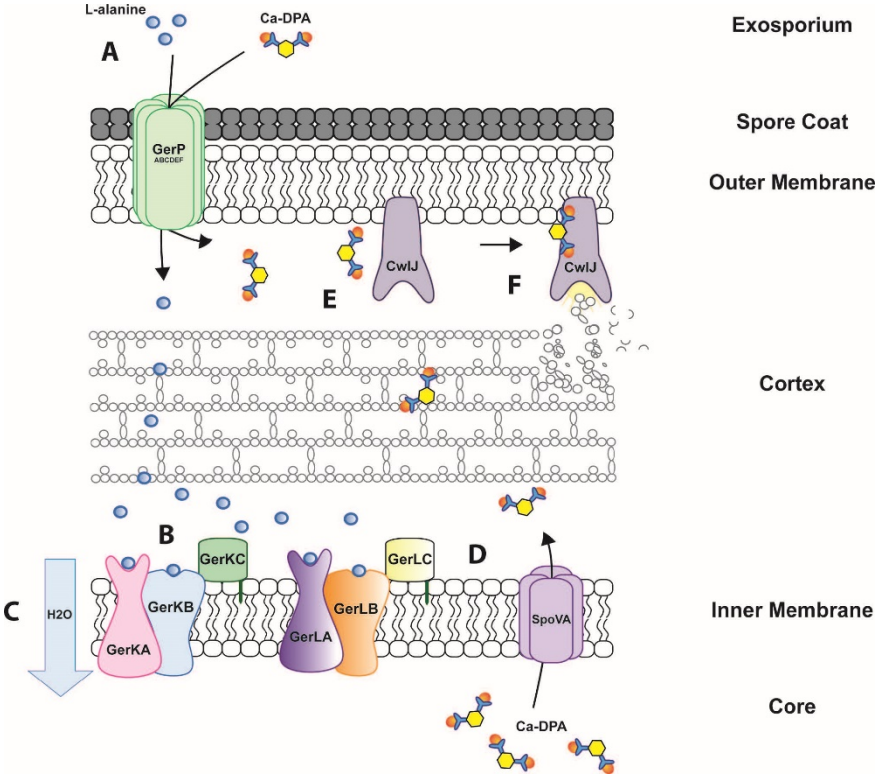

3.5. O gene *yaaH* (*sleL*) em *Bacillus atrophaeus* e *Geobacillus stearothermophilus*

O gene *yaaH* (sleL) em *B. atrophaeus* e *G. stearothermophilus* codifica a proteína de germinação YaaH (Uniprot ID P37531). Esta proteína YaaH (SleL), uma N-acetilglucosaminidase, é uma enzima do córtex que apoia sua hidrolisação, durante o proceso de germinação, por fendas de peptidoglicanos de esporos apenas parcialmente degradados, reconhecendo resíduos delta-lactama do ácido murâmico específicos para peptidoglicanos de esporos (DRIKS & EICHENBERGER, 2016). Sugere-se que a inativação do gene *yaaH* não prejudicaria a germinação do esporo ou sua resistência ao calor, clorofórmio ou lisozima, no entanto, afetaria a germinação induzida pela L-alanina (KODAMA *et al.*, 1999).

O genoma dos esporos de *B. atrophaeus* e *G. stearothermophilus* apresenta um tamanho de 4.152.603 pb e 2.859.252 pb, respectivamente, ambos conservando o gene *yaaH* (sleL) em seu genoma que codifica a proteína de germinação de esporos YaaH (Uniprot ID P37531). O gene *yaaH* em *B. atrophaeus* tem 1.281 pb e em *G. stearothermophilus* tem 1.287 pb. Ao comparar a sequência nucleotídica de *yaaH* em *G. stearothermophilus* versus o genoma de *yaaH* em *B. atrophaeus*, verificou-se que apresentam apresenta uma homologia de 69% (https://blast.ncbi.nlm.nih.gov/Blast.cgi) (Figura 0-6).

Figura 0-6: Comparação da sequência de nucleotídeos para o gene yaaH em G. stearothermophilus *vs.* B. atrophaeus *(https://blast.ncbi.nlm.nih.gov/Blast.cgi)*

```
Query: None Query ID: lcl|Query_13655 Length: 1287>
Sequence ID: Query_13657 Length: 1281 Range 1: 583 to 1236
Score:242 bits(267), Expect:4e-67,
Identities:456/660(69%),  Gaps:12/660(1%), Strand: Plus/Plus
Query  598   ATTGTCGCCACCGCCAGACGGTATGGCTTCCGCGACATCCATTTTGATTTTGAATATTTG  657
              ||||| || || || |||   ||||| || || || || |||||||| |||||||| ||
Sbjct  583   ATTGTTGCGACTGCTAGAAAATATGGATTTCGGGATATTCATTTTGACTTTGAATACTTA  642
Query  658   CGCCCGGAAGACCGTGAGGCGTATAATGCGTTTTTGCGCAAAGCGAAACGGCGATTTGA-  716
              || || |||||    || || ||||||  |||| ||||  |||| | |  |  |||| |
Sbjct  643   CGTCCTGAAGATAAAGAAGCCTATAATCAGTTTCTGCGTGAAGCAAGA--GATATTTTAC  700
Query  717   AC-GGGAAGGATGGATGATGTCGACCGCCCTGGCGCCAAAAACGAGCGCCACCCAGCGCG  775
              || ||||||| ||| |||| || || || || || || ||||| || || || ||    |
Sbjct  701   ACAGGGAAGGCTGGCTGATCTCTACGGCACTTGCCCCGAAAACCAGTGCAACTCAAAAAG  760
Query  776   GACGTTGGTACGAAGCCCATGACTACCGCGCCCATGGACAAATTGCCGACTTTGTCGTCA  835
              |    ||||| || || ||||| ||    || || ||| | ||||  |||||||| || |
Sbjct  761   GCAAATGGTATGAGGCTCATGATTATAAGGCTCACGGAGAGATTGTGGACTTTGTTGTGA  820
Query  836   TAATGACGTATGAGTGGGGCTACAGCGGCGGTCC-GCCGATGCCGGTCTCCCCCATCGGC  894
              | ||||| ||||| ||||| || |||||||||| ||  | ||| || || || || ||
Sbjct  821   TTATGACATATGAATGGGGGTATAGCGGCGGTCCGGCTCAAGCC-GTTTCTCCTATAGGA  879
Query  895   CCTGTCCGCCGTGTCCTCAAGTACGCCGTCTCGGAAATGCCTCCCGGAAAGATTTTAATG  954
              || |||||   |||| |  | || ||  |  | ||||||||| |    || ||  | |||
Sbjct  880   CCCGTCCGGGATGTCATTGAATATGCTTTAACTGAAATGCCTGCAAACAAAATCGTTATG  939
Query  955   GGGCAAAATTTGTATGGTTATGATTGGACACTGCCGTACGTACCG--GGCGGA-CCGTAC  1011
              || || ||||| || || |||||||||| ||||||||  ||||  ||||||  | ||
Sbjct  940   GGACAGAATTTATACGGATATGATTGGACCTTGCCGTAC--ACCGCTGGCGGAGACCTA-  996
Query  1012  GCCCGCGCCATCAGCCCGCAGCAGGCCATCGCCCTCGCCGCGAAGTATAACGTCGCGATT  1071
              ||    ||  |||| |||||||||| || |  || ||||   |  |||| |  || ||
Sbjct  997   GCGAAAGCTCTCAGTCCGCAGCAGGCGATTGTACTGGCCGGCCAAAATAATGCAGCAATC  1056
Query  1072  GAATACGACACCGAGGCGCAGGCGCCGCATTTTCGCTACCGCGATGAAAACGGGCGCGAG  1131
               |||||||        | ||||| ||    ||||||||   ||||  ||||       ||
Sbjct  1057  CAATACGATGAAACATCTCAGGCTCCCTTCTTTCGCTATACCGATTCAAACAACAAACAG  1116
Query  1132  CACGAAGTATGGTTTGAGGACGCCCGCTCCATTCAGGCAAAATTCAATCTCGTGAAAGAA  1191
              || || |||||||| || ||||| || |||||||| |||||||||||  |  | || |||
Sbjct  1117  CATGAGGTATGGTTCGAAGACGCACGTTCCATTCAAGCAAAATTCAATTTAATTAAGGAA  1176
Query  1192  CTTGGCCTGCGCGGAGTCAGCTATTGGAAACTGGGCTTCGATTTCCCGCAAAACTGGCTG  1251
              ||     |  | ||  ||||||||||||||| ||  ||  |||||| ||||||||||
Sbjct  1177  CTGAATTTAAGAGGGATCAGCTATTGGAAACTCGGGCTCTCTTTCCCTCAAAACTGGCTG  1236
```

3.6. Resistência a esporos

3.6.1. Resistência geral

As células bacterianas vivem em ambientes ricos em nutrientes ou com escassez aos mesmos. Para que as bactérias sobrevivam, elas devem se adaptar rapidamente às mudanças nas condições ambientais. Condições ricas em nutrientes levam a uma diminuição no tempo de duplicação da massa e a um aumento no tamanho das células, enquanto as condições pobres em nutrientes reduzem o crescimento e reduzem o tamanho das células. Neste contexto, a esporulação de bactérias em diferentes condições ambientais fornece ao esporo diferentes capacidades de resistência (SETLOW, 2006; WANG & LEVIN, 2009).

3.6.2. Específico para produtos químicos

Os esporos podem ser extremamente resistentes a uma variedade de produtos químicos, incluindo ácidos, bases, agentes oxidantes, alquilantes, aldeídos e solventes orgânicos. Com algumas substâncias químicas parece ocorrer dano a membrana interna do esporo, de modo que essa membrana se rompe após a germinação e crescimento de esporos. Para outros agentes, como o glutaraldeído, o mecanismo de eliminação de esporos não é claro (SETLOW, 2006).

Com o revestimento de esporos protegendo o núcleo de uma ampla variedade de agressões químicas e biológicas, tem-se um processo de exclusão passiva de enzimas degradativas produzidas por outras bactérias e moléculas tóxicas no ambiente (DRIKS & EICHENBERGER, 2016).

Conforme descrito por Setlow (2006), os fatores que são importantes na resistência química dos esporos variam com o produto químico, mas incluem: (i) a desintoxicação pelas proteínas do revestimento de esporos que provavelmente reagem com ele; (ii) a impermeabilidade da membrana interna do esporo para restringir o acesso ao núcleo do esporo; (iii) como proteção do DNA de esporos por sua saturação com pequenas proteínas de esporos solúveis em ácido (SASP) do tipo α/ß; e (iv) reparo de DNA para agentes que matam esporos por danos no DNA.

3.7. Metodologias de Descontaminação

Existem várias metodologias para a descontaminação de instalações de assistência médica, laboratórios de diagnóstico e pesquisa e instalações de produção de vacinas.

Comumente são usados gás de formaldeído, peróxido de hidrogênio vaporizado ou em fase de vapor, gás dióxido de cloro ou peróxido de hidrogênio ionizado.

3.7.1. Formaldeído

A eficácia do gás de formaldeído é altamente dependente da temperatura ambiente e da umidade, deixando um resíduo em pó branco "metenamina" em todas as superfícies quando neutralizada com gás amônia (Comunicação pessoal). O processo de descontaminação com gás de formaldeído tem a desvantagem de potencializar a re-polimerização em superfícies mais frias, não sendo desativada pelo processo de neutralização de amônia (LUFTMAN, 2005).

Demonstrado com agente mutagênico, sugere-se que o formaldeído mate os esporos, pelo menos em parte, por danos no DNA, pode entrar no núcleo do esporo. No entanto, o mecanismo preciso do dano ao DNA por este agente, causando a morte de esporos e a mutagênese, não é conhecido. Em estudos, verificou-se um aumento significativo na reticulação de DNA-proteína em esporos tratados com formaldeído (LOSHON *et al.*, 1999).

3.7.2. Dióxido de cloro

O mecanismo de ação do gás dióxido de cloro para matar esporos não está bem definido. Poderoso oxidante, se comporta como um radical livre por causa da presença de um elétron não pareado em seu orbital molecular. Sua atividade antimicrobiana se dá pela desnaturação de proteínas, afetando a viabilidade e a integridade dos esporos (RASTOGI *et al.*, 2010). O gás dióxido de cloro não mata os esporos por danos no DNA, mas parece danificar a camada de esporos. Os esporos expostos ao dióxido de cloro podem sofrer as etapas iniciais da germinação dos esporos, mas seu processo de germinação e crescimento não são concluídos provavelmente devido a algum dano na membrana, seja pela oxidação de ácidos graxos ou proteínas da membrana ou por ambos (YOUNG & SETLOW, 2003). Deve ser ressaltado ser um produto altamente corrosivo para metal de carbono e soldas não passivadas em equipamentos de aço inoxidável, como caixas de filtro HEPA.

3.7.3. Peróxido de hidrogênio vaporizado(Vaporized Hydrogen Peroxide) ou Peróxido de hidrogênio em fase de vapor (Vapor Phase Hydrogen Peroxide)

Os sistemas de peróxido de hidrogênio vaporizados ou em fase de vapor usam 30% a 35% de peróxido de hidrogênio, o qual é vaporizado para descontaminação das superfícies. A diferença entre os dois sistemas é a umidade inicial do controle, sendo ambos mais eficaz em superfícies não porosas do que em porosas (GORDON *et al.*, 2012). O processo no qual o vapor de peróxido de hidrogênio inativa os esporos não é completamente conhecido.

A decomposição deste produção com ação decontaminante gera espécies reativas de oxigênio. Pensa-se que os danos nos revestimentos de esporos por radicais hidroxila podem matar os esporos, pelo menos em parte, por danos no DNA (KHADRE & YOUSEF, 2001; SETLOW & SETLOW, 1993). O peróxido de hidrogênio vaporizado, devido à sua natureza vaporosa, tem problemas para chegar a locais difíceis, requerendo a utilização de ventiladores para forçar a circulação do vapor nas salas. Pode danificar revestimentos epóxi, sendo corrosivo para superfícies de metal de carbono e delaminar acabamentos anodizados no equipamento (Comunicação pessoal).

3.7.4. Peróxido de hidroênio ionizado

O peróxido de hidrogênio ionizado é uma tecnologia recente desenvolvida para a descontaminação de superfícies. Utiliza uma baixa concentração de peróxido de hidrogênio (7,8%), misturada com o ar, ionizada através de um arco de plasma frio, gerando espécies reativas de oxigênio como um meio de descontaminação. Por ser a mais nova tecnologia disponível para procediemtnso de decontaminação ambiental, seus problemas de aplicação e incompatibilidade ainda não foram documentados. Em testes recentes (Comunicação pessoal), o sistema de peróxido de hidrogênio ionizado apresenta padrões semelhantes à difusão semelhantes a um sistema gasoso, não mostrando danos a componentes eletrônicos.

Em estudos realizados usando um princípio semelhante para gerar espécies reativas de oxigênio e investigar seus efeitos nos esporos de *Cordyceps pruinosa*, verificou-se que a morfologia do esporo mudou drasticamente após o tratamento. Os esporos achataram, sugerindo que o espaço intracelular foi esvaziado de seu conteúdo e que a deformação da parede celular poderia afetar a viabilidade dos esporos quando

a parede celular perdeu suas funções responsáveis pelo controle da permeabilidade da parede celular e manutenção da rigidez estrutural. Além disso, com um tempo de tratamento de exposição mais longo, a recuperação da análise de DNA da eletroforese em gel de agarose mostrou uma redução mais significativa na intensidade da banda dos esporos tratados. A quantidade reduzida de DNA nos esporos tratados com plasma é possivelmente o resultado de degradação ou vazamento de DNA através da parede celular danificada (KIM *et al.*, 2016).

4. Referêcias

ALBINA, E.; BENGTSSON, U.; FORSTER, J.; HAAS, B. *et al.*, 2011, **EPIZONE** Workshop Formaldehyde Replacement, Central Veterinary Institute, Wageningen UR, Lelystad, The Netherlands.

CANO, R. J.; BORUCKI, M. K. Revival and identification of bacterial spores in 25- to 40-million-year-old Dominican amber. **Science**, v. 268, n. 5213, p. 1060-1064, May 19 1995.

COGLIANO, V. J.; GROSSE, Y.; BAAN, R. A.; STRAIF, K. *et al.* Meeting Report: Summary of IARC monographs on formaldehyde, 2-butoxyethanol, and 1-tert-butoxy-2-propanol. **Environmental Health Perspectives**, v. 113, n. 9, p. 1205-1208, 2005.

COWAN, A. E.; KOPPEL, D. E.; SETLOW, B.; SETLOW, P. A soluble protein is immobile in dormant spores of *Bacillus subtilis*; but is mobile in germinated spores: Implications for spore dormancy. **Proceedings of the National Academy of Sciences**, v. 100, n. 7, p. 4209, 2003.

DRIKS, A. *Bacillus subtilis* spore coat. **Microbiology and Molecular Biology Reviews**, v. 63, n. 1, p. 1-20, Mar 1999.

DRIKS, A.; EICHENBERGER, P. The spore coat. **Microbiology Spectrum**, v. 4, n. 2, Apr 2016.

EPA. Formaldehyde emission standards for composite wood products (RIN 2070-AJ44). **Environmental Protection Agency** : 40 CFR 770 2016.

GORDON, D.; CARRUTHERS, B.-A.; THERIAULT, S. Gaseous decontamination methods in high-containment laboratories. **Applied Biosafety**, v. 17, n. 1, p. 31-39, 2012.

KERNS, W. D.; PAVKOV, K. L.; DONOFRIO, D. J.; GRALLA, E. J. *et al.* Carcinogenicity of formaldehyde in rats and mice after long-term inhalation exposure. **Cancer Research**, v. 43, n. 9, p. 4382-4392, Sep 1983.

KHADRE; YOUSEF, A. E. Sporicidal action of ozone and hydrogen peroxide: a comparative study. **International Journal of Food Microbiology**, v. 71, n. 2-3, p. 131-138, Dec 30 2001.

KIM, J. Y.; LEE, I. H.; KIM, D.; KIM, S. H. *et al.* Effects of reactive oxygen species on the biological, structural, and optical properties of *Cordyceps pruinosa* spores. **RSC Advances**, v. 6, n. 36, p. 30699-30709, 2016. 10.1039/C5RA28107E.

KOCHAN, T. J.; FOLEY, M. H.; SHOSHIEV, M. S.; SOMERS, M. J. *et al.* Updates to *Clostridium difficile* Spore Germination. **Journal of Bacteriology**, v. 200, n. 16, Aug 15 2018.

KODAMA, T.; TAKAMATSU, H.; ASAI, K.; KOBAYASHI, K. *et al.* The *Bacillus subtilis yaaH* gene is transcribed by SigE RNA polymerase during sporulation, and its product is involved in germination of spores. **Journal of Bacteriology**, v. 181, n. 15, p. 4584-4591, Aug 1999.

LACH, V. H. A study of conventional formaldehyde fumigation methods. **Journal of Applied Bacteriology**, v. 68, n. 5, p. 471-477, May 1990.

LEGGETT, M. J.; MCDONNELL, G.; DENYER, S. P.; SETLOW, P. *et al.* Bacterial spore structures and their protective role in biocide resistance. **Journal of Applied Microbiology**, v. 113, n. 3, p. 485-498, Sep 2012.

LOSHON, C. A.; GENEST, P. C.; SETLOW, B.; SETLOW, P. Formaldehyde kills spores of *Bacillus subtilis* by DNA damage and small, acid-soluble spore proteins of the alpha/beta-type protect spores against this DNA damage. **Journal of Applied Microbiology**, v. 87, n. 1, p. 8-14, Jul 1999.

LUFTMAN, H. S. Neutralization of formaldehyde gas by ammonium bicarbonate and ammonium carbonate. **Applied Biosafety**, v. 10, n. 2, p. 101-106, 2005.

MOIR, A.; COOPER, G. Spore germination. **Microbiology Spectrum**, v. 3, n. 6, Dec 2015.

NAKAMURA, L. K. Taxonomic relationship of black-pigmented *Bacillus subtilis* strains and a proposal for *Bacillus atrophaeus* sp. nov. **International Journal of Systematic and Evolutionary Microbiology**, v. 39, n. 3, p. 295-300, 1989.

NAZINA, T. N.; TOUROVA, T. P.; POLTARAUS, A. B.; NOVIKOVA, E. V. *et al.* Taxonomic study of aerobic thermophilic bacilli: descriptions of *Geobacillus subterraneus* gen. nov., sp. nov. and *Geobacillus uzenensis* sp. nov. from petroleum reservoirs and transfer of *Bacillus stearothermophilus*, *Bacillus thermocatenulatus*, *Bacillus thermoleovorans, Bacillus kaustophilus, Bacillus thermodenitrificans* to *Geobacillus* as the new combinations *G. stearothermophilus*, *G. thermocatenulatus, G. thermoleovorans, G. kaustophilus, G. thermoglucosidasius and G. thermodenitrificans.* **International Journal of Systematic and Evolutionary Microbiology**, v. 51, n. 2, p. 433-446, 2001.

NICHOLSON, W. L.; MUNAKATA, N.; HORNECK, G.; MELOSH, H. J. *et al.* Resistance of *Bacillus* endospores to extreme terrestrial and extraterrestrial environments. **Microbiology and Molecular Biology Reviews**, v. 64, n. 3, p. 548-572, Sep 2000.

RASTOGI, V. K.; RYAN, S. P.; WALLACE, L.; SMITH, L. S. *et al.* Systematic evaluation of the efficacy of chlorine dioxide in decontamination of building interior

surfaces contaminated with anthrax spores. **Applied and Environmental Microbiology**, 76, n. 10, p. 3343-3351, May 2010.

SANTO, L. Y.; DOI, R. H. Ultrastructural analysis during germination and outgrowth of *Bacillus subtilis* spores. **Journal of Bacteriology**, v. 120, n. 1, p. 475-481, Oct 1974.

SELLA, S. R. B. R.; VANDENBERGHE, L. P. S.; SOCCOL, C. R. Life cycle and spore resistance of spore-forming *Bacillus atrophaeus*. **Microbiological Research**, v. 169, n. 12, p. 931-939, Dec 2014.

SETLOW, B.; SETLOW, P. Binding of small, acid-soluble spore proteins to DNA plays a significant role in the resistance of *Bacillus subtilis* spores to hydrogen peroxide. **Applied and Environmental Microbiology**, v. 59, n. 10, p. 3418-3423, Oct 1993.

SETLOW, P. Spores of Bacillus subtilis: their resistance to and killing by radiation, heat and chemicals. **Journal of Applied Microbiology**, v. 101, n. 3, p. 514-525, Sep 2006.

SETLOW, P. Germination of spores of Bacillus species: what we know and do not know. **Journal of Bacteriology**, v. 196, n. 7, p. 1297-1305, Apr 2014.

WANG, J. D.; LEVIN, P. A. Metabolism, cell growth and the bacterial cell cycle. **Nature Reviews Microbiology**, v. 7, n. 11, p. 822-827, Nov 2009.

YOUNG, S. B.; SETLOW, P. Mechanisms of killing of *Bacillus subtilis* spores by hypochlorite and chlorine dioxide. **Journal of Applied Microbiology**, v. 95, n. 1, p. 54-67, 2003.

CAPÍTULO 1 - Determining the effectiveness of decontaminating with Ionized Hydrogen Peroxide

1. Introduction

Ionized Hydrogen Peroxide (iHP) is a new technology used for the decontamination of surfaces or laboratory areas. It utilizes a low concentration of hydrogen peroxide (H_2O_2) at 7.8% mixed with air and ionized through a cold plasma arc. This technology generates reactive oxygen species (ROS) as a means of decontamination. Members of the reactive oxygen species in the air include ozone, atomic oxygen, superoxide, peroxide, and hydroxyl radicals (GAUNT *et al.,* 2006; DAS & ROYCHOUDHURY, 2014). In addition to these, H_2O_2 generates oxidative stress that attacks multiple molecular targets, including nucleic acids, enzymes, cell wall proteins, and lipids (HALL *et al.,* 2007; MELLY *et al.,* 2002).

There have been other hydrogen peroxide systems that have been used in the past to decontaminate surfaces, laboratories, and HEPA filters, but their lack of penetration is a concern (JIA *et al.*, 2013). Since iHP is the newest technology available, its application and incompatibility issues have not been documented. In preliminary test trials (personal communication), the ionized hydrogen peroxide system presents diffusion like- patterns similar to a gaseous system. One of the advantages of using hydrogen peroxide is that it does not leave any residue after the decontamination process since it breaks down into water and oxygen (GALVIN *et al.*, 2012; KLAPES & VESLEY, 1990; MCDONNELL, 2017). The purpose of this particular study is to evaluate the diffusion effect of ionized hydrogen peroxide and its decontamination capabilities using biological and enzyme indicators.

2. Materials and Methods

2.1. Biological Indicator and Enzyme Indicator

To evaluate the effectiveness and diffusion of the decontamination process, biological indicators of *Bacillus atrophaeus* ATCC 9372 in stainless steel disks and Tyvek® envelope (Catalog No. GRS-090, Population 2.2x106, D-Value: 0.7 minutes, Mesa Labs, Lakewood, CA, USA) along with biological indicators of *Geobacillus stearothermophilus* ATCC 12980 in stainless steel disks with Tyvek®

envelope (Catalog HMV-091, Population 2.0 x 106, D-Value: 1.7 minutes, Mesa Labs, Lakewood, CA, USA) and in stainless steel strips (Catalog SBC-327, Population 1.9 x 106, D-Value: 2.4 minutes, Mesa Labs, Lakewood, CA, USA) were used.

In addition to the biological indicators, tAK enzyme indicators (Protak Scientific, Redhill, Surrey, UK.) were used alongside the biological indicators. The tAK enzymes indicators are made of thermostable Adenylate Kinase (tAK) from thermophilic bacteria found in hot springs (*Sulpholobus acidocaldarius*) (HESP *et al.*, 2010; BACKMANN *et al.,* 1998). The tAK enzyme is a phosphotransferase enzyme that catalyzes the reversible formation of adenosine triphosphate (ATP) and adenosine monophosphate (AMP) (HATHAWAY *et al.,* 2015). Its composition has been modified with luciferase/luciferin assay to emit fluorescence with the production of ATP that can be measured with a luminometer.

2.2. Decontamination Setup

A fumigation room with a volume of 880 ft^3 (8ft x 11ft x10ft) was used for the decontamination trials. This gas-tight room has air pressure resistant doors and bioseal dampers to isolate the room during decontamination procedures. During the decontamination process, empty animal cages (2.75ft x 2.75ft x 7ft) were placed inside the fumigation room to create fumigant distribution restrictions. Spore indicators and enzyme indicators were placed in eleven locations throughout the decontamination room in the corners in high and low positions and underneath or behind the animal cages.

2.3. Decontamination Process

Generation of ionized hydrogen peroxide was done with the use of the SteraMist Environmental System equipment (TOMI Environmental Solutions, Beverly Hills, CA, USA) at a rate of 25ml/min and 20 psi of air pressure through the plasma arc.

The total room volume was adjusted to 900ft^3 for ease of dose calculations, and the disinfection solution used was SteraMist Solution (TOMI Environmental

Solutions, Beverly Hills, CA, USA), with 7.8% H_2O_2 at the dose of 0.5 ml per ft^3. Air sampling monitors for measuring concentrations of 0_3 and H_2O_2 were located inside the room, and the bioseal dampers and the pneumatic gasketed door were closed before the start of the fumigation to provide a gas-tight room. The total spray time per decontamination trial was 18 minutes, and the contact periods that started at the end of the spray times were for 1 hour, 2 hours, 6 hours, and 12 hours. For each decontamination period, a total of three trials were done. The samples were collected and processed after a 30 minutes ventilation period of the room.

Room environmental conditions during decontamination were measured using a temperature and humidity sensor (Velocicalc, Model 9555P, Probe Model 966, TSI Incorporated, Shoreview, MN, USA). Also, Hydrogen Peroxide and Ozone levels were measured using a portable gas detector (PortaSens II, Model C16, Analytical Technology, Inc., Collegeville, PA, USA) with smart sensor modules for ozone (O_3, 1-5 ppm, Part No. H10-00-1008) and hydrogen peroxide (H_2O_2, 10-100 ppm, Part No. H10-00-1042).

2.4. Evaluation of Inactivation Effectiveness

The biological indicators of *B. atrophaeus* were incubated at 37°C in Soybean Casein Digest Medium (Red Releasat®, RM/100, MesaLabs, Lakewood, CA, USA) and indicators of *G. stearothermophilus* were incubated at 56°C in Soybean Casein Digest Medium (Purple Releasat®, PM/100, MesaLabs, Lakewood, CA, USA). All biological indicators were incubated for seven days.

The reduction of enzyme activity was analyzed by a luminometer (Model PR2A, Protak Scientific, Red Hill Surrey, UK) according to manufacturer's instructions. The luminometer data was analyzed using Protak's Athena Software.

Graphing and statistical software used for data analysis was GraphPad Prism 8 (Graphpad Software Inc., La Jolla, CA, USA). The graphs are presented using a median with interquartile range because of the variability in environmental conditions during the decontamination process.

3. Results

Parameters as microbial growth and enzyme activity were placed side by side in eleven locations throughout the decontamination room, including the corners in high and low positions and underneath or behind the animal cages, as shown in figures 1-1 through 1-7. The purpose was to simulate the decontamination scenario that is typical to formaldehyde gas decontamination of animal cages. A typical formaldehyde decontamination cycle for this room is 2:30 hrs of formaldehyde injection, overnight contact time (≥12 hrs), followed by neutralization of formaldehyde of 2:30 hrs and finally ventilation of the room for a minimum of two hours before biological indicators are extracted wearing protective equipment.

Figure 1-1: Fumigation Room Decontamination Setup.

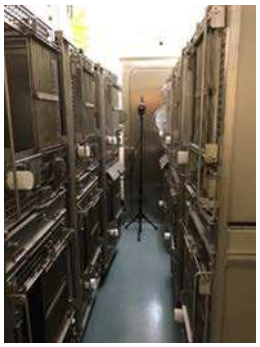

Figure 1-2: Portasens II - Parametric testing of O3 and H2O2 concentrations during decontamination.

Figure 1-3: Sample 3 located behind the iHP application nozzle.

Figure 1-4: Sample 4 located behind the iHP application nozzle. Also, view decontamination equipment.

Figure 1-5: Sample 8 located away from the nozzle in a low position.

Figure 1-6: Sample 11 located behind a cage

Figure 1-7: Sample 5 located behind the iHP application nozzle and location of sample 11.

The environmental conditions during the decontamination trials were in average temperatures from 22.3°C to 23.9°C and humidity from 57.2% to 72.7%. The observed

hydrogen peroxide readings during the decontamination of the room were from 53.3 ppm to a max of 111.1 ppm, and the Portasens II ozone sensor reached its detection limit of 6.01 ppm in two minutes into the injection of the ionized hydrogen peroxide.

3.1. Biological Indicators Results

Biological indicator results for the four different contact times of ionized hydrogen peroxide (iHP decontamination are described as follows.

For the one-hour iHP decontamination contact time (Table 1-1), the biological indicators of *B. atrophaeus* resulted in an inactivation of 31 out of 33 samples for a 94% inactivation rate, the *G. stearothermophilus* in SS disks resulted in an inactivation of 18 out of 22 for an 82% inactivation rate, and the *G. stearothermophilus* samples in SS strips resulted in an inactivation of 29 out of 33 samples for a 88% inactivation rate.

Table 1-1: Evaluation of inactivation effectiveness after 1-hour iHP exposure. Spore samples results for B. atrophaeus achieved a 94% inactivation rate, G. stearothermophilus in SS disks achieved an 82% inactivation rate, and G. stearothermophilus in SS strips achieved an 88% inactivation rate. Empty cells indicate no sample on this location.

iHP 1hr	*B. atrophaeus* SS Disks				*G. stearothermophilus* SS Disks			*G. stearothermophilus* SS Strips			
Room Position	Test 1	Test 2	Test 2	Test 3	Test 2	Test 2	Test 3	Test 1	Test 2	Test 2	Test 3
Positive Control	Pos	Pos	Pos	Pos	Pos	Pos	Pos	Pos	Pos	Pos	Pos
Negative Control	Neg	Neg	Neg	Neg	Neg	Neg	Neg	Neg	Neg	Neg	Neg
1	Neg	Neg	Neg	Neg	Pos	Pos	Neg	Pos	Neg	Neg	Neg
2	Neg	Neg	Neg	Neg	Pos	Pos	Neg	Neg	Neg	Neg	Neg
3	Neg	Neg	Neg	Neg	Neg	Neg	Neg	Neg	Neg	Neg	Neg
4	Neg	Neg		Neg	Neg		Neg	Neg	Neg		Neg
5	Neg	Pos	Pos	Neg	Neg	Neg	Neg	Pos	Neg	Neg	Neg
6	Neg	Neg	Neg	Neg	Neg	Neg	Neg	Neg	Neg	Neg	Neg
7	Neg			Neg			Neg	Pos			Neg
8	Neg			Neg			Neg	Neg			Neg
9	Neg			Neg			Neg	Pos			Neg
10	Neg			Neg			Neg	Neg			Neg
11	Neg			Neg			Neg	Neg			Neg

For the two hours iHP decontamination contact time (Table 1-2), the biological indicators of *B. atrophaeus* resulted in an inactivation of 32 out of 33 samples for a 97% inactivation rate, the *G. stearothermophilus* in SS disks resulted in an inactivation of 15 out of 22 for a 68% inactivation rate. The *G. stearothermophilus* samples in SS strips resulted in an inactivation of 22 out of 33 samples for a 67% inactivation rate.

Table 1-2: Evaluation of inactivation effectiveness after 2-hours iHP exposure. Spore sample results for B. atrophaeus achieved a 97% inactivation rate, G. stearothermophilus in SS disks achieved a 68% inactivation rate, and G. stearothermophilus in SS strips achieved a 67% inactivation rate. Empty cells indicate no sample on this location.

iHP 2hrs	*B. atrophaeus* SS Disks				*G. stearothermophilus* SS Disks			*G. stearothermophilus* SS Strips			
Room Position	Test 1	Test 2	Test 2	Test 3	Test 2	Test 2	Test 3	Test 1	Test 2	Test 2	Test 3
Positive Control	Pos	Pos	Pos	Pos	Pos	Pos	Pos	Pos	Pos	Pos	Pos
Negative Control	Neg	Neg	Neg	Neg	Neg	Neg	Neg	Neg	Neg	Neg	Neg
1	Pos	Neg	Neg	Neg	Pos	Pos	Neg	Pos	Pos	Pos	Neg
2	Neg	Neg	Neg	Neg	Pos	Pos	Pos	Neg	Pos	Pos	Neg
3	Neg	Neg	Neg	Neg	Pos	Pos	Neg	Neg	Pos	Pos	Neg
4	Neg	Neg		Neg	Neg		Neg	Neg	Pos		Neg
5	Neg	Neg	Neg	Neg	Neg	Neg	Neg	Neg	Neg	Neg	Neg
6	Neg	Neg	Neg	Neg	Neg	Neg	Neg	Neg	Pos	Pos	Neg
7	Neg			Neg			Neg	Neg			Neg
8	Neg			Neg			Neg	Neg			Neg
9	Neg			Neg			Neg	Pos			Neg
10	Neg			Neg			Neg	Neg			Neg
11	Neg			Neg			Neg	Neg			Neg

For the six hours iHP decontamination contact time (Table 1-3), the biological indicators of *B. atrophaeus* resulted in an inactivation of 44 out of 44 samples for a 100% inactivation rate, the *G. stearothermophilus* in SS disks resulted in an inactivation of 44 out of 44 for a 100% inactivation rate, and the *G. stearothermophilus* samples in SS strips resulted in an inactivation of 20 out of 22 samples for a 91% inactivation rate.

Table 1-3: Evaluation of inactivation effectiveness after 6-hours iHP exposure. Spore sample results for B. atrophaeus achieved a 100% inactivation rate, G. stearothermophilus in SS disks achieved a 100% inactivation rate, and G. stearothermophilus in SS strips achieved a 91% inactivation rate. Empty cells indicate no sample on this location.

iHP 6hrs	*B. atrophaeus* SS Disks					*G. stearothermophilus* SS Disks					*G. stearothermophilus* SS Strips		
Room Position	Test 1	Test 1	Test 2	Test 2	Test 3	Test 1	Test 1	Test 2	Test 2	Test 3	Test 2	Test 2	Test 3
Positive Control	Pos	Pos	Pos	Pos	Pos	Pos	Pos	Pos	Pos	Pos	Pos	Pos	Pos
Negative Control	Neg	Neg	Neg	Neg	Neg	Neg	Neg	Neg	Neg	Neg	Neg	Neg	Neg
1	Neg	Neg	Neg	Neg	Neg	Neg	Neg	Neg	Neg	Neg	Pos	Pos	Neg
2	Neg	Neg	Neg	Neg	Neg	Neg	Neg	Neg	Neg	Neg	Neg	Neg	Neg
3	Neg	Neg	Neg	Neg	Neg	Neg	Neg	Neg	Neg	Neg	Neg	Neg	Neg
4	Neg	Neg	Neg		Neg	Neg	Neg	Neg		Neg	Neg		Neg
5	Neg	Neg	Neg	Neg	Neg	Neg	Neg	Neg	Neg	Neg	Neg	Neg	Neg
6	Neg	Neg	Neg	Neg	Neg	Neg	Neg	Neg	Neg	Neg	Neg	Neg	Neg
7	Neg	Neg			Neg	Neg	Neg			Neg			Neg
8	Neg	Neg			Neg	Neg	Neg			Neg			Neg
9	Neg	Neg			Neg	Neg	Neg			Neg			Neg
10	Neg	Neg			Neg	Neg	Neg			Neg			Neg
11	Neg	Neg			Neg	Neg	Neg			Neg			Neg

For the 12 hours iHP decontamination contact time (Table 1-4), the biological indicators of *B. atrophaeus* resulted in an inactivation of 44 out of 44 samples for a 100% inactivation rate, the *G. stearothermophilus* in SS disks resulted in an inactivation of 44 out of 44 for a 100% inactivation rate. The *G. stearothermophilus* samples in SS strips resulted in an inactivation of 22 out of 22 samples for a 100% inactivation rate.

Table 1-4: Evaluation of inactivation effectiveness after 12-hours iHP exposure. Spore sample results for B. atrophaeus achieved a 100% inactivation rate, G. stearothermophilus in SS disks achieved a 100% inactivation rate, and G. stearothermophilus in SS strips achieved a 100% inactivation rate. Empty cells indicate no sample on this location.

iHP 12hrs	*B. atrophaeus* SS Disks					*G. stearothermophilus* SS Disks					*G. stearothermophilus* SS Strips		
Room Position	Test 1	Test 1	Test 2	Test 2	Test 3	Test 1	Test 1	Test 2	Test 2	Test 3	Test 2	Test 2	Test 3
Positive Control	Pos	Pos	Pos	Pos	Pos	Pos	Pos	Pos	Pos	Pos	Pos	Pos	Pos
Negative Control	Neg	Neg	Neg	Neg	Neg	Neg	Neg	Neg	Neg	Neg	Neg	Neg	Neg
1	Neg	Neg	Neg	Neg	Neg	Neg	Neg	Neg	Neg	Neg	Neg	Neg	Neg
2	Neg	Neg	Neg	Neg	Neg	Neg	Neg	Neg	Neg	Neg	Neg	Neg	Neg
3	Neg	Neg	Neg	Neg	Neg	Neg	Neg	Neg	Neg	Neg	Neg	Neg	Neg
4	Neg	Neg	Neg		Neg	Neg	Neg	Neg		Neg	Neg		Neg
5	Neg	Neg	Neg	Neg	Neg	Neg	Neg	Neg	Neg	Neg	Neg	Neg	Neg
6	Neg	Neg	Neg	Neg	Neg	Neg	Neg	Neg	Neg	Neg	Neg	Neg	Neg
7	Neg	Neg			Neg	Neg	Neg			Neg			Neg
8	Neg	Neg			Neg	Neg	Neg			Neg			Neg
9	Neg	Neg			Neg	Neg	Neg			Neg			Neg
10	Neg	Neg			Neg	Neg	Neg			Neg			Neg
11	Neg	Neg			Neg	Neg	Neg			Neg			Neg

For all decontamination trials, a comparison graph of pass rate percentage per spore type and contact time is shown in Figure 1-8.

Figure 1-8: Percentage pass rate of biological indicators per decontamination trail.

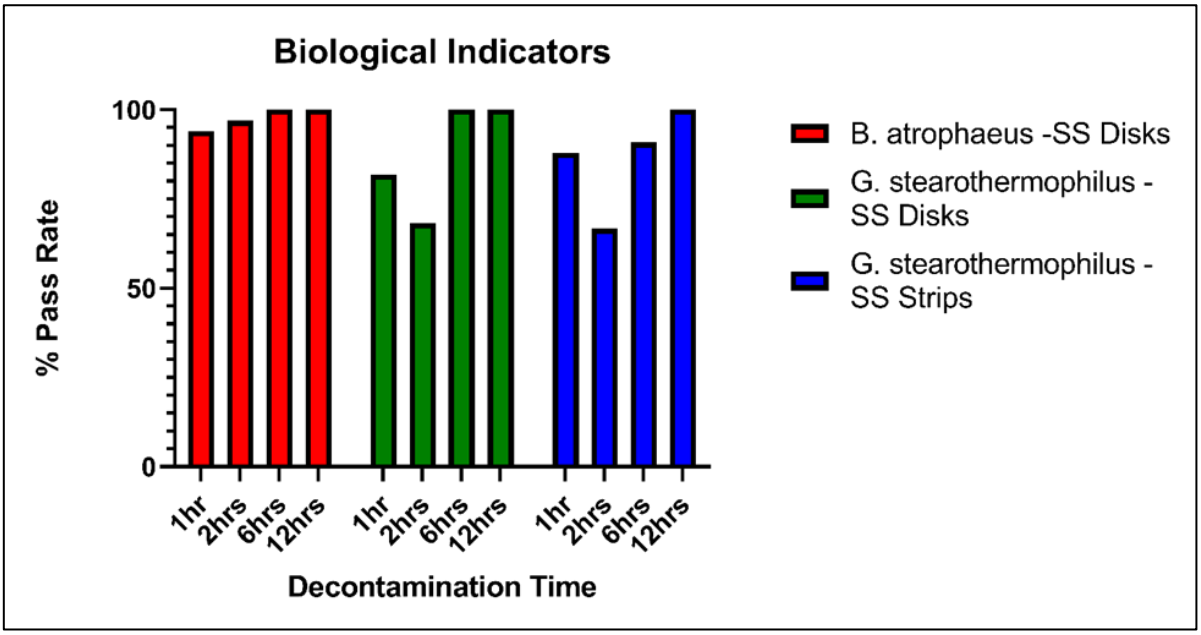

3.2. Enzyme Indicators Results

The luminometer reading of the production of fluorescent ATP from the residual enzyme activity in relative light units (RLU) for both positive and negative controls, as well as the 11 samples in the room, is shown in Figure 1-9. The measure of residual enzyme activity indicated that as the contact time of iHP decontamination increased, an increase in inactivation of enzyme activity was observed in parallel.

Figure 1-9: Remaining fluorescence tAK activity after the decontamination process. Data are presented as the median with interquartile range.

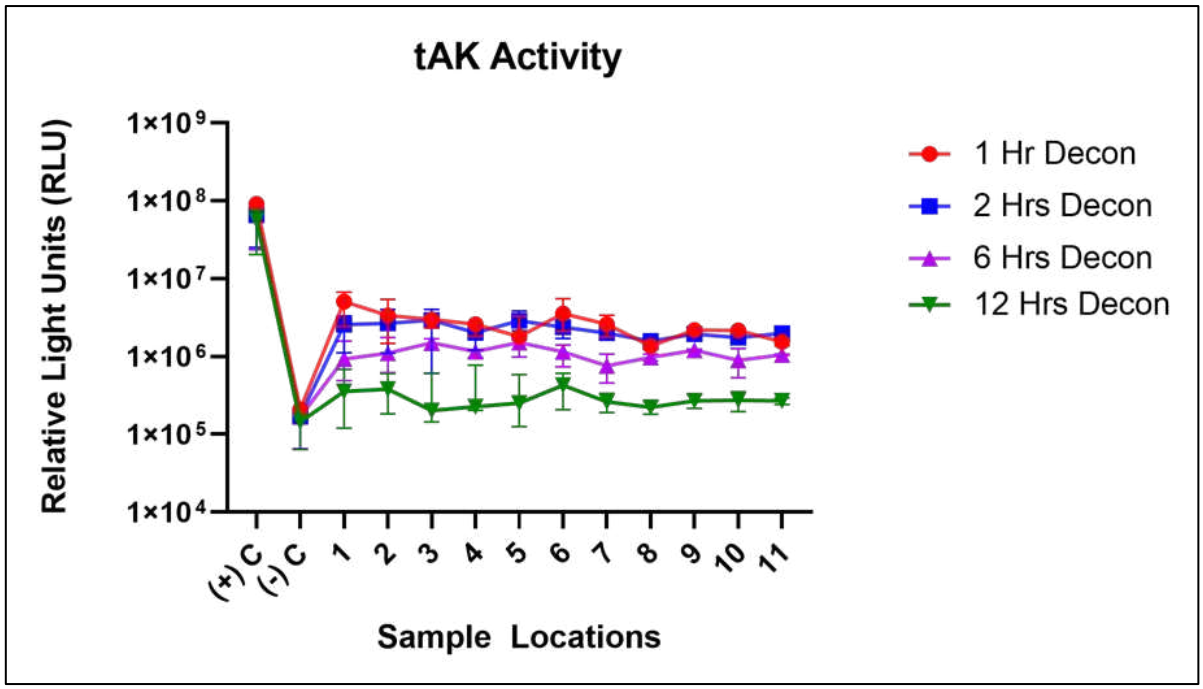

In addition to the review of the RLU inactivation, data were also analyzed comparing the positive control for each decontamination trial (N_0) versus each sample (N) in the trial. The resulting calculation of N divided by N_0 provided us with the relative inactivation of the enzyme compared to its control. The data results for each decontamination trial (1hr, 2hrs, 6hrs, 12hrs) are graphed in Figure 1-10.

Figure 1-10: tAK inactivation (N/N_0) after decontamination trials of 1hr, 2hrs, 6hrs, and 12hrs. Data are presented as the median with interquartile range.

.

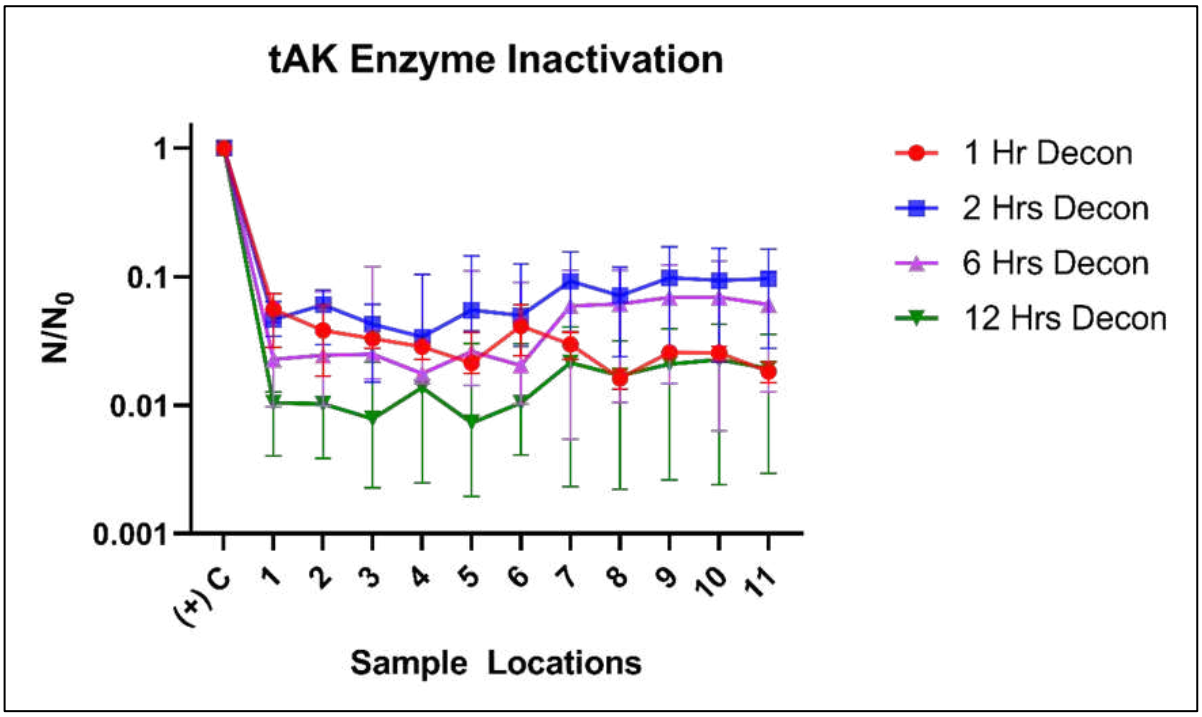

4. Discussion and Conclusion

In order to determine the quantitative measurements of the effects of the ionized hydrogen peroxide decontamination process, both biological spore and enzyme indicators were utilized. Previous studies have demonstrated that spore and enzyme indicators have similar inactivation profiles (MCLEOD *et al.,* 2017). Therefore it was possible to use the enzyme indicators as a means to measure the inactivation of the luciferase/luciferin reaction of the enzyme in relative light units providing us with a standardized reading in the room.

For the decontamination of 1 hr, 2 hrs, 6 hrs, and 12 hrs, the biological indicators of *B. atrophaeus* in stainless steel (SS) Disk, and Tyvek® envelope has a rate of inactivation of 94%, 97%, 100%, and 100%, respectively. For *G. stearothermophilus* in SS disk and Tyvek® envelope, it has an inactivation rate of 82%, 68%, 100%, and 100%, respectively and, for *G. stearothermophilus* in SS strips it has an inactivation rate of 88%, 67%, 91%, and 100%.

The use of biological or enzyme indicators that are inoculated on non-porous surfaces like stainless steel disks is preferred because paper base indicators have the potential for false-negative results that may limit the evaluation of a proper decontamination cycle to be achieved (GORDON *et al.*, 2011).

Studies utilizing *B. subtilis* spores with decontamination using formaldehyde gas and vaporized hydrogen peroxide have found that small, acid-soluble proteins protect the DNA from damage during decontamination and plays a role in the resistance of the spores (LOSHON *et al.,* 1999; SETLOW & SETLOW, 1993). This resistant capability could explain in part the repair or survival of spores if they are not completely damaged during the decontamination.

In a similar inactivation, a study using formaldehyde gas, exposure of spores to 10 hours of contact time, and 1,100 ppm of gas, the treatment inactivated ≥ 50% of spore strips with approximately the same spore count per indicator as to the samples used on our studies (ROGERS *et al.*, 2007).

Although Pottage *et al*. (2012) did not find a difference between non-enveloped and enveloped biological indicators during his decontamination studies, a difference was observed between non-enveloped and Tyvek® enveloped *G. sterothermophilus*. However, the variability of biological indicator inactivation in our *G. sterothermophilus* results could be due to the difference in the D-value of the samples.

Our results from this study also suggest that *G. stearothermophilus* is more resistant to ionized hydrogen peroxide than *B. atrophaeus,* which is similar to the findings from several other decontamination studies with hydrogen peroxide (KLAPES & VESLEY, 1990; ROGERS *et al.*, 2005; POTTAGE *et al.*, 2010).

Traditionally, biological (spores) indicators have been used to validate decontamination processes with the final readout (pass/fail) of these indicators completed after seven days of incubation. Unfortunately, biological spore indicators do not provide a quantitative way to determine their pass/fail limits. In contrast, enzyme indicators, provide a measurement of residual enzyme (tAK) activity, which can be a tool for evaluation of diffusion, penetration, quantification, and 3D mapping of the fumigation process. Enzyme indicators have excellent potential to replace the use of biological indicators. Nevertheless, correlation studies need to be carried out to thoroughly assess the inactivation readout of the enzyme in comparison to the specific biological indicator of use.

In conclusion, obtained results show that ionized hydrogen peroxide inactivates spores of *B. atrophaeus* and *G. stearothermophilus* and that the residual tAK activity indicates a gas-like fumigant diffusion due to the uniformity of the inactivation on different sample locations without the use of oscillating fans and a higher inactivation of the enzyme indicators as the contact time is extended.

5. Future Directions

In future directions, one activity would be to investigate what causes the reduction of inactivation at two hours of contact time compared to the one hour and the six hours. Also test if changing environmental conditions have a negative effect on the results of the decontaminations.

Additionally, review the inactivation of the tAK enzyme indicators with the use of formaldehyde gas. On a pilot study (Data not shown), the inactivation of the tAK enzyme was at levels close to the negative control. As Hathaway *et al.* (2015) mentions, the inhibition of the luciferin/luciferase indicator system used for the detection of the activity of the tAK enzyme could be affected by the decontamination systems.

As Pottage *et al.* (2012) found that methicillin-resistant *Staphylococcus aureus* is more resistant to vaporized hydrogen peroxide than commercial *G. stearothermophilus* biological indicators. It is vital that a new methodology to evaluate decontamination effectiveness needs to be done for each decontamination technology utilized. One approach could be the use of enzyme indicators that provides quick quantitative data to correlate the inactivation of a specific pathogen to the inactivation of the enzyme, taking into consideration the limit of detection of the enzyme indicator.

6. References

BACKMANN, J.; SCHAFER, G.; WYNS, L.; BONISCH, H. Thermodynamics and kinetics of unfolding of the thermostable trimeric adenylate kinase from the archaeon *Sulfolobus acidocaldarius*. **Journal of Molecular Biology**, v. 284, n. 3, p. 817-833, Dec 4 1998.

DAS, K.; ROYCHOUDHURY, A. Reactive oxygen species (ROS) and response of antioxidants as ROS-scavengers during environmental stress in plants. **Frontiers in Environmental Science**, v. 2, n. 53, 2014-December-02 2014.

GALVIN, S.; BOYLE, M.; RUSSELL, R. J.; COLEMAN, D. C. *et al.* Evaluation of vaporized hydrogen peroxide, Citrox and pH neutral Ecasol for decontamination of an enclosed area: a pilot study. **Journal of Hospital Infection**, v. 80, n. 1, p. 67-70, Jan 2012.

GAUNT, L. F.; BEGGS, C. B.; GEORGHIOU, G. E. Bactericidal action of the reactive species produced by gas-discharge nonthermal plasma at atmospheric pressure: a review. **IEEE Transactions on Plasma Science**, v. 34, n. 4, p. 1257-1269, 2006.

GORDON, D.; MADDEN, B.; KRISHNAN, J.; KLASSEN, S. *et al.* Implications of paper vs stainless steel biological indicator substrates for formaldehyde gas decontamination. **Journal of Applied Microbiology**, v. 110, n. 2, p. 455-462, Feb 2011.

HALL, L.; OTTER, J. A.; CHEWINS, J.; WENGENACK, N. L. Use of hydrogen peroxide vapor for deactivation of *Mycobacterium tuberculosis* in a biological safety cabinet and a room. **Journal of Clinical Microbiology**, v. 45, n. 3, p. 810-815, Mar 2007.

HATHAWAY, H. J.; SUTTON, J. M.; JENKINS, A. T. Study into the kinetic properties and surface attachment of a thermostable adenylate kinase. **Biochemistry and Biophysics Reports**, v. 1, p. 1-7, May 2015.

HESP, J. R.; POOLMAN, T. M.; BUDGE, C.; BATTEN, L. *et al.* Thermostable adenylate kinase technology: a new process indicator and its use as a validation tool for the reprocessing of surgical instruments. **Journal of Hospital Infection**, v. 74, n. 2, p. 137-143, Feb 2010.

JIA, H. Q.; LI, Y. J.; SUN, B.; ZHAO, S. Q. *et al.* Evaluation of vaporized hydrogen peroxide fumigation as a method for the bio-decontamination of the high efficiency

particulate air filter unit. **Biomedical and Environmental Sciences**, v. 26, n. 2, p. 110-117, Feb 2013.

KLAPES, N. A.; VESLEY, D. Vapor-phase hydrogen peroxide as a surface decontaminant and sterilant. **Applied and Environmental Microbiology**, 56, n. 2, p. 503-506, Feb 1990.

LOSHON, C. A.; GENEST, P. C.; SETLOW, B.; SETLOW, P. Formaldehyde kills spores of *Bacillus subtilis* by DNA damage and small, acid-soluble spore proteins of the alpha/beta-type protect spores against this DNA damage. **Journal of Applied Microbiology**, v. 87, n. 1, p. 8-14, Jul 1999.

MCDONNELL, G. E. **Antisepsis, Disinfection, and Sterilization: Types, Action, and Resistance**. American Society of Microbiology, John Wiley & Son, 2017. 9781683673071.

MCLEOD, N. P.; CLIFFORD, M.; SUTTON, J. M. Evaluation of novel process indicators for rapid monitoring of hydrogen peroxide decontamination processes. **PDA Journal of Pharmaceutical Science and Technology**, v. 71, n. 5, p. 393-404, 2017.

MELLY, E.; COWAN, A. E.; SETLOW, P. Studies on the mechanism of killing of *Bacillus subtilis* spores by hydrogen peroxide. **Journal of Applied Microbiology**, v. 93, n. 2, p. 316-325, 2002.

POTTAGE, T.; MACKEN, S.; WALKER, J. T.; BENNETT, A. M. Meticillin-resistant *Staphylococcus aureus* is more resistant to vaporized hydrogen peroxide than commercial *Geobacillus stearothermophilus* biological indicators. **Journal of Hospital Infection**, v. 80, n. 1, p. 41-45, Jan 2012.

POTTAGE, T.; RICHARDSON, C.; PARKS, S.; WALKER, J. T. *et al.* Evaluation of hydrogen peroxide gaseous disinfection systems to decontaminate viruses. **Journal of Hospital Infection**, v. 74, n. 1, p. 55-61, Jan 2010.

ROGERS, J. V.; CHOI, Y. W.; RICHTER, W. R.; RUDNICKI, D. C. *et al.* Formaldehyde gas inactivation of *Bacillus anthracis*, *Bacillus subtilis*, and *Geobacillus stearothermophilus* spores on indoor surface materials. **Journal of Applied Microbiology**, v. 103, n. 4, p. 1104-1112, Oct 2007.

ROGERS, J. V.; SABOURIN, C. L.; CHOI, Y. W.; RICHTER, W. R. *et al.* Decontamination assessment of *Bacillus anthracis*, *Bacillus subtilis*, and *Geobacillus stearothermophilus* spores on indoor surfaces using a hydrogen peroxide gas generator. **Journal of Applied Microbiology**, v. 99, n. 4, p. 739-748, 2005.

SETLOW, B.; SETLOW, P. Binding of small, acid-soluble spore proteins to DNA plays a significant role in the resistance of *Bacillus subtilis* spores to hydrogen peroxide. **Applied and Environmental Microbiology**, v. 59, n. 10, p. 3418-3423, Oct 1993.

CAPÍTULO 2 - Mechanisms of Sporicidal Activity induced by Ionized Hydrogen Peroxide in the Inactivation of Spores of *Bacillus atrophaeus* and *Geobacillus stearothermophilus*.

1. Introduction

As previously described in Capítulo 1, the decontamination with ionized hydrogen peroxide (iHP) at 1 hr, 2 hrs, 6 hrs, and 12 hrs, observed a rate of inactivation for biological indicators of *Bacillus atrophaeus* in stainless steel (SS) Disk in Tyvek® envelope of 94%, 97%, 100%, and 100%, respectively. For *Geobacillus stearothermophilus* in SS disk and Tyvek® envelope, an inactivation rate of 82%, 68%, 100%, and 100%, was observed respectively and, for *G. stearothermophilus* in SS strips an inactivation rate of 88%, 67%, 91%, and 100% was observed. What is not well understood is the mechanisms of inactivation of the spores that affect germination and growth.

The ionized hydrogen peroxide (iHP) system utilized in this study sprays a 7.8% H_2O_2 solution mixed with air and ionized through a cold plasma arc. This ionization process generates reactive oxygen species (ROS) that could include ozone, atomic oxygen, superoxide, peroxide, and hydroxyl radicals (GAUNT *et al.,* 2006; DAS & ROYCHOUDHURY, 2014).

On studies done using a similar principle for generating ROS and investigating its effects on spores of *Cordyceps pruinosa*, the morphology of the spore changed dramatically after treatment. The spores flattened, suggesting that the intracellular space was emptied of its contents and that the cell wall deformation could affect spore viability when the cell wall lost its functions that control cell wall permeability and ability to maintain structural rigidity (KIM *et al.*, 2016). Also, with longer exposure treatment time, the recovery of DNA was evaluated through analysis of agarose gel electrophoresis. The results showed a more significant reduction in the band intensity of the treated spores. The reduced amount of DNA in the plasma-treated spores is possibly a result of either degradation or leakage of DNA through the damaged cell wall (KIM *et al.*, 2016).

The purpose of this particular study was to review the effects of ionized hydrogen peroxide (iHP) in the structure of the spores of *B. atrophaeus* and *G. stearothermophilus* by observing its effects using Transmission Electron Microscopy (TEM) and also by

evaluating the existence of DNA damage by fluorescence-based quantitative polymerase chain reaction (qPCR).

2. Materials and Methods

2.1. Sample Preparations for Decontamination

Spores of *B. atrophaeus* (ATCC 9372, Mesa Labs, Lakewood, CA, USA) were grown at 37°C on Tryptic Soy Broth (TSB) Media for 14 days in a shaker incubator at 100 revs/min and *G. stearothermophilus* (ATCC 12980, Mesa Labs, Lakewood, CA, USA) were grown at 56°C on TSB Media for 14 days in a shaker incubator at 100 revs/min. After the incubation period, both samples were centrifuged at 2500 rcf for 20 min at 4°C. The supernatant was discarded, and the pellet was resuspended in Electropure Water (>14 MΩ-cm). This process was repeated four times for each spore type.

Spore quantification was done by serial dilution and inoculation in blood agar plates. The spore counts for *B. atrophaeus* (ATCC 9372) varied between 1.28 x 10^9 to 1.65 x 10^9 per ml, Figure 2-1.

Decontamination samples of the produced spores were created by placing 400µl of spore sample suspensions in 6-well plates and allowed to dry overnight inside a biological safety cabinet (BSC). After drying, the spore samples were stored in a 4°C refrigerator until used for decontamination.

Figure 2-1: B. atrophaeus spore quantification by serial dilution.

Figure 2-2: Placement of decontamination samples inside the animal cage.

Figure 2-3: Measurement of environmental conditions during room decontaminations.

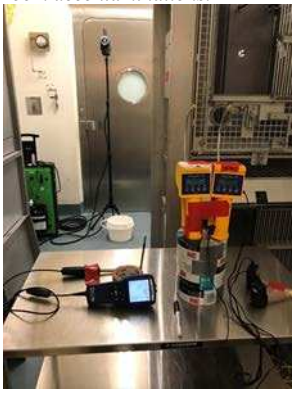

2.2. Decontamination Procedure

A fumigation room with a volume of 880 ft^3 (8ft x 11ft x10ft) was used for the decontamination trials. This gas-tight room has air pressure resistant doors and bioseal dampers to isolate the room during decontamination procedures. Decontamination samples of *B. atrophaeus* and *G. stearothermophilus* were placed inside animal cages(2.75ft x 2.75ft x 7ft) facing away from the ionized hydrogen peroxide (iHP) spray nozzle, as seen in Figure 2-2. Room environmental conditions during decontamination were measured using a temperature and humidity sensor (Velocicalc, Model 9555P, Probe Model 966, TSI Incorporated, Shoreview, MN, USA.), (Figure 2-3). Hydrogen peroxide and ozone levels were measured using a portable gas detector (PortaSens II, Model C16, Analytical Technology, Inc., Collegeville, PA, USA.) with smart sensor modules for ozone (O_3, 1-5 ppm, Part No. H10-00-1008) and hydrogen peroxide (H_2O_2, 10-100 ppm, Part No. H10-00-1042).

Generation of iHP was done with the use of the SteraMist Environmental System equipment (TOMI Environmental Solutions, Beverly Hills, CA, USA) at a rate of 25 ml/min and 20 psi of air pressure through the plasma arc. The total room volume was adjusted to 900 ft^3 for ease of dose calculations, and the disinfection solution used was SteraMist Solution (TOMI Environmental Solutions, Beverly Hills, CA, USA), with 7.8% H_2O_2 at the dose of 0.5 ml per ft^3. Air sampling monitors for measuring concentrations of 0_3 and H_2O_2 were located inside the room, and the bioseal dampers and the door with a pneumatic gasket were closed before the start of the fumigation to provide a gas-tight room. The total spray time per decontamination trial was 18 minutes, and the contact periods that started at the end of the spray times were for 1 hour, 2 hours, 6 hours, and 12 hours. The samples were collected and re-suspended for processing after a 30minute ventilation period of the room. In total, three different decontaminations were done for each contact time.

Validation of decontamination procedures was done by using biological indicators of *B. atrophaeus* (ATCC 9372, Mesa Labs, Lakewood, CA, USA) on Stainless Steel Disk and Tyvek® Envelope (Population $2.2x10^6$, D-Value of 0.7 minutes) and biological indicators of *G. stearothermophilus* (ATCC 12980, Mesa

Labs, Lakewood, CA, USA) on Stainless Steel Disk and Tyvek® Envelope (Population 2.0 x 106, D-Value: 1.7 minutes).

Verification for inactivation of the biological indicators by the decontamination process was done by inoculating the *B. atrophaeus* biological indicators in Soybean Casein Digest Medium (Red Releasat®, RM/100, MesaLabs, Lakewood, CA, USA) and incubated for seven days at 37°C. The verification inactivation of the biological indicators of *G. stearothermophilus* was done by inoculating them in Soybean Casein Digest Medium (Purple Releasat®, PM/100, MesaLabs, Lakewood, CA, USA), and incubated for seven days at 56°C.

2.3. Preparation of Transmission Electron Microscopy Samples

The exposed decontamination samples utilized for Transmission Electron Microscopy (TEM) were re-suspended with 400 µl of a solution of 2% glutaraldehyde plus 2% paraformaldehyde and stored in a 4°C refrigerator. The fixation procedure used was modified from that of Berryman & Rodewald (BERRYMAN & RODEWALD, 1990). Samples were centrifuged, and the pellet was washed three times with 0.1M cacodylate buffer for 10 minutes. Depending on the pellet form and size, agar was added to consolidate the pellet for staining and polymerization.

To stain the pellet, a solution of 1% osmium oxide (OsO_4) was added and set for one hour at room temperature, followed by two washes with distilled water for 5 minutes each. Also, a solution of 2% uranyl acetate was added to stain the pellet, and the sample was placed in a 60°C oven for 20 minutes. After the heating period, three washes were done with 50%, 75%, and 95% ethanol for 10 minutes each. The three stages of diluted ethanol were followed by three washes of the pellet with 100% ethanol for 10 minutes each.

For polymerization, the pellet was washed twice with propylene oxide (PO) for 10 minutes each. Followed by infiltration of 50% PO – 50% Poly/Bed 812 Resin and placed in a rocking table for 1 hour at room temperature. After the 50:50 infiltration period, the solution was removed, and a 25% PO - 75% Poly/Bed 812 Resin was added to the sample for additional infiltration of the resin. The sample was placed in a rocking table for 1 hour at room temperature. After the 25:75%

infiltration period, the solution was removed, and a 100% Poly/Bed 812 Resin was added, the sample was placed in a rocking table for 1 hour at room temperature.

After the first 100% Poly/Bed 812 Resin infiltration period, the pellet was removed from the tube and cut into small sections of approximately two mm^3 and placed in a new tube containing 100% Poly/Bed 812 Resin and set overnight in a rocking table at room temperature. At the end of the overnight infiltration period, the samples were placed in a polymerization tube and set for hardening in a 60°C oven overnight.

After hardening, the hard epoxy resin containing the spore samples were cut into ultrathin sections using a diamond knife and placed into an objective disk and prepared for imaging. TEM images were obtained using a JEOL JEM-1400 microscope (JEOL, Ltd., Tokyo, Japan).

2.4. Preparation of DNA samples

The exposed and non-exposed decontamination samples utilized for DNA extraction were re-suspended with 400 µl of Dulbecco's phosphate buffer saline (DPBS) solution and stored in a minus 20°C freezer for further processing.

Since one of the goals of the study was to evaluate the potential DNA damage caused by the decontamination activity, no mechanical action could be done to the spore samples because of the potential of damaging the DNA as well. Multiple DNA extraction techniques were evaluated (ROSE *et al.*, 2011), and a decision was made to extract DNA, utilizing a protocol with phenol/chloroform/isoamyl alcohol extraction followed by ethanol precipitation. The extraction procedure was modified from Ausubel *et al*. (2003) and Sargent (1980).

The exposed and non-exposed decontamination samples were allowed to thaw on ice, and an equal volume of phenol/chloroform/isoamyl alcohol was added to the sample to initiate the DNA extraction in a 1.5 ml microcentrifuge tube. The samples were vortexed vigorously for 10 sec at room temperature followed by a pulse microcentrifugation at maximum speed (<21,000 rcf) for 15 sec also at room temperature. After the centrifugation process, the top aqueous phase was removed and transferred to a new tube. The transferred quantities varied between 200µl and 300µl.

A salt solution of 3M sodium acetate (pH 5.2), at 1/10 of the volume calculated from the original sample suspension, was added to a vial containing the aqueous phase transferred with the DNA. The solution was mixed by gentle agitation of the tube several times (~10 times). After this, 2 to 2.5 volumes of chilled 100% ethanol (-80°C) calculated after the salt addition was added and mixed by inverting tubes multiple times (~10 times). The tubes with the alcohol and the samples were placed in crushed ice for 30 minutes.

After the cool-down period, the DNA extraction samples were microcentrifuge at 16,000 rcf for 10 minutes at 4°C. The alcohol supernatant was removed, and then one ml of 70% ethanol at room temperature was added to the tubes. The samples were mixed by inverting tubes several times (~10 times) followed by microcentrifugation at 21,000 rcf for 15 minutes at room temperature. The 70% ethanol supernatant was removed, and the tubes with the DNA samples were allowed to dry inside a biosafety cabinet overnight. After the drying period, the DNA was re-suspended with 100 µl of molecular biology grade water (AccuGENE, Cat No. 51200, Lonza, USA), and the DNA concentration and purity were measured by spectrophotometry (NanoDrop, ND-1000, NanoDrop Technologies, Wilmington, DE, USA). The extracted DNA samples were stored in a minus 20°C freezer.

2.5. Quantitative polymerase chain reaction (qPCR) assays

To quantify potential damage to the spore core DNA caused by iHP decontamination, the gene *yaaH* that produces the spore germination protein YaaH was used as a template for the quantitative polymerase chain reaction (qPCR) assays. Quantitative polymerase chain reaction (qPCR) was chosen over gel electrophoresis because this assay can indicate how much of a specific DNA or gene is present in the sample in real-time (THORNTON & BASU, 2015; GARIBYAN & AVASHIA, 2013). In addition, real-time qPCR has been used to identify *G. stearothermophilus* in samples of canned food (NAKANO, 2015) and as a reliable detection method for *B. anthracis* spores (JANSE *et al.,* 2010).

The gene *yaaH* for *B. atrophaeus* (ATCC 9372) has 1,281 bases pair (bp), and for *G. stearothermophilus* (ATCC 12980), it has 1,287 bp. Since there is only a 69% alignment nucleotide similarity between the sequences for the *yaaH* gene in

B. atrophaeus (ATCC 9372) and *G. stearothermophilus*, different primer sets were needed for each spore type. The nucleotide sequence comparison for *G. stearothermophilus yaaH* gene versus the *B. atrophaeus yaaH* gene can be seen in Figure 2-4.

Figure 2-4: Nucleotide sequence comparison for G. stearothermophilus *yaaH gene vs.* B. atrophaeus *yaaH gene.(https://blast.ncbi.nlm.nih.gov/Blast.cgi).*

```
Query: None Query ID: lcl|Query_13655 Length: 1287>
Sequence ID: Query_13657 Length: 1281 Range 1: 583 to 1236
Score:242 bits(267), Expect:4e-67,
Identities:456/660(69%),  Gaps:12/660(1%), Strand: Plus/Plus
Query  598   ATTGTCGCCACCGCCAGACGGTATGGCTTCCGCGACATCCATTTTGATTTTGAATATTTG  657
              ||||| || || || |||   ||||| || || || || |||||||| |||||||| ||
Sbjct  583   ATTGTTGCGACTGCTAGAAAATATGGATTTCGGGATATTCATTTTGACTTTGAATACTTA  642
Query  658   CGCCCGGAAGACCGTGAGGCGTATAATGCGTTTTTGCGCAAAGCGAAACGGCGATTTGA-  716
              || || |||||    || || ||||||  |||| ||||  |||| | |  |  |||| |
Sbjct  643   CGTCCTGAAGATAAAGAAGCCTATAATCAGTTTCTGCGTGAAGCAAGA--GATATTTTAC  700
Query  717   AC-GGGAAGGATGGATGATGTCGACCGCCCTGGCGCCAAAAACGAGCGCCACCCAGCGCG  775
              || ||||||| ||| |||| || || || || || || ||||| || || || ||    |
Sbjct  701   ACAGGGAAGGCTGGCTGATCTCTACGGCACTTGCCCCGAAAACCAGTGCAACTCAAAAAG  760
Query  776   GACGTTGGTACGAAGCCCATGACTACCGCGCCCATGGACAAATTGCCGACTTTGTCGTCA  835
              |    ||||| || || ||||| ||    || || ||| | ||||  |||||||| || |
Sbjct  761   GCAAATGGTATGAGGCTCATGATTATAAGGCTCACGGAGAGATTGTGGACTTTGTTGTGA  820
Query  836   TAATGACGTATGAGTGGGGCTACAGCGGCGGTCC-GCCGATGCCGGTCTCCCCCATCGGC  894
              | ||||| ||||| ||||| || ||||||||||| ||  | ||| || || || || ||
Sbjct  821   TTATGACATATGAATGGGGGTATAGCGGCGGTCCGGCTCAAGCC-GTTTCTCCTATAGGA  879
Query  895   CCTGTCCGCCGTGTCCTCAAGTACGCCGTCTCGGAAATGCCTCCCGGAAAGATTTTAATG  954
              || |||||   |||| |  | || ||  |  | ||||||||| |    || ||  | |||
Sbjct  880   CCCGTCCGGGATGTCATTGAATATGCTTTAACTGAAATGCCTGCAAACAAAATCGTTATG  939
Query  955   GGGCAAAATTTGTATGGTTATGATTGGACACTGCCGTACGTACCG--GGCGGA-CCGTAC  1011
              || || ||||| || || ||||||||||  ||||||||  ||||  ||||||  | ||
Sbjct  940   GGACAGAATTTATACGGATATGATTGGACCTTGCCGTAC--ACCGCTGGCGGAGACCTA-  996
Query  1012  GCCCGCGCCATCAGCCCGCAGCAGGCCATCGCCCTCGCCGCGAAGTATAACGTCGCGATT  1071
              ||    ||  |||| |||||||||| || |  || ||||   |  |||| |  || ||
Sbjct  997   GCGAAAGCTCTCAGTCCGCAGCAGGCGATTGTACTGGCCGGCCAAAATAATGCAGCAATC  1056
Query  1072  GAATACGACACCGAGGCGCAGGCGCCGCATTTTCGCTACCGCGATGAAAACGGGCGCGAG  1131
               |||||||        | ||||| ||    ||||||||   ||||  ||||       ||
Sbjct  1057  CAATACGATGAAACATCTCAGGCTCCCTTCTTTCGCTATACCGATTCAAACAACAAACAG  1116
Query  1132  CACGAAGTATGGTTTGAGGACGCCCGCTCCATTCAGGCAAAATTCAATCTCGTGAAAGAA  1191
              || || |||||||| || ||||| || |||||||| |||||||||||| |  | || |||
Sbjct  1117  CATGAGGTATGGTTCGAAGACGCACGTTCCATTCAAGCAAAATTCAATTTAATTAAGGAA  1176
Query  1192  CTTGGCCTGCGCGGAGTCAGCTATTGGAAACTGGGCTTCGATTTCCCGCAAAACTGGCTG  1251
              ||     |  | ||  |||||||||||||||| ||  ||  ||||||  ||||||||||||
Sbjct  1177  CTGAATTTAAGAGGGATCAGCTATTGGAAACTCGGGCTCTCTTTCCCTCAAAACTGGCTG  1236
```

Preliminary primer selection was considered using NCBI's Primer BLAST tool (YE *et al.*, 2012), and final selections for optimization and validations were made using DNASTAR Lasergene Software (DNASTAR, Inc., Madison, WI, USA) as previously described by Bustin and Huggett and Thornton & Basu (BUSTIN & HUGGETT, 2017; HORNTON & BASU, 2015).

The criteria for primer set selection was that its elongation product could produce both short and long segments of the *yaaH* gene in order to be able to evaluate quantitative damages to the segments (RAYMAEKERS *et al.*, 2009;

FAJARDO-CAVAZOS *et al*., 2010). Also, the short and long primer sets needed to fall within the elongation product of the primers used to generate the plasmids for developing the standard curve for quantification. Since there was no history of the using the *yaaH* gene for quantification of damage and the primer selection needed to be optimized for use, short and long primers were selected in an attempt to match proximity to the 5' end as well as the 3' end of the plasmids to be generated. The list of primer sets identified for this study for the *yaaH* gene of *B. atrophaeus* and *G. stearothermophilus* to be evaluated and optimized for this study are shown in Table 2-1. All primers were purchased from Integrated DNA Technologies (Coralville, IA, USA). For naming purposes, all primer pairs to be analyzed were named using the 5' end position of the corresponding spore *yaaH* gene oligonucleotides as previously described by Fajardo-Cavazos *et al*. (2010).

Table 2-1: List of primer sets for the yaaH gene of B. atrophaeus *and* G. stearothermophilus *to be evaluated and optimized for this study.*

Name	Product Length (bp)	Upper Primer Location (from 5' end)	Lower Primer Location (from 3' end)	To be used to generate
B. atrophaeus – yaaH Gene - Primer Set 1 (BA-*yaaH*-124F, BA-*yaaH*-966R	863	124 .. 147	986 .. 966	Plasmid
B. atrophaeus – yaaH Gene - Primer Set 2 (BA-*yaaH*-171F, BA-*yaaH*-830R)	680	171 .. 191	850 .. 830	Long Segment
B. atrophaeus – yaaH Gene - Primer Set 3 (BA-*yaaH*-314F, BA-*yaaH*-423R)	132	314 .. 332	445 .. 423	Short Segment
B. atrophaeus – yaaH Gene - Primer Set 4 (BA-*yaaH*-314F, BA-*yaaH*-958R)	668	314 .. 332	981 .. 958	Long Segment
B. atrophaeus – yaaH Gene - Primer Set 5 (BA-*yaaH*-730F, BA-*yaaH*-830R)	121	730 .. 749	850 .. 830	Short Segment
G. stearothermophilus – yaaH Gene - Primer Set 1 (GS-*yaaH*-124F, GS-*yaaH*-1188R)	1084	124 .. 140	1207 .. 1188	Plasmid
G. stearothermophilus – yaaH Gene - Primer Set 2 (GS-*yaaH*-85F, GS-*yaaH*-1074R)	1011	85 .. 104	1095 .. 1074	Plasmid
G. stearothermophilus – yaaH Gene - Primer Set 3 (GS-*yaaH*-190F, GS-*yaaH*-724R)	558	190 .. 212	747 .. 724	Long Segment
G. stearothermophilus – yaaH Gene - Primer Set 4 (GS-*yaaH*-190F, GS-*yaaH*-360R)	190	190 .. 212	379 .. 360	Short Segment
G. stearothermophilus – yaaH Gene - Primer Set 5 (GS-*yaaH*-190F, GS-*yaaH*-844R)	678	190 .. 212	867 .. 844	Long Segment
G. stearothermophilus – yaaH Gene - Primer Set 6 (GS-*yaaH*-447F, GS-*yaaH*-844R)	421	447 .. 466	867 .. 844	Long Segment
G. stearothermophilus – yaaH Gene - Primer Set 7 (GS-*yaaH*-804F, GS-*yaaH*-844R)	64	804 .. 827	867 .. 844	Short Segment

The fluorescence-based qPCR methodology of absolute quantification was selected to evaluate any DNA damage to the decontamination samples produced by ionized hydrogen peroxide due to its capacity to detect and measure small amounts of DNA (BUSTIN *et al.*, 2009). This methodology uses a known copy number of standards with a known concentration. This quantification methodology

required multiple experiments to be executed before the evaluation of the decontamination samples could be completed.

First was the development of plasmids for the *yaaH* gene of *B. atrophaeus* and *G. stearothermophilus* to generate a copy number of standards to create a quantitative standard curve to compare with and quantify the potential damage to the DNA. The second set of experiments was the verification of amplification for all short and long primers for the *yaaH* gene of *B. atrophaeus* and *G. stearothermophilus*. The third set of experiments was the optimization of the reaction conditions by optimization of the annealing temperature using a temperature gradient test for selected primers that showed non-optimal results from the verification of the amplification. And the fourth set of experiments was the measurement of the limit of detection (LOD) of the selected primers versus the quantitative standard curve. The fluorescence quantification of possible DNA damage to the spores of *B. atrophaeus* and *G. stearothermophilus* was done using SYBR Green (BIORAD, Hercules, CA, USA) and a real-time thermal cycler C1000 Touch (BIORAD, Hercules, CA, USA).

The optimization and validation of the primers which were used to evaluate the potential damage to the DNA segment encoding the *yaaH* gene of *B. atrophaeus* (ATCC 9372) and *G. stearothermophilus* (ATCC 12980) caused by the decontamination with iHP, were evaluated following the recommendation of Raymaekers, et al. (RAYMAEKERS *et al.,* 2009).

2.5.1. Plasmid development

Plasmids for the selected target gene needed to be created as templates for the absolute quantification of any DNA damage to the decontamination samples produced by iHP. The following primer pair (BA-*yaaH*-124F, BA-*yaaH*-966R) was selected for the *yaaH* gene of *B. atrophaeus* (ATCC 9372) because it amplifies 863 bp fragment from nucleotide 124 to 986. The nucleotide sequence can be seen in Table 2-2. The plasmids were used as a known copy number of standards with a known concentration for quantification in the qPCR reaction.

Table 2-2: Nucleotide sequence for generation of B. atrophaeus *plasmids.*

Primer Set Name	Primer Names	Nucleotide Sequence
BA – yaaH Gene - Primer Set 1	BA-*yaaH*-124F	5' – CCGATTGCAGGACAGTTTTATGAT – 3'
	BA-*yaaH*-966R	5' – CCAGCGGTGTACGGCAAGGTC – 3'

For the *yaaH* gene of *G. stearothermophilus* (ATCC 12980), two primer sets were selected to generate two different plasmids for evaluation. The first primer set (GS-*yaaH*-124F, GS-*yaaH*-1188R) with the nucleotide sequence information shown in Table 2-3, was used to produce GS Plasmid A, amplifying a 1,084 bp fragment from nucleotide 124 to 1207.

Table 2-3: Nucleotide sequence for generation of G. stearothermophilus *plasmid A.*

Primer Set Name	Primer Names	Nucleotide Sequence
GS – yaaH Gene - Primer Set 1	GS-*yaaH*-124F	5' – CAGGCGCTCGTGATTCC – 3'
	GS-*yaaH*-1188R	5' – CTCCGCGCAGGCCAAGTTCT – 3'

The second primer set (GS-*yaaH*-85F, GS-*yaaH*-1074R) with the nucleotide sequence information shown in Table 2-4 was used to produce GS plasmid B, amplifying a 1,011 bp fragment from nucleotide 85 to 1095.

Table 2-4: Nucleotide sequence for generation of G. stearothermophilus *plasmid B.*

Primer Set Name	Primer Names	Nucleotide Sequence
GS – yaaH Gene - Primer Set 2	GS-*yaaH*-85F	5' - GCGAACAAGCTGCCAAATCC – 3'
	GS-*yaaH*-1074R	5' - CGCCTGCGCCTCGGTGTCGTAT – 3'

Each polymerase chain reaction (PCR) for the construction of the plasmids included 10 µl of 2.5X Taq DNA polymerase master mix (5PRIME HotMasterMix, Quantabio, Beverly. MA, USA), 0.25 µl of 20 µM forward primer, 0.25 µl of 20 µM reverse primer and 12.5 µl of molecular grade water and 2 µl of control sample for a 25 µl reaction.

Thermal cycler equipment (Applied Biosystems, Foster City, CA, USA) was used to generate the DNA segments encoding the *yaaH* gene of *B. atrophaeus* (ATCC 9372) and *G. stearothermophilus* (ATCC 12980). The PCR initial process to produce the BA-*yaaH* plasmid (124F, 966R) was done with an initialization temperature of 94°C for 5 minutes, then 35 cycles of denaturation at 94°C for 30 seconds, annealing at 57.5°C for 1 minute and elongation at 72°C for 1 minute. At the end of the 35 repeats, a final elongation

period at 72°C for 7 minutes, then the material remained indefinitely at 4°C. In addition, this PCR process to produce the BA-*yaaH* plasmid (124F, 966R) was repeated using elongation temperatures of 57.7°C, 59°C and 60°C.

The PCR initial process to produce the GS-*yaaH* plasmid A (124F, 1188R) and GS-*yaaH* plasmid B (85F, 1074R) was done with an initialization temperature of 94°C for 5 minutes, then 35 cycles of denaturation at 94°C for 30 seconds, annealing at 59°C for 1 minute and elongation at 72°C for 1 minute. At the end of the 35 repeats, a final elongation period at 72°C for 7 minutes, then the material remained indefinitely at 4°C.

The cloning process for all PCR products to generate the plasmids for this study started with a cloning reaction using 4 µl of the PCR product, 1 µl of salt (1.2 M NaCl; 0.06 M MgCl2) and 1 µl of the TOPO4 vector and was incubated at room temperature for 5 minutes. Both the salt and the TOPO4 vector are provided by the TOPO TA Cloning Kit (Invitrogen, Carlsbad, CA, USA). The second step of the cloning process was the transformation of the *Escherichia coli* chemically competent cells by adding 2 µl of the cloning reaction to the TOP10 One Shot chemically competent cells (Invitrogen, Carlsbad, CA, USA) and incubated on ice for 5 minutes, followed by a 30 seconds heat shock at 42°C, all per manufacturer's instructions.

After the ligation of the PCR product and the transformation of the plasmid in chemically competent *E. coli*, between 10 µl and 100 µl were plated on super optimal broth with batabolite repression (SOC) agar plates with 100 µg/mL ampicillin for selection of cultures and placed in an incubator at 37°C overnight. Samples from the representative colonies were collected and grown in SOC media with 100µg/mL of ampicillin for 24 hrs, and then plasmids were extracted using ZR Plasmid Miniprep – Classic Kit (Zymo Research, Irving, CA, USA) following the manufacturer's instructions.

The plasmids extracted were enzyme digested using the restriction enzyme EcoRI and the EcoRI buffer (New England BioLabs, Inc. Ipswich, MA, USA), and the resulting products were evaluated by electrophoresis for verification of the proper size of the plasmid insert.

2.5.2. Verification of Amplification of the Short and Long primers

The short and long primers for the *yaaH* gene target for *B. atrophaeus* and *G. stearothermophilus* were tested against its corresponding plasmids. Each nucleotide sequence for the short and long primer sets is listed in Table 2-5 for the *B. atrophaeus* primers and in Table 2-6 for the *G. stearothermophilus* primers.

Table 2-5: B. atrophaeus *gene yaaH primers sequence evaluated for this study.*

Primer Set Name	Product Length (bp)	Forward Nucleotide Sequence (5' – 3' direction)	Reverse Nucleotide Sequence (5' – 3' direction)	Optimal Annealing Temp	Melting Temp.
BA *yaaH* Primer Set 2	680bp	GTCCATCGCCCGTCAGTTCAA	CGCCGCTATACCCCCATTCAT	56.6°C	76.7°C
BA *yaaH* Primer Set 3	132bp	AGCCACGCGGAACTCAGGT	TTGTCATCGGGGGCTCTTCTAAA	56.2°C	77.2°C
BA *yaaH* Primer Set 4	668bp	AGCCACGCGGAACTCAGGT	GGTGTACGGCAAGGTCCAATCATA	55.9°C	76.8°C
BA *yaaH* Primer Set 5	121bp	CTTGCCCCGAAAACCAGTGC	CGCCGCTATACCCCCATTCAT	53.9°C	73.0°C

Table 2-6: G. stearothermophilus *gene yaaH primer sequence evaluated for this study.*

Primer Set Name	Product Length (bp)	Forward Nucleotide Sequence (5' – 3' direction)	Reverse Nucleotide Sequence (5' – 3' direction)	Optimal Annealing Temp	Melting Temp.
GS *yaaH* Primer Set 3	558bp	ATTGCCCGCCGGTTTTCCATTCC	CAGGGCGGTCGACATCATCCATCC	62.3°C	81.6°C
GS *yaaH* Primer Set 4	190bp	ATTGCCCGCCGGTTTTCCATTCC	CTTCGCGGGCGCTTGCTTCC	61.9°C	81.6°C
GS *yaaH* Primer Set 5	678bp	ATTGCCCGCCGGTTTTCCATTCC	ACCGCCGCTGTAGCCCCACTCATA	62.4°C	82.1°C
GS *yaaH* Primer Set 6	421bp	GCCGCCGCTTGACGACTTTC	ACCGCCGCTGTAGCCCCACTCATA	60.4°C	81.2°C
GS *yaaH* Primer Set 7	64bp	CGCCCATGGACAAATTGCCGACTT	ACCGCCGCTGTAGCCCCACTCATA	55.2°C	71.8°C

The qPCR cycle for the verification of the short primers was done with an initialization temperature of 95°C for 3 minutes, then 40 cycles of denaturation at 95°C for 5 seconds, annealing at 56.0°C for 30 seconds and followed by a plate read. The qPCR cycle for the verification of the long primers was done with an initialization temperature of 95°C for 3 minutes, then 40 cycles of

denaturation at 95°C for 5 seconds, annealing at 58.0°C for 1 minute and followed by a plate read. The experiments were performed using SYBR Green (BIORAD, Hercules, CA, USA) utilizing a real-time thermal cycler C1000 Touch equipment (BIORAD, Hercules, CA, USA).

2.5.3. Optimization of Reaction Conditions

A group of primers was selected from the verification of the amplification process to optimize the reaction conditions. A temperature gradient test was done to identify the best annealing temperature conditions of the qPCR test. The experiments were performed using SYBR Green (BIORAD, Hercules, CA, USA) utilizing a real-time thermal cycler C1000 Touch equipment (BIORAD, Hercules, CA, USA).

The qPCR cycling conditions for optimization of the short primers of *B. atrophaeus* and *G. stearothermophilus* was done with an initialization temperature of 95°C for 3 minutes, then 40 cycles of denaturation at 95°C for 5 seconds, then gradient annealing temperatures of 54.0°C, 54.7°C, 56.0°C, 57.9°C, 60.4°C, 62.3°C, 63.5°C, and 64.0°C for 20 seconds each followed by a plate read. At the end of the cycle, a melt curve test of 65°C to 95°C with increments of 0.5°C for 5 seconds was done.

The qPCR cycling conditions for optimization of the long primers of *B. atrophaeus* and *G. stearothermophilus* was done with an initialization temperature of 95°C for 3 minutes, then 40 cycles of denaturation at 95°C for 5 seconds, then gradient annealing temperatures of 56.0°C, 56.7°C, 58.0°C, 60.0°C, 62.4°C, 64.3°C, 65.5°C, and 66.0°C for 40 seconds each followed by a plate read.

At the end of the cycles, both temperature gradient tests included a melt curve analysis of 65°C to 95°C with increments of 0.5°C for 5 seconds to review the effectiveness of each primer with different annealing temperature and the detection of primer dimers.

2.5.4. Measurement of the Limit of Detection (LOD)

Assays of the limit of detection (LOD) were performed using SYBR Green (BIORAD, Hercules, CA, USA) utilizing a real-time thermal cycler C1000 Touch equipment (BIORAD, Hercules, CA, USA).

Plasmids generated for the *B. atrophaeus* and *G. stearothermophilus* spores were selected for the qPCR assays as a template. The concentration of the chosen plasmids was measured using a NanoDrop Spectrophotometer (NanoDrop Technologies, Wilmington, DE, USA). With that concentration, the initial gene copy quantity was estimated to calculate the standard curve of 10-fold serial dilutions. In order to improve the accuracy of the LOD in the qPCR analysis, three technical replicates (n=3) were used from these serial dilutions (FOROOTAN *et al.*, 2017; STOKDYK *et al.*, 2016).

3. Results

3.1. Transmission Electron Microscopy (TEM)

The results of the visual verification of the effects in the structure of the spores of *B. atrophaeus* caused by the iHP decontamination process at different decontamination times (Control, 1hr, 2hrs, 6hrs, 12hrs) can be observed in the following micrographs, where different spore structures can be seen. These are the Outer Spore Coat (OC), the Inner Spore Coat (IC), the Cortex (CT), the Inner Membrane (IM), and the Core (CO) were the DNA resides. Arrows indicate the location of the damage.

The following micrographs in Figure 2-5, Figure 2-6, and Figure 2-7 present views of the damage to the spore structures caused by the decontamination process with iHP at different exposure times. All figures start with Panel A, which shows the spore structures of non-exposed control samples. Panel B shows the initial damages to the OC after one hour of decontamination. The two-hour decontamination results are shown in Panel C, where damage can be observed to the OC and the IC. Panel D shows the result of the six-hour decontamination cycle where damages to both spore coats and some initial effects in the IM are observed. The effects of the 12-hour decontamination can be seen in Panel E, where damage can be seen to IM accompanied by the release of CO material. Figure 2-5 presents a view of a whole spore. Figure 2-6, presents a higher magnification of the outer layers of the spores and Figure 2-7, presents a higher magnification of the inner membranes and the core.

Figure 2-5: Progression of decontamination effects of iHP in the spores of B. atrophaeus*. (A) non-exposed; (B) 1hr exposure; (C) 2 hrs exposure; (D) 6 hrs exposure; (E) 12 hrs exposure. OC – Outer Spore Coat, IC – Inner Spore Coat, CT – Cortex, IM – Inner Membrane, CO – Core.*

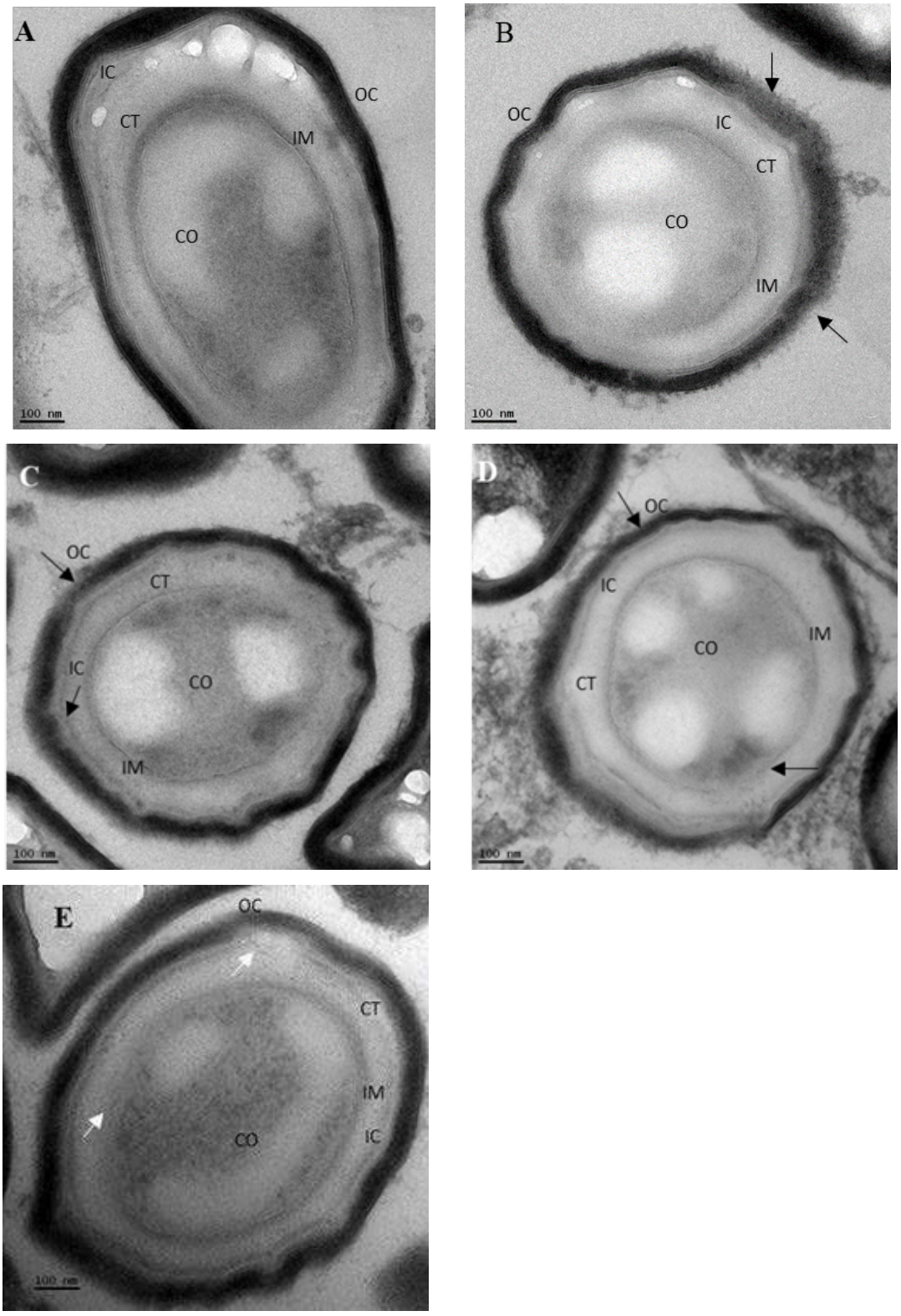

Figure 2-6: Progression of decontamination effects of iHP in the spore coat of B. atrophaeus *spores. (A) Non-exposed control; (B) 1hr exposure; (C) 2 hrs exposure; (D) 6 hrs exposure; (E) 12 hrs exposure. SC – Outer Spore Coat, IC – Inner Coat, CT – Cortex, IM – Inner Membrane, CO – Core.*

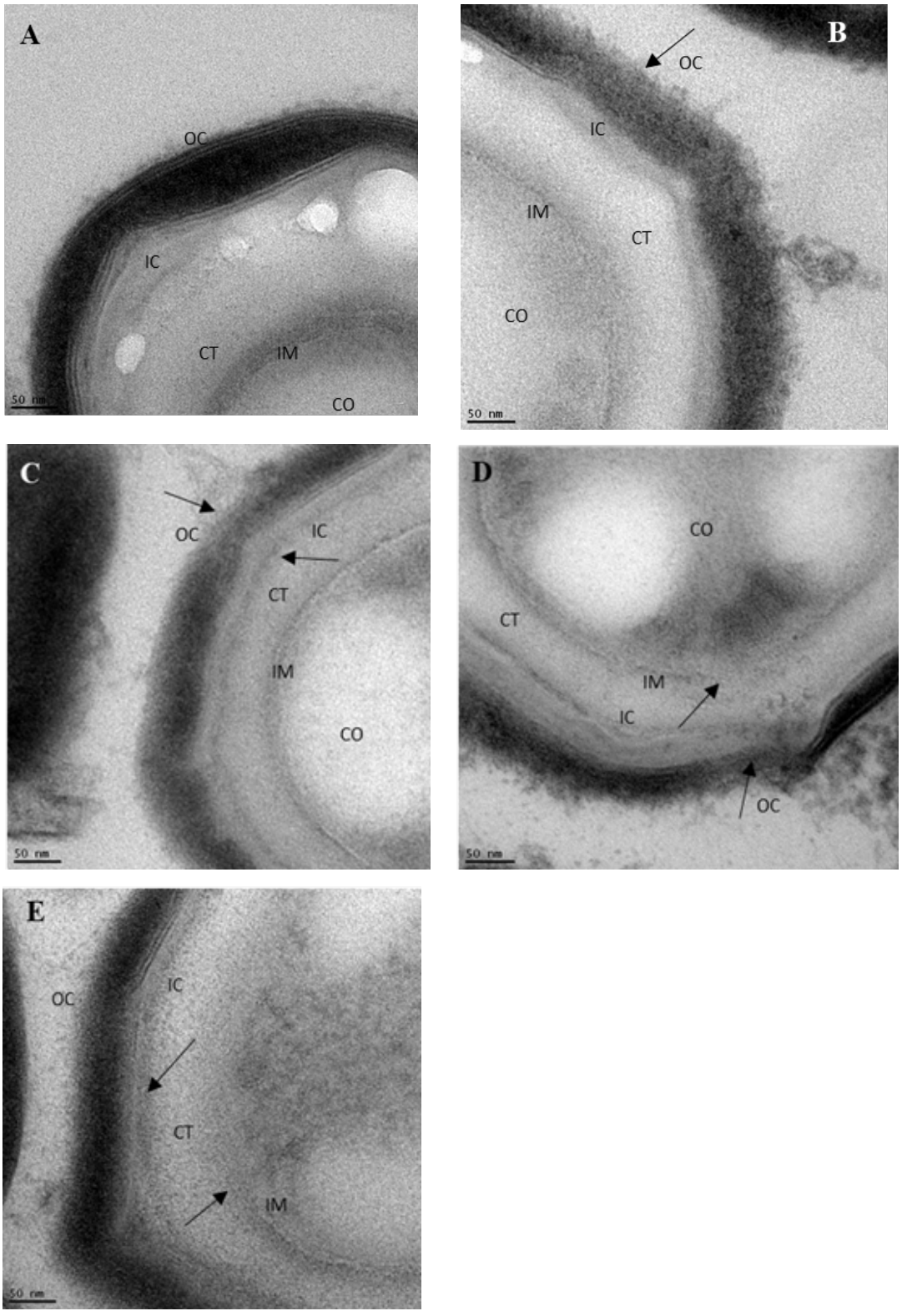

Figure 2-7: Progression of decontamination effects of iHP in the spore coat of B. atrophaeus *spores. (A) Non-Exposed Control; (B) 1hr exposure; (C) 2 hrs exposure; (D) 6 hrs exposure; (E) 12 hrs exposure. SC – Outer Spore Coat, IC – Inner Coat, CT – Cortex, IM – Inner Membrane, CO – Core.*

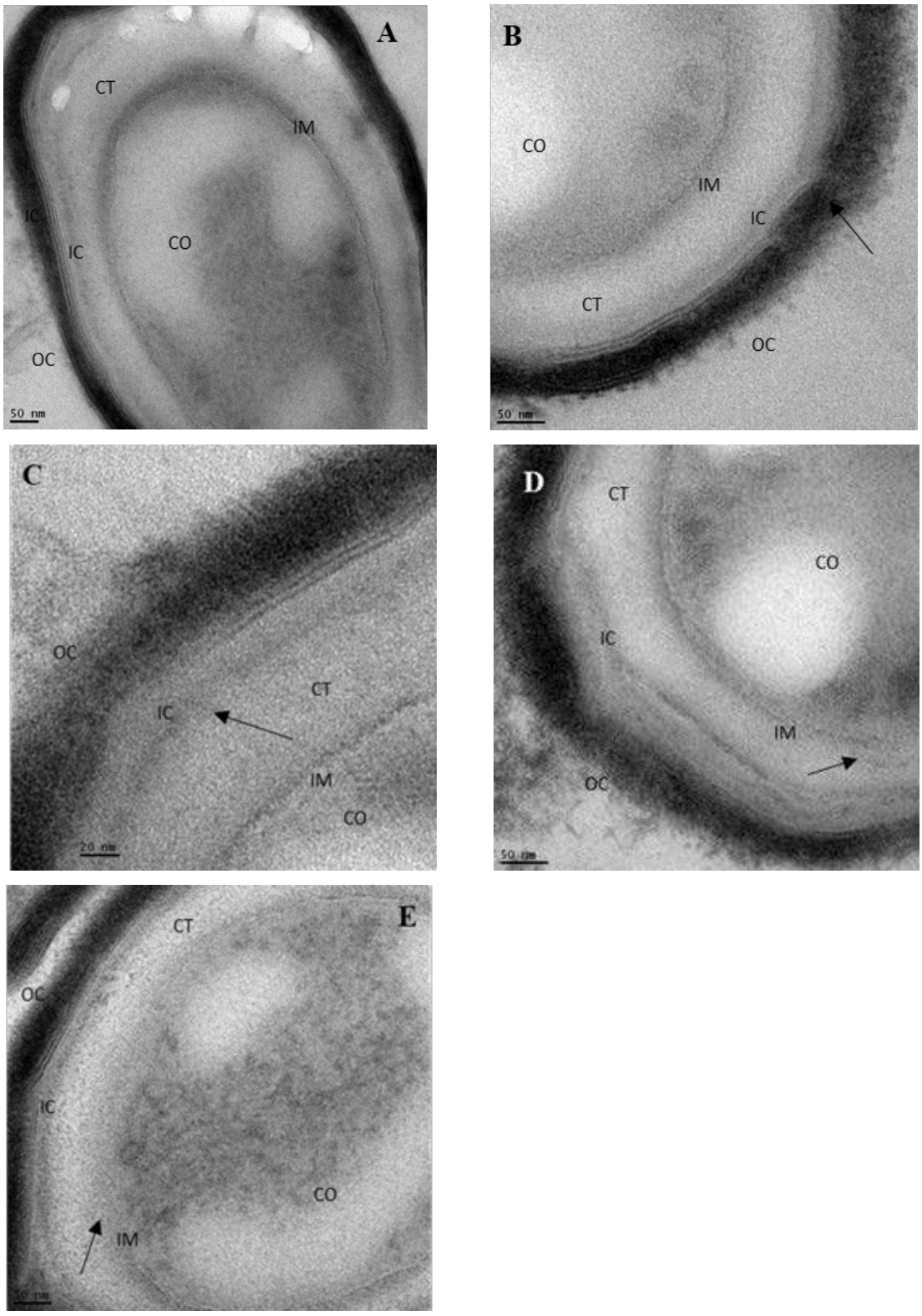

The micrograph of spores of *G. stearothermophilus* after the decontamination process in Figure 2-8 shows the damage to the spore after 12-hour decontamination with iHP, which is consistent with the results of the *B. atrophaeus* spores.

Figure 2-8: View of Geobacillus stearothermophilus *spore after iHP decontamination with 12 hours contact time. (A) Arrows indicate damages to the spore coat and the inner membrane; (B) Arrow indicate damage to the inner membrane and release of core material; (C) Arrows indicate damages to the spore coat and the inner membrane, also show the release of core material; (D) Arrow shows the release of the core material. SC – Outer Spore Coat, IC – Inner Coat, CT – Cortex, IM – Inner Membrane, CO – Core.*

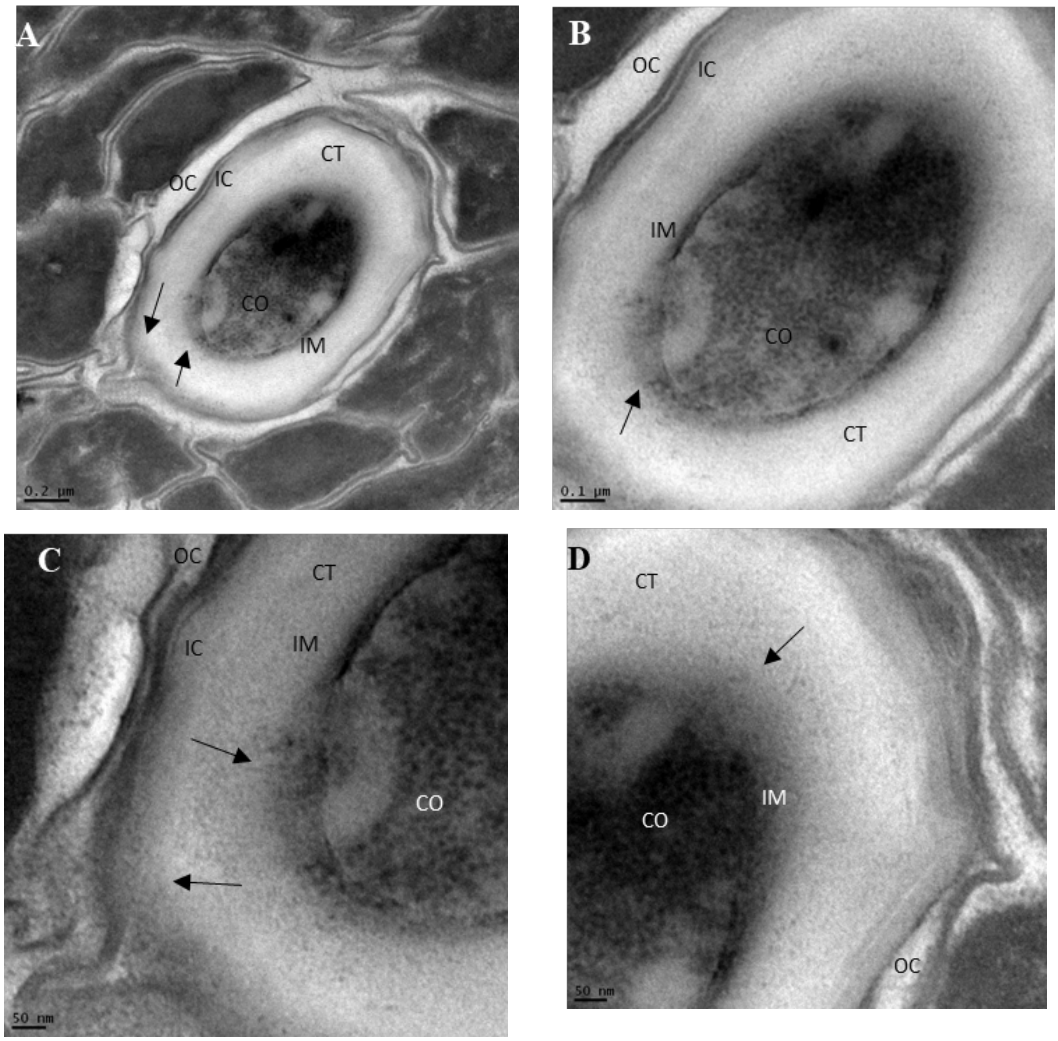

3.2. Quantitative Polymerase Chain Reaction (qPCR) assays

3.2.1. Plasmid Development

The PCR products using template DNA extracted from the non-exposed samples for each spore type and BA Primer Set 1 (BA-*yaaH*-124F, BA-*yaaH*-966R), GS Primer Set 1 (GS-*yaaH*-124F, GS-*yaaH*-1188R) and GS Primer Set 2 (GS-*yaaH*-85F, GS-*yaaH*-1074R) were analyzed by gel electrophoresis, and the results are presented in Figure 2-9.

Figure 2-9: Results of the verification of amplicons by gel electrophoresis for primers of yaaH gene of B . atrophaeus (BA) and G. Stearothermophilus (GS). Lane 1-100bp Ladder, Lane 2 BA yaaH (124F,966R) #26, Lane 3 BA yaaH (124F,966R)#27, Lane 4- Negative control (124F,966R), Lane 5 - GS yaaH (124F, 1188R)#62A, Lane 6 - GS yaaH (124F, 1188RR)#61A, Lane 7 – Negative Control (124F, 1188R), Lane 8 - GS yaaH (85F, 1074R)#62B, Lane 9 - GS yaaH (85F, 1074R)#61B, Lane 10 – Negative Control (85F, 1074R).

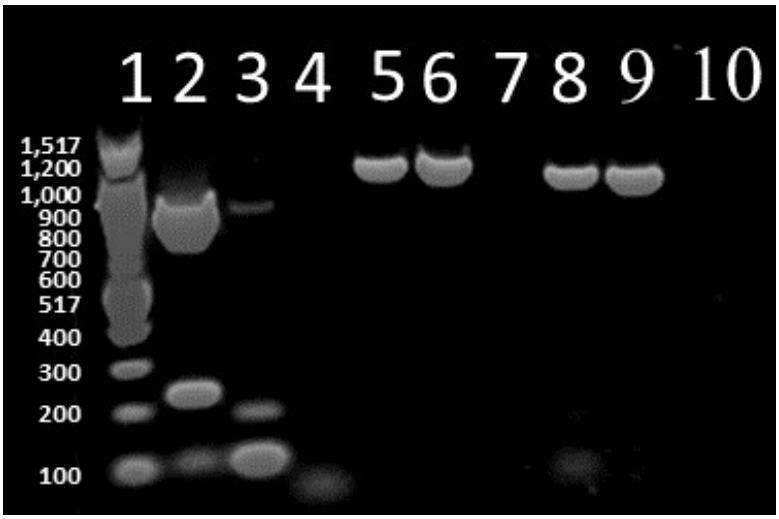

The PCR reaction from the BA Primer Set 1 (BA-*yaaH*-124F, BA-*yaaH*-966R) produced multiple bands in the gel electrophoresis analysis. Therefore the segment of the lane that created the appropriate product size was excised from the gel to evaluate its possibility to produce the BA *yaaH* plasmid.

The PCR product was extracted from the gel by using the QIAquick Gel Extraction Kit (QIAGEN, Germantown, MD, USA). The resultant product was cloned into One Shot Top10 chemically competent *E. coli* and plated on SOC agar plates with 100 µg/mL of ampicillin. The product evaluated did not produce any cell colonies The PCR product from GS Primer Set 1 (GS-*yaaH*-124F, GS-*yaaH*-1188R) and GS Primer Set 2 (GS-*yaaH*-85F, GS-*yaaH*-

1074R) that was cloned into One Shot Top10 chemically competent *E. coli* and plated on SOC agar plates with 100 µg/mL of ampicillin which resulted in the appropriate colonies.

Because no viable cloned *E. coli* cells were produced from the initial cloning attempt with BA Primer 1, the PCR process was repeated with extracted DNA of non-exposed *B. atrophaeus* spores and the BA Primer Set 1 (BA-*yaaH*-124F, BA-*yaaH*-966R) using increased annealing temperatures of 57.5°C, 59°C, and 60°C. The results of the PCR process were analyzed by gel electrophoresis (Figure 2-10).

Figure 2-10: Results of the verification of amplicons by gel electrophoresis for primers of yaaH gene of B . atrophaeus (BA) using different annealing temperatures. Lane 1-100bp Ladder, Lane 2 BA yaaH (124F,966R) at 57.5°C, Lane 3 Negative control (124F,966R), Lane 4- BA yaaH (124F,966R) at 59°C, Lane 5 - Negative control (124F,966R), Lane 6 - BA yaaH (124F,966R) at 60°C, Lane 7 – Negative control (124F,966R).

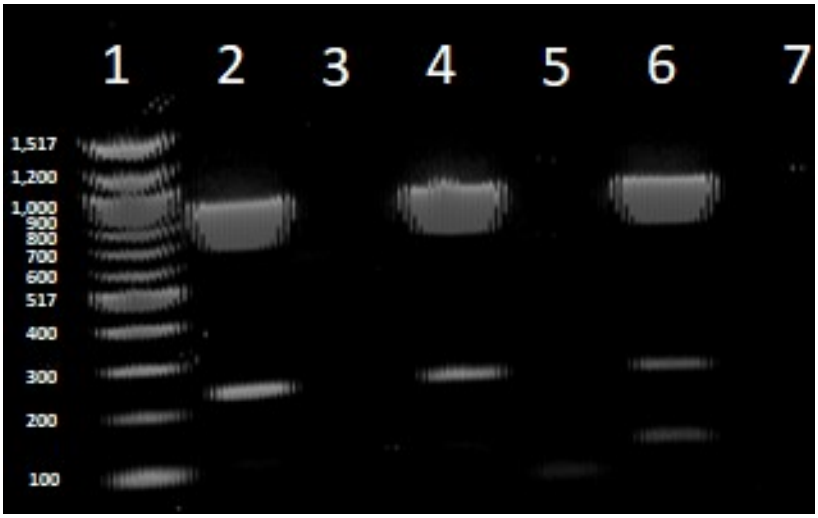

The PCR products from the different annealing temperatures were cloned into One Shot Top10 chemically competent *E. coli* and plated on SOC agar plates with 100 µg/mL of ampicillin to produce the appropriate colonies.

A single colony for each cloning of the PCR product was picked, and they were grown in SOC media with 100 µg/mL of ampicillin. The plasmids were extracted from the resultant overnight culture and enzyme digested using the restriction enzyme. Gel electrophoresis was used to analyze the resultant

plasmid product of the restriction enzyme digestion to verify the proper size of the plasmid inserts (Figure 2-11).

Figure 2-11: Size verificaction using gel eletrophoresis of the resultant plasmid product for the yaaH gene of B. atrophaeus (BA) and G. stearothermophilus (GS) after restriction enzyme digestion. Lane 1 - 100bp ladder, Lane 2 – BA plasmid DHB 100-I, Lane 3 - BA plasmid DHB 100-II, Lane 4 - BA plasmid DHB 100-III, Lane 5 - BA plasmid DHB 100-IV, Lane 6 - BA plasmid DHB 100-V, Lane 7 - BA plasmid DHB 100-VI, Lane 8 - BA plasmid DHB 100-VII, Lane 9 - BA plasmid DHB 50-I, Lane 10 - BA plasmid DHB 50-II, Lane 11 - BA plasmid 1A-1, Lane 12 - BA plasmid 1A-2, Lane 13 – GS plasmid 61B-I, Lane 14 - GS plasmid 61B-2, Lane 15 - GS plasmid 61B-3, Lane 16 - GS plasmid 61A-1, Lane 17 - GS plasmid 61A-2, Lane 18 - GS plasmid 61A-3.

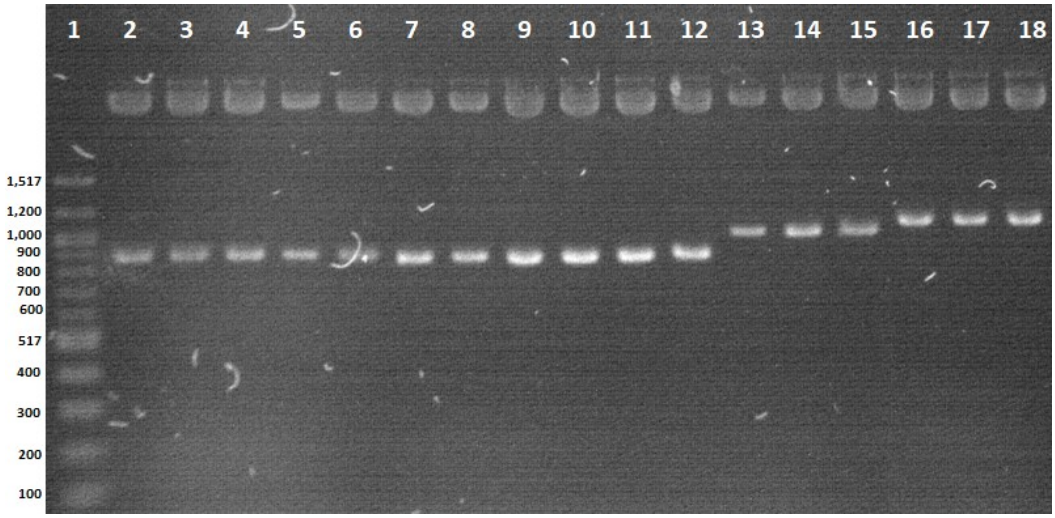

From the gel electrophoresis analysis, plasmids "BA Plasmid DHB100-VI", "GS Plasmid 61A-2", and "GS Plasmid 61B-2" were selected for this study as templates for the quantitative analysis of potential DNA damage.

3.2.2. Verification of Amplification of the Short and Long primers

Long and short primer sets for *B. atrophaeus* were verified utilizing plasmid "BA Plasmid DHB100-VI", and the long and short primer sets *G. stearothermophilus* was confirmed using both plasmids "GS Plasmid 61A-2" and "GS plasmid 61B-2" to determine if these primers were able to produce the proper amplification without producing subproducts such as primer dimers.

Figure 2-12 shows the visual amplification results in relative fluorescence units (RFU), and cycle amplification number (Cq) of the *B. atrophaeus* short primers BA *yaaH* Primer Set 3, BA *yaaH* Primer Set 5 and the *G. stearothermophilus* short primers GS *yaaH* Primer Set 4 and GS *yaaH* Primer

Set 7. The quantitative data results can be seen in Table 2-7 for *B. atrophaeus* short primers and in Table 2-8 for the *G. stearothermophilus* short primers.

Figure 2-12: Amplification curve of short primers BA yaaH primer Set 3, BA yaaH primer Set 5, GS yaaH primer Set 4, and GS yaaH primer Set 7 for the selection of short primers for analysis of decontamination test samples of B. atrophaeus and G. stearothermophilus *DNA.*

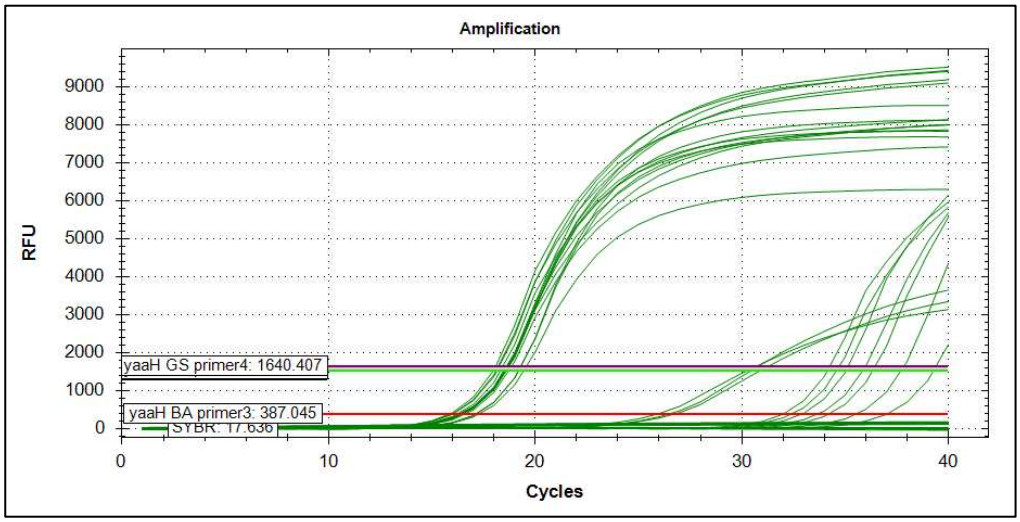

Table 2-7: Results of the verification of Short and Long primers for the yaaH gene of B. atrophaeus *versus the plasmid "BA Plasmid DHB100-VI".*

Primer Set Name	Target Lenght	Plasmid	Fluorescence	Sample Cq Mean Value	NTC Cq Mean Values
BA *yaaH* Primer Set 2	Long	BA Plasmid DHB100-VI	SYBR	18.57	0.00, 36.87, 38.39
BA *yaaH* Primer Set 3	Short	BA Plasmid DHB100-VI	SYBR	26.43	0.00, 0.00, 0.00
BA *yaaH* Primer Set 4	Long	BA Plasmid DHB100-VI	SYBR	18.55	38.84, 37.91, 37.16
BA *yaaH* Primer Set 5	Short	BA Plasmid DHB100-VI	SYBR	18.51	34.58, 35.05, 34.15

Table 2-8: Results of the verification of short and long primers for the yaaH gene of G. stearothermophilus *versus the plasmids "GS Plasmid 61A-2" and "GS plasmid 61B-2."*

Primer Set Name	Target	Plasmid	Fluorescence	Sample Cq Mean Value	NTC Cq Mean Values
GS *yaaH* Primer Set 3	Long	GS Plasmid 61A-2	SYBR	16.81	36.78, 36.67, 36.53
GS *yaaH* Primer Set 4	Short	GS Plasmid 61A-2	SYBR	18.64	0.00, 0.00, 39.40
GS *yaaH* Primer Set 5	Long	GS Plasmid 61A-2	SYBR	17.27	0.00, 0.00, 0.00
GS *yaaH* Primer Set 6	Long	GS Plasmid 61A-2	SYBR	17.14	0.00, 0.00, 0.00
GS *yaaH* Primer Set 7	Short	GS Plasmid 61A-2	SYBR	19.32	37.76, 36.38, 35.92
GS *yaaH* Primer Set 3	Long	GS plasmid 61B-2	SYBR	16.29	36.78, 36.67, 36.53
GS *yaaH* Primer Set 4	Short	GS plasmid 61B-2	SYBR	18.19	0.00, 0.00, 39.40
GS *yaaH* Primer Set 5	Long	GS plasmid 61B-2	SYBR	16.61	0.00, 0.00, 0.00
GS *yaaH* Primer Set 6	Long	GS plasmid 61B-2	SYBR	16.55	0.00, 0.00, 0.00
GS *yaaH* Primer Set 7	Short	GS plasmid 61B-2	SYBR	18.60	37.76, 36.38, 35.92

Figure 2-13 shows the visual amplification results in RFU, and cycle amplification number (Cq) of the *B. atrophaeus* long primer BA *yaaH* Primer Set 2, BA *yaaH* Primer Set 4 and the *G. stearothermophilus* long primers GS *yaaH* Primer Set 3, GS *yaaH* Primer Set 5 and GS *yaaH* Primer Set 6. The quantitative data results can be seen in Table 2-7 for *B. atrophaeus* long primers and in Table 2-8 for the *G. stearothermophilus* long primers.

Figure 2-13: Amplification curve of long primers BA yaaH Primer Set 2, BA yaaH Primer Set 4, GS yaaH Primer Set 3, GS yaaH Primer Set 5 and GS yaaH Primer Set 6 for the selection of long primers for analysis of decontamination test samples of B. atrophaeus and G. stearothermophilus DNA.

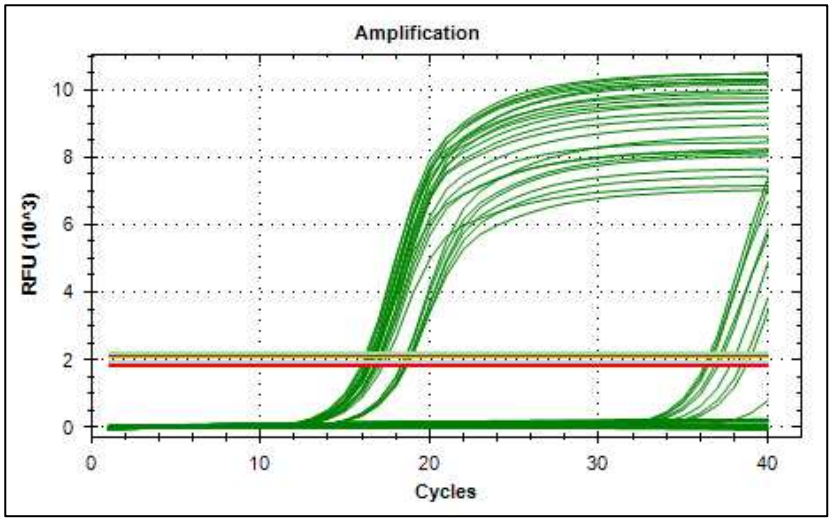

The results of the verification of the primers for *yaaH* gene of *B. atrophaeus* showed that BA *yaaH* Primer Set 2, BA *yaaH* Primer Set 3, BA *yaaH* Primer Set 4, and BA *yaaH* Primer Set 5 needed to be optimized before they could be used, because BA *yaaH* primers 2, 4 and 5 produced primer dimmers in the control sample (NTC) and BA *yaaH* Primer Set 3 had a delayed start in the quantification as evidenced by the increased Cq value compared to the other BA *yaaH* primers. It was determined that all *B. atrophaeus* primers needed to be optimized.

In addition, the results of the verification for the *yaaH* gene of *G. stearothermophilus* showed that good amplification both in the detection of the fluorescent signal crossing the background threshold (Cq value) and the lack of

developing primer dimers for GS *yaaH* Primer Set 6. Primer sets GS *yaaH* Primer Set 4 and GS *yaaH* Primer Set 5 were also suitable, although one of the NTC samples Cq value was observed on the last quantification cycle (39.40) in one of the three technical replicates. It was determined that only *G. stearothermophilus* primers GS *yaaH* Primer Set 3 and GS *yaaH* Primer Set 7 needed to be optimized.

Also, since both *G. stearothermophilus* plasmids (61A-2 and 61B-2) resulted in similar Cq outputs, GS plasmid 61A-2 was selected for further use along with BA plasmid DHB100-VI for the *B. atrophaeus* samples.

3.2.3. Optimization of Reaction Conditions

The selected primers and plasmids from the verification of the amplification process were optimized by temperature gradient test to identify the best annealing temperature conditions to run the qPCR test. The resultant data of the temperature gradient test for selected short and long primers of the *yaaH* gene of *B. atrophaeus* can be seen in Table 2-9.

Table 2-9: Optimization results of B. atrophaeus *for both short and long primers for the yaaH Gene that needed a more detailed optimization analysis.*

Primer Set Name	Target Lenght	Plasmid	Temperature (°C)	Sample Cq Values	NTC Cq Mean Values
BA *yaaH* Primer Set 2	Long	BA Plasmid DHB100-VI	66.0	17.14, 17.66	0.00, 0.00
			65.5	18.24, 17.73	36.14, 0.00
			64.3	17.25, 18.01	0.00, 0.00
			62.4	17.76, 17.65	38.47, 37.06
			60.0	18.29, 18.24	0.00, 0.00
			58.0	18.60, 18.71	0.00, 0.00
			56.7	18.93, 18.24	0.00, 0.00
			56.0	19.38, 19.47	0.00, 0.00
BA *yaaH* Primer Set 3	Short	BA Plasmid DHB100-VI	64.0	20.24, 20.59	0.00, 0.00
			63.5	20.32, 20.56	0.00, 0.00
			62.3	20.14, 20.17	0.00, 0.00
			60.4	20.44, 20.83	0.00, 0.00
			57.9	21.24, 22.05	0.00, 0.00
			56.0	23.67, 23.85	0.00, 0.00
			54.7	24.06, 24.39	0.00, 0.00
			54.0	24.23, 25.09	0.00, 0.00
BA *yaaH* Primer Set 4	Long	BA Plasmid DHB100-VI	66.0	18.27, 18.63	0.00, 36.88
			65.5	19.21, 18.15	0.00, 0.00
			64.3	18.18, 21.33	36.55, 0.00
			62.4	18.10, 18.44	0.00, 37.58
			60.0	18.61, 18.74	0.00, 0.00
			58.0	20.04, 18.60	0.00, 0.00
			56.7	20.83, 18.52	38.79, 37.60
			56.0	18.83, 19.45	0.00, 37.41
BA *yaaH* Primer Set 5	Short	BA Plasmid DHB100-VI	64.0	16.49, 16.44	34.83, 34.69
			63.5	16.40, 35.27	34.24, 33.33
			62.3	15.98, 16.08	33.93, 34.29
			60.4	16.10, 16.78	32.84, 33.94
			57.9	15.76, 15.95	35.43, 34.31
			56.0	15.78, 16.00	35.10, 34.43
			54.7	15.73, 15.66	35.41, 33.19
			54.0	15.88, 27.29	0.00, 33.51

The resultant data of the temperature gradient test for selected short and long primers of the *yaaH* gene of *G. stearothermophilus* can be seen in Table 2-10.

Table 2-10: Optimization results of G. stearothermophilus *for both short and long primers for the yaaH Gene that needed a more detailed optimization analysis.*

Primer Set Name	Target	Plasmid	Temperature	Sample Cq Mean Value	NTC Cq Mean Values
GS *yaaH* Primer Set 3	Long	GS Plasmid 61A-2	66.0	18.15, 0.00	0.00, 0.00
			65.5	18.66, 18.22	0.00, 0.00
			64.3	18.30, 17.75	0.00, 0.00
			62.4	18.04, 18.07	0.00, 0.00
			60.0	18.13, 17.82	0.00, 0.00
			58.0	17.78, 18.30	0.00, 0.00
			56.7	18.04, 18.09	0.00, 39.04
			56.0	18.59, 18.32	0.00, 0.00
GS *yaaH* Primer Set 7	Short	GS Plasmid 61A-2	64.0	18.19, 18.27	37.02, 37.42
			63.5	18.08, 17.92	35.72, 34.93
			62.3	17.71, 17.56	35.30, 35.22
			60.4	17.53, 37.19	35.59, 36.02
			57.9	17.40, 17.32	34.72, 36.16
			56.0	17.25, 17.21	34.73, 34.91
			54.7	17.18, 17.22	34.45, 35.52
			54.0	17.30, 34.27	34.84, 36.79

The visual results of the short and long primer gradient tests can be seen in Figure 2-14 and Figure 2-15, respectively.

Figure 2-14: Gradient annealing temperature test for short primers BA yaaH Primer Set 3 and GS yaaH Primer Set 4 against BA Plasmid DHB100-VI and GS Plasmid 61A-2. (A) Plate setup, (B) Amplification graph with Cq value, (C) Melt Curve (D) Melt Peak.

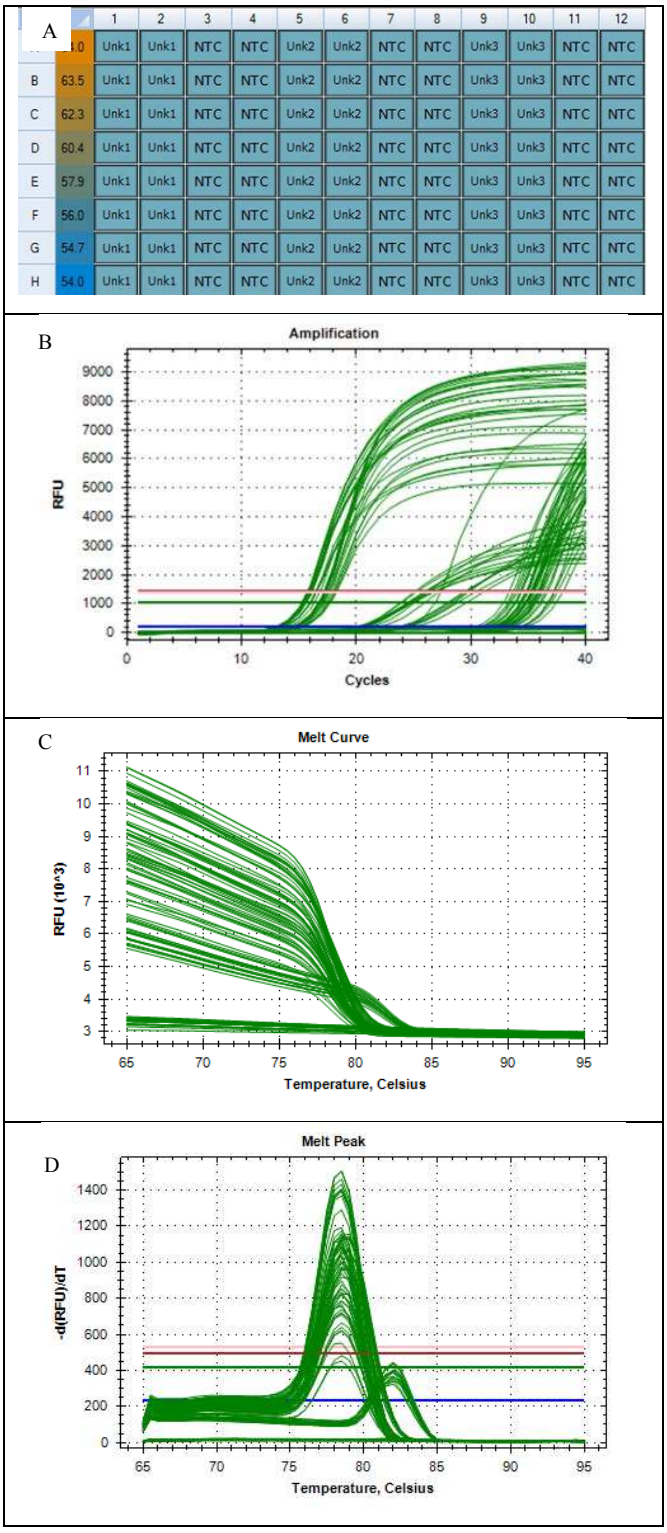

Figure 2-15: Gradient annealing temperature test for long primers BA yaaH Primer Set 2 and GS yaaH Primer Set 5 against BA Plasmid DHB100-VI and GS Plasmid 61A-2. (A) Plate setup, (B) Amplification graph with Cq value, (C) Melt Curve (D) Melt Peak.

A

		1	2	3	4	5	6	7	8	9	10	11	12
A	66.0	Unk1	Unk1	NTC	NTC	Unk2	Unk2	NTC	NTC	Unk3	Unk3	NTC	NTC
B	65.5	Unk1	Unk1	NTC	NTC	Unk2	Unk2	NTC	NTC	Unk3	Unk3	NTC	NTC
C	64.3	Unk1	Unk1	NTC	NTC	Unk2	Unk2	NTC	NTC	Unk3	Unk3	NTC	NTC
D	62.4	Unk1	Unk1	NTC	NTC	Unk2	Unk2	NTC	NTC	Unk3	Unk3	NTC	NTC
E	60.0	Unk1	Unk1	NTC	NTC	Unk2	Unk2	NTC	NTC	Unk3	Unk3	NTC	NTC
F	58.0	Unk1	Unk1	NTC	NTC	Unk2	Unk2	NTC	NTC	Unk3	Unk3	NTC	NTC
G	56.7	Unk1	Unk1	NTC	NTC	Unk2	Unk2	NTC	NTC	Unk3	Unk3	NTC	NTC
H	56.0	Unk1	Unk1	NTC	NTC	Unk2	Unk2	NTC	NTC	Unk3	Unk3	NTC	NTC

B

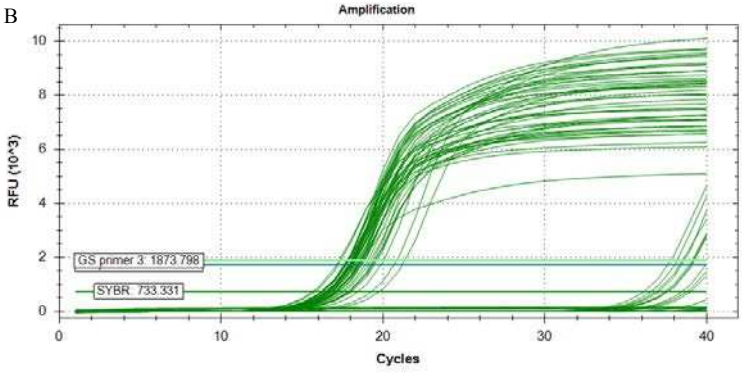

C

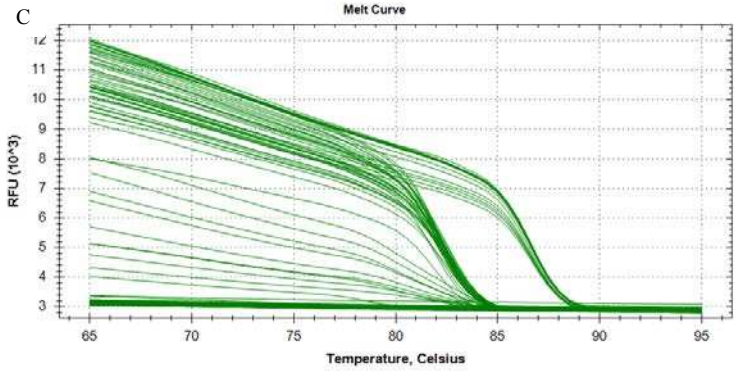

D

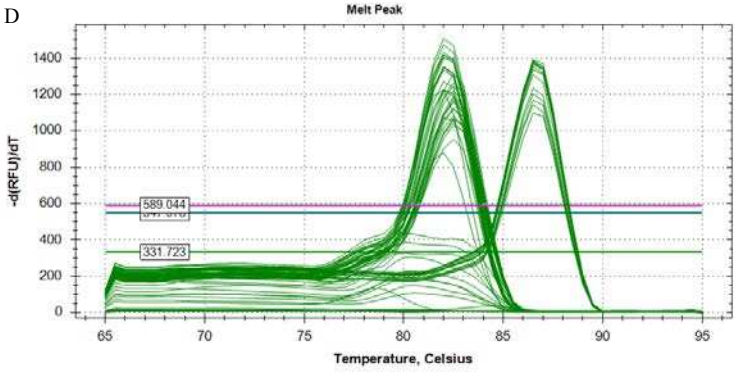

The results of the initial analysis during verification of the primers and the analysis of the gradient temperature test provided a reference to run all qPCR plates using the same annealing temperature of 60°C but modifying the annealing time to 20 seconds for the short primers and 40 seconds for the long primers.

The qPCR thermal cycling conditions that were elected to evaluate the decontamination cycles were a hold temperature of 95°C for 3 minutes, followed by 45 cycles at 95°C for 5 seconds an annealing temp of 60°C for 20 seconds for the short primers and 40 seconds for the long primers. The melt curve analysis was done from 65°C to 95°C.

Even though other primers were suitable for the analysis of the samples, the final selected pairs of primers for each bacteria type can be seen in Table 2-11.

Table 2-11: Selected primer sets for the evaluation of decontamination samples.

Type	Primer Set Name	Product Length
Short *B. atrophaeus* Primer	BA *yaaH* Primer Set 3	132bp
Long *B. atrophaeus* Primer	BA *yaaH* Primer Set 2	680bp
Short *G. stearothermophilus* Primer	GS *yaaH* Primer Set 4	190bp
Long *G. stearothermophilus* Primer	GS *yaaH* Primer Set 5	678bp

3.2.4. Measurement of the Level of Detection (LOD)

Plasmids “BA plasmid DHB 100-VI” with a concentration of 277.1 ng/µl and insert size of 863 bp and “GS plasmid 61A-2” with a concentration of 153.8 ng/µl and insert size of 1084 bp were selected for the qPCR assays as a template. It was calculated that plasmid “BA plasmid DHB 100-VI” had $5.24x10^{10}$ molecules per µl and “GS plasmid 61A-2” had $2.78\ x10^{10}$ molecules per µl. The standard curve consisting of 10-fold serial dilutions of the stock concentration was made after this calculation. Three technical replicates were used for each standard. The results of the limit of detection (LOD) experiments can be seen in Table 2-12.

Table 2-12: Results of the limit of detection (LOD) for the BA yaaH Primer Set 2, BA yaaH Primer Set 3, GS yaaH Primer Set 4, GS yaaH Primer Set 5.

Primer name	**Efficiency**	**R^2**	**Slope**	**y-Intercept**
BA *yaaH* Primer Set 2	83.8%	0.965	-3.783	41.347
BA *yaaH* Primer Set 3	69.4%	0.946	-4.371	49.035
GS *yaaH* Primer Set 4	101.0%	0.975	-3.299	37.687
GS *yaaH* Primer Set 5	73.6%	0.977	-4.177	43.409

The visual results of the limit of detection tests can be seen in Figure 2- 16 and Figure 2-17, respectively.

Figure 2- 16: Visual result of the limit of detection (LOD) experiment of the short primers for the yaaH gene of B. atrophaeus *(BA yaaH Primer Set 3) and* G. stearothermophilus*(GS yaaH Primer Set 4). Panel A- Amplification cycle, Panel B – Standard Curve for quantification, Panel C – Melt Curve, Panel D- Melt Peak.*

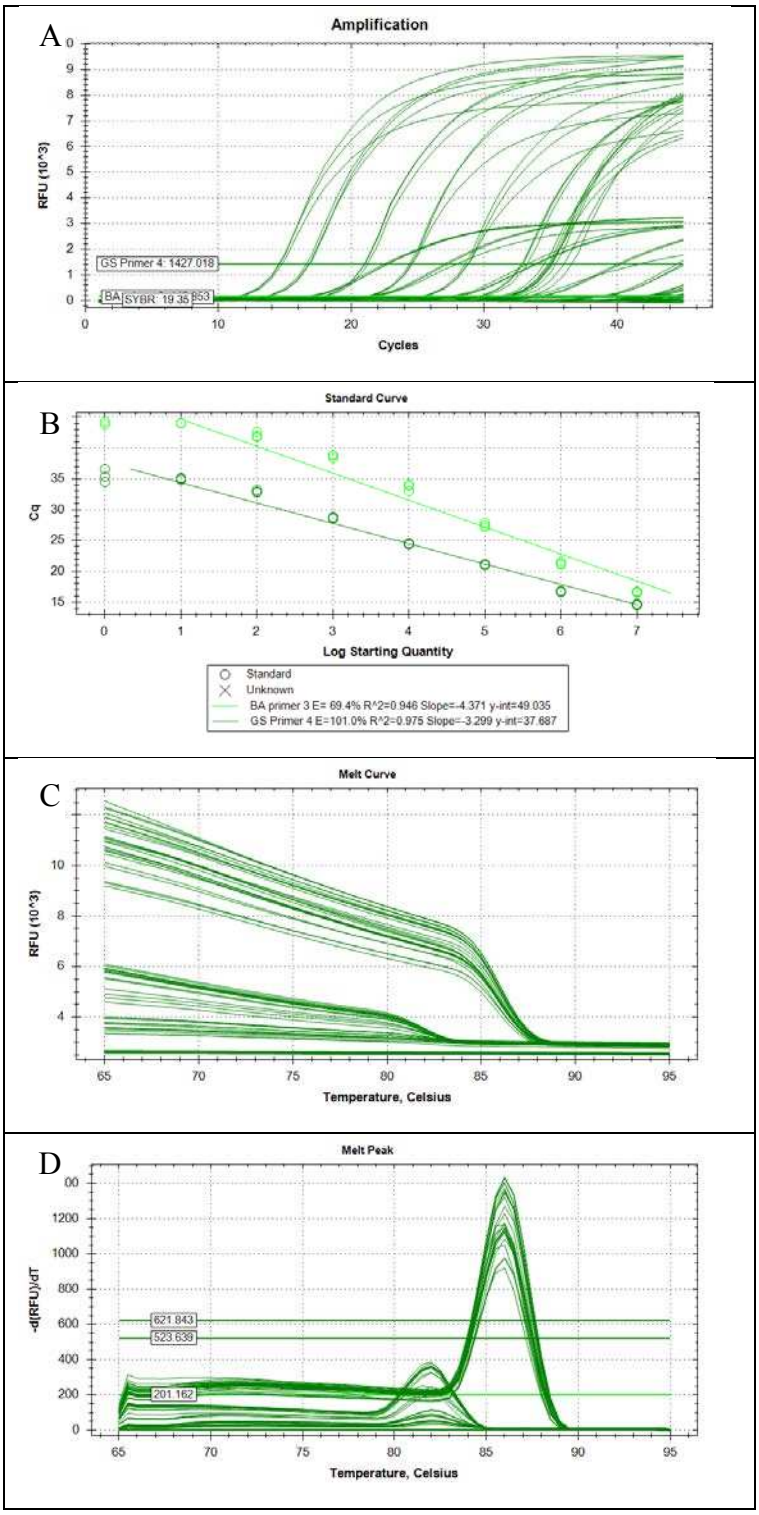

Figure 2-17: Visual result of the Limit of Detection (LOD) experiment of the Long primers for the yaaH gene of Bacillus atrophaeus (BA yaaH Primer Set 2) and Geobacillus stearothermophilus (GS yaaH Primer Set 5). *Panel A- Amplification cycle, Panel B – Standard Curve for quantification, Panel C – Melt Curve, Panel D- Melt Peak.*

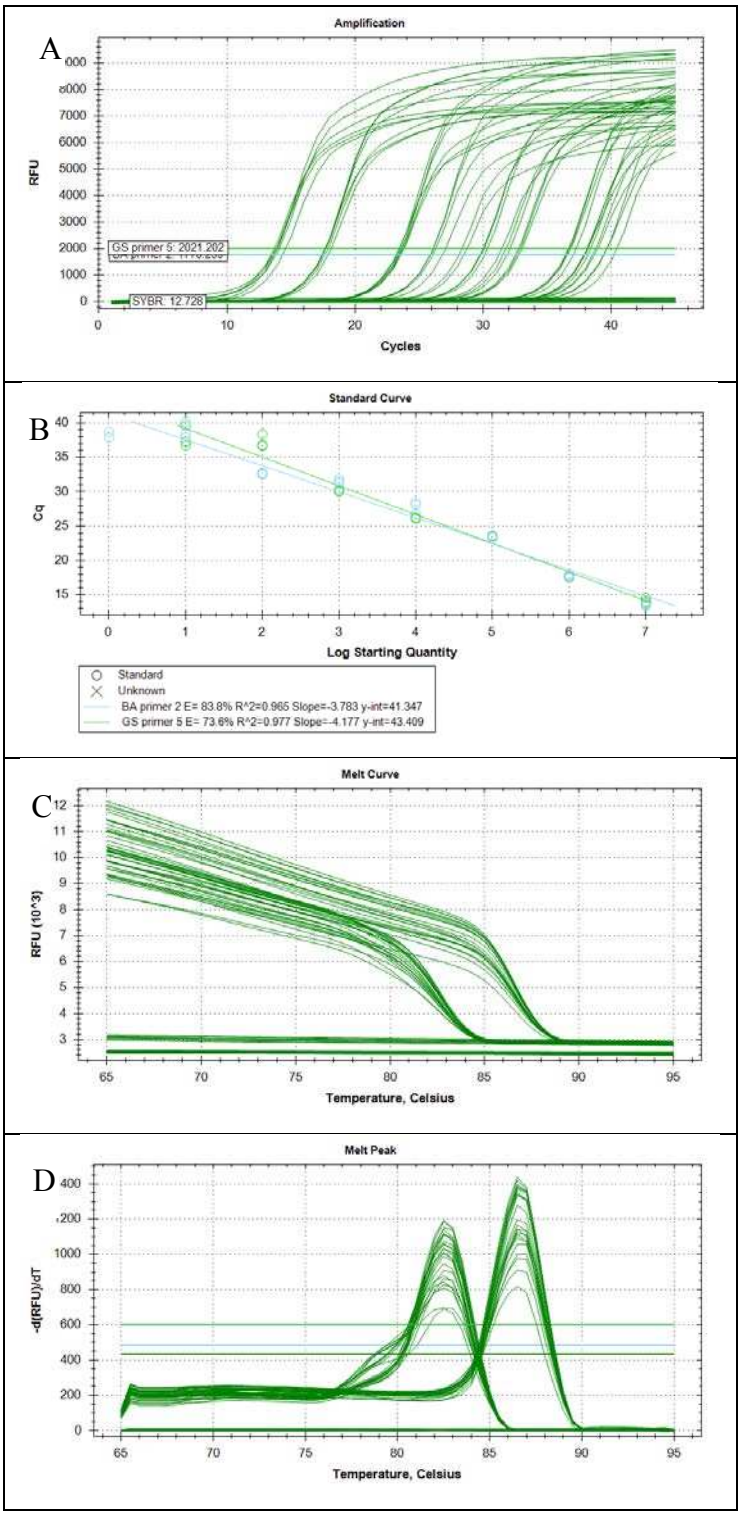

It was determined that the primer sets BA *yaaH* Primer Set 2, BA *yaaH* Primer Set 3, GS *yaaH* Primer Set 4, and GS *yaaH* Primer Set 5 provided an adequate limit of detection (LOD) to be able to quantify the potential damage to the DNA caused by the iHP decontamination process in the *yaaH* gene of *B. atrophaeus* and *G. stearothermophilus*.

3.2.5. Quantitative Analysis of Decontamination Samples

All samples used for the analysis of DNA damage resulted from three different decontamination tests for each contact time. DNA was extracted from at least three samples for each decontamination trial. For fluorescence-based qPCR analysis, all samples tested were run with three technical triplicates. The number of samples analyzed by qPCR can be seen in Table 2-13.

Table 2-13: Number of Decontamination samples per contact time of 1 hour, 2 hours, 6 hours, and 12 hours analyzed by qPCR.

Decontamination Test	*Bacillus atrophaeus* Number of Samples Analyzed per Contact time	*Geobacillus stearothermophilus* Number of Samples Analyzed per Contact time
Test 1	N = 6	N = 6
Test 2	N = 6	N = 6
Test 3	N = 3	N = 3

The exclusion criteria used from qPCR results were made by looking at the melt curve produced by each sample product. The samples that did not generate an appropriate melt curve were excluded from the qPCR analysis (PRYOR & WITTWER, 2006; RUIJTER *et al.*, 2019). Representative visual results of the qPCR analysis to quantify the damage to the DNA of the *B. atrophaeus* spores at the different decontamination tests of the can be seen in Figure 2-18 and Figure 2-19.

Figure 2-18: Representative visual results of the qPCR analysis for DNA damage on the decontamination samples of the B. atrophaeus spores using the short primer "BA yaaH Primer Set 3". Panel A- Amplification cycle, Panel B – Standard Curve for quantification, Panel C – Melt Curve, Panel D- Melt Peak.

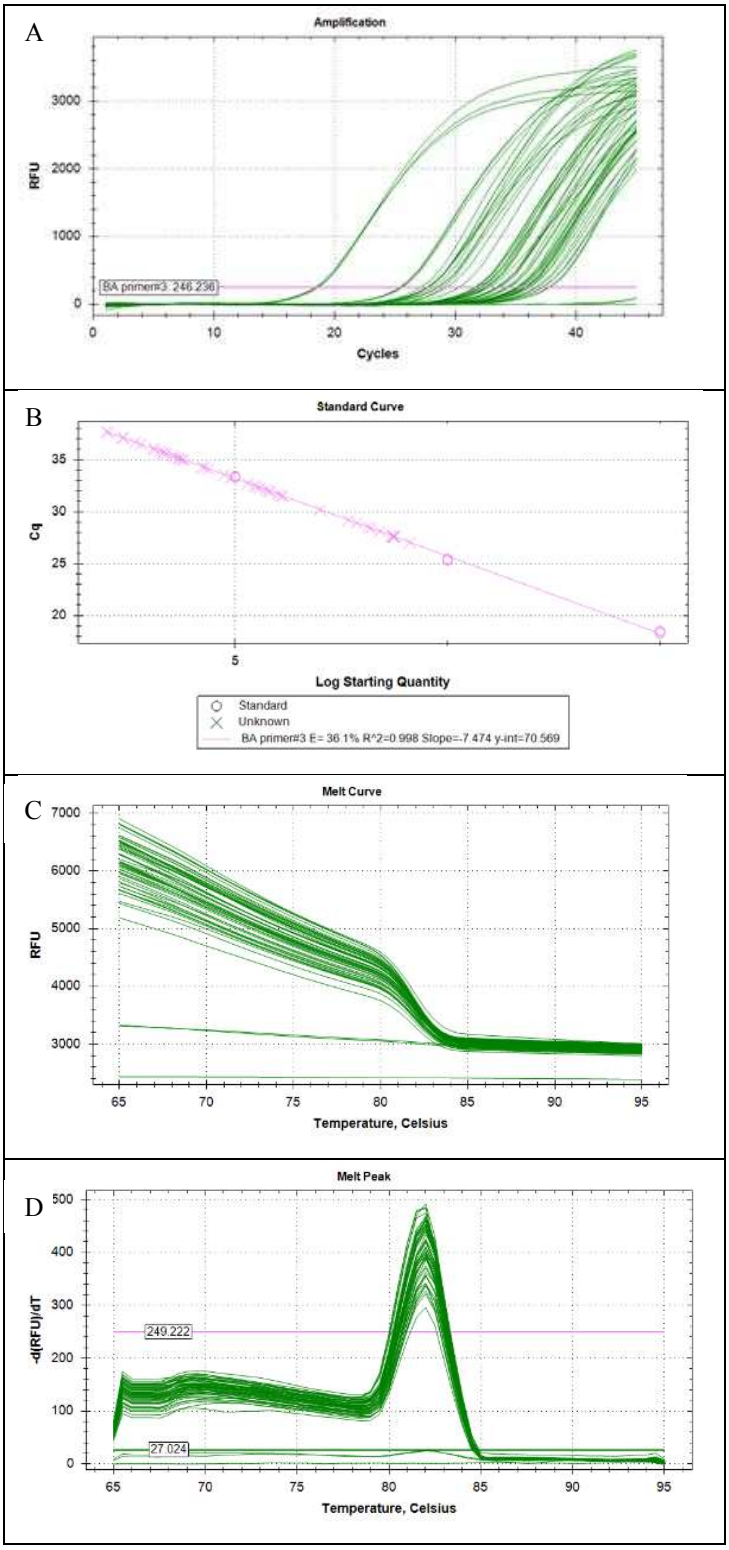

Figure 2-19: Representative visual results of the qPCR analysis for DNA damage on the decontamination samples of the B. atrophaeus *spores using the long primer "BA yaaH Primer Set 2". Panel A- Amplification cycle, Panel B – Standard Curve for quantification, Panel C – Melt Curve, Panel D- Melt Peak.*

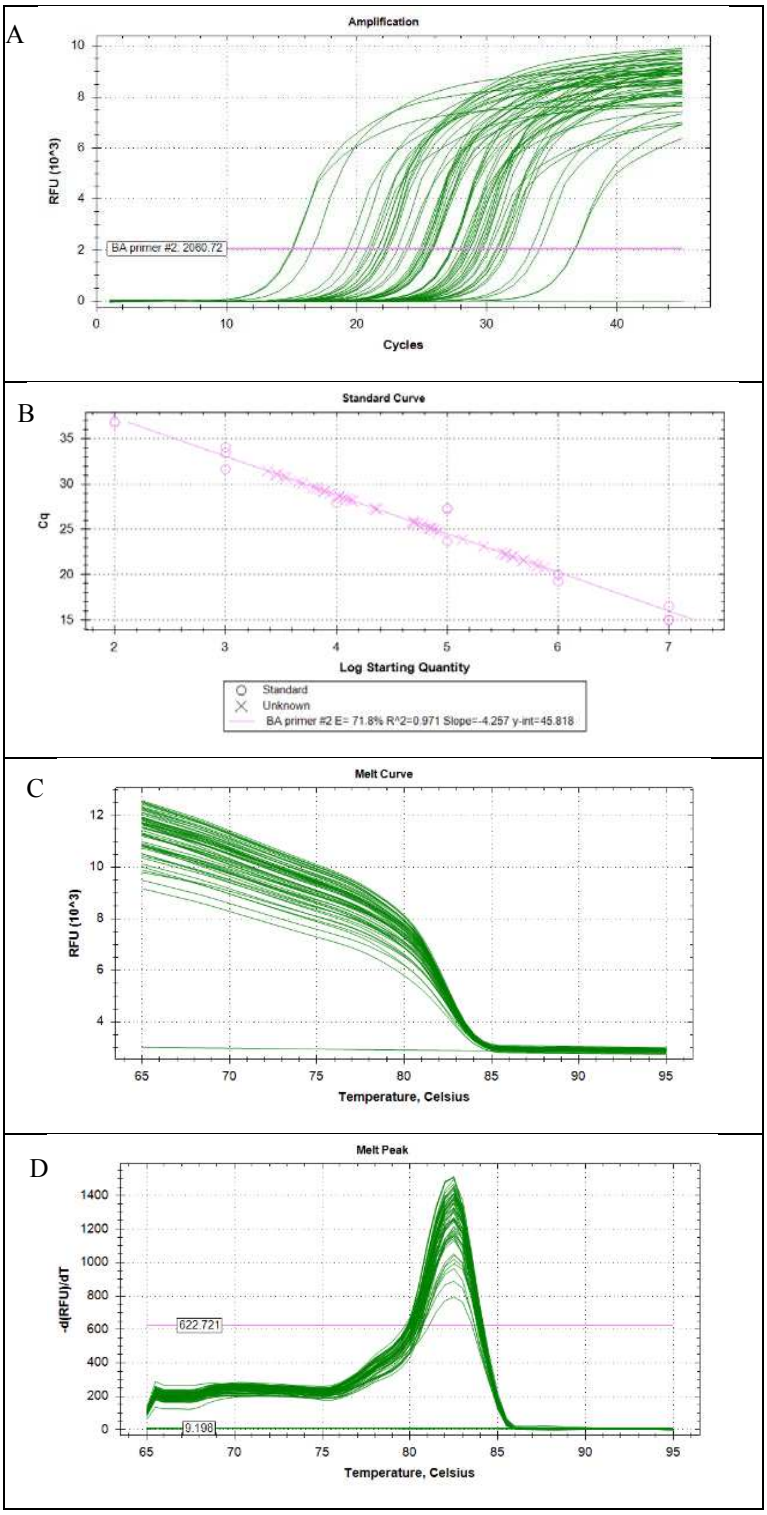

Representative visual results of the qPCR analysis to quantify the damage to the DNA of the *G. stearothermophilus* spores at the different decontamination tests of the can be seen in Figure 2-20 and Figure 2-21.

Figure 2-20: Representative visual results of the qPCR analysis for DNA damage on the decontamination samples of the G. stearothermophilus spores using the short primer "GS yaaH Primer Set 4". Panel A- Amplification cycle, Panel B – Standard Curve for quantification, Panel C – Melt Curve, Panel D- Melt Peak.

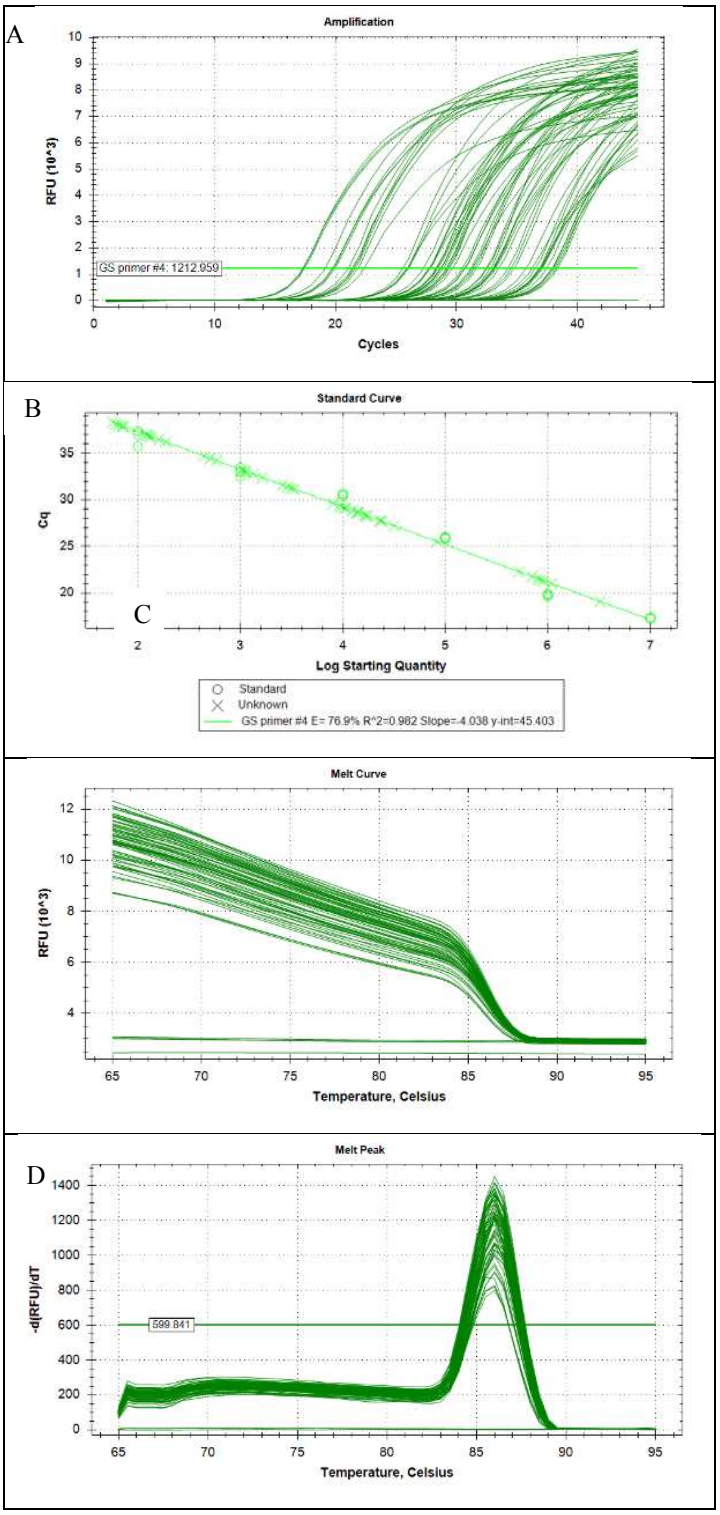

Figure 2-21: Representative visual results of the qPCR analysis for DNA damage on the decontamination samples of the G. stearothermophilus spores using the long primer "GS yaaH Primer Set 5". Panel A- Amplification cycle, Panel B – Standard Curve for quantification, Panel C – Melt Curve, Panel D- Melt Peak.

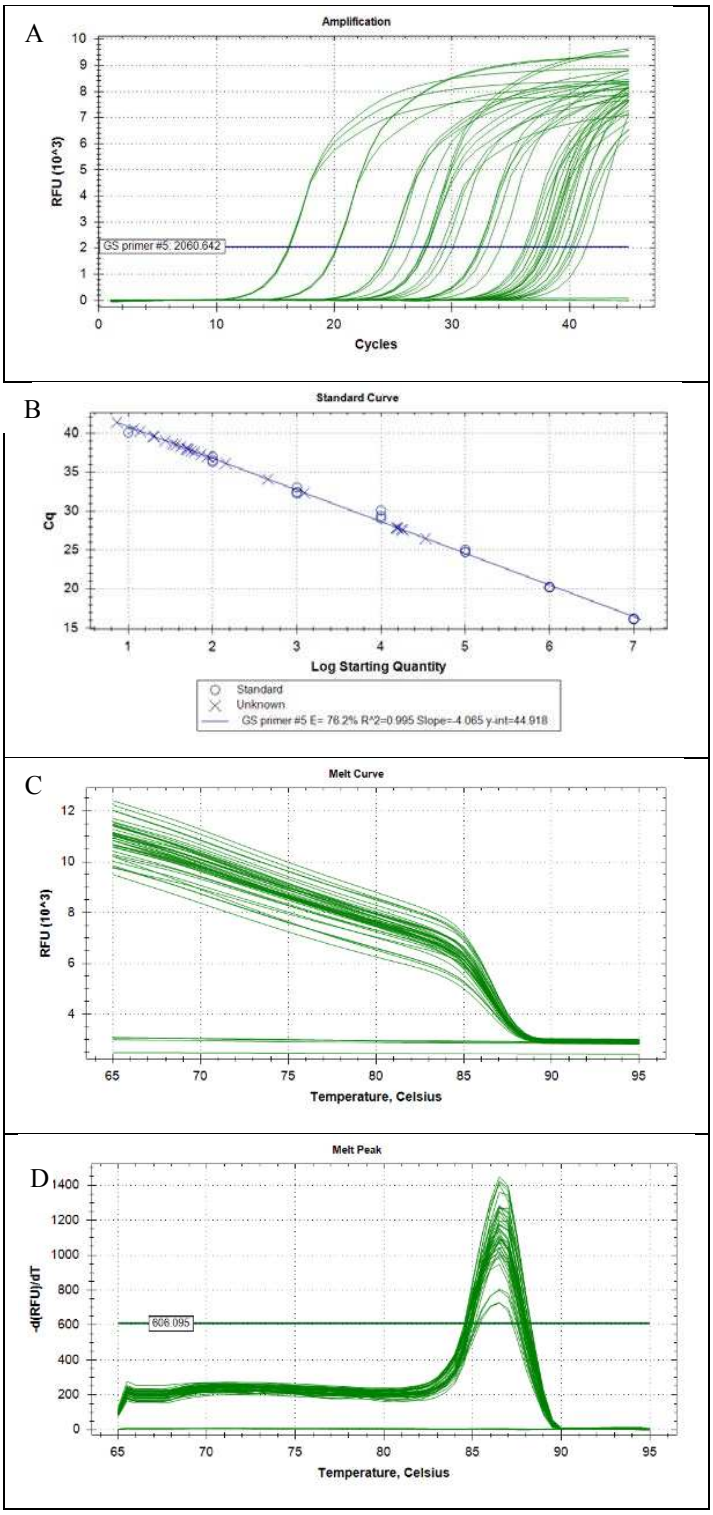

The compiled quantitative result of the damage caused to the DNA of the *B. atrophaeus* spores can be seen in Table 2-14 and Figure 2-22. The effects of the decontamination to short DNA segment (132bp) of the *yaaH* gene using "BA *yaaH* Primer Set 3" presents a linear degradation starting at approximately 489,000 copies and ending on 49,600 copies. On the other hand, the damage to the long DNA segment (680bp) of the *yaaH* gene using "BA *yaaH* Primer Set 2" presents biphasic mode, starting with approximately 392,000 copies with a very rapids degradation for the 1-hour decontamination, followed by a plateau or refractory effect in damage for the 2 hours, then another rapid deterioration for the 6 hours and a plateau in degradation for the 12 hours decontamination ending in approximately 181,000 copies.

Table 2-14: Quantification data of the qPCR analysis for DNA damage on the decontamination samples of the B. atrophaeus spores. Data are presented as the median with interquartile range.

iHP Decontamination Time	Quantification of Short (132bp) DNA segment using "BA *yaaH* Primer Set 3"	Quantification of Long (680bp) DNA segment using "BA *yaaH* Primer Set 2"
Control	489,096	392,229
1 hour	265,833	58,525
2 hours	126,673	59,967
6 hours	87,614	20,412
12 hours	49,600	18,114

Figure 2-22: Results of the qPCR analysis to the damage to the yaaH gene of the Bacillus atrophaeus spores. Data are presented as the median with interquartile range.

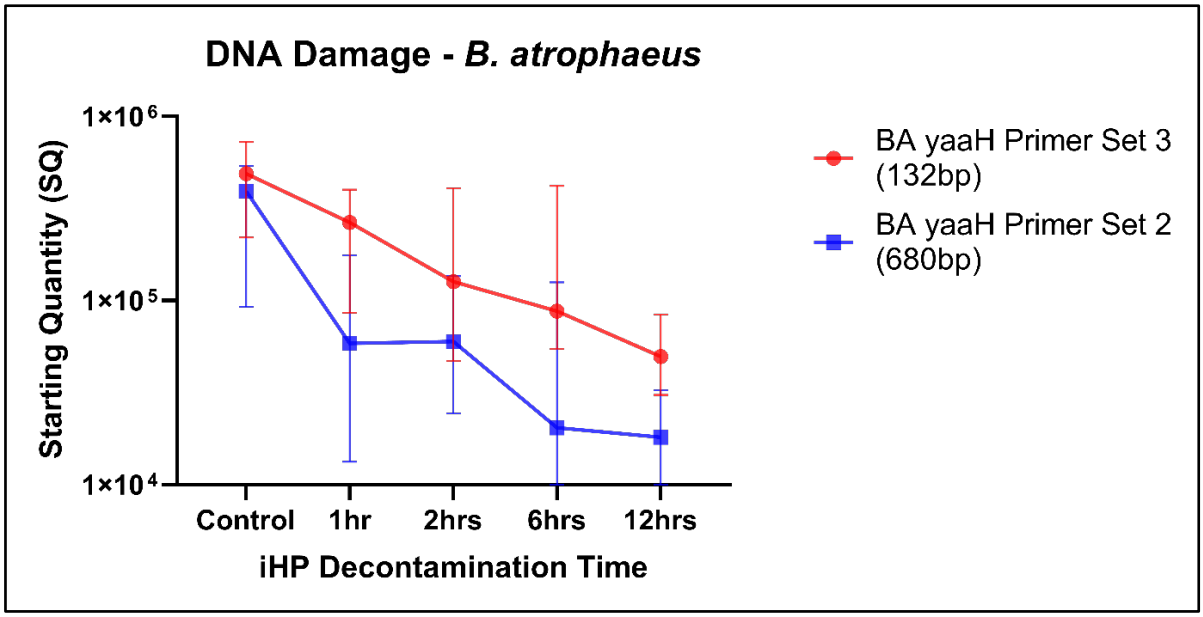

The compiled quantitative result of the damage caused to the DNA of the *G. stearothermophilus* spores can be seen in Table 2-15 and Figure 2-23. The effects of the decontamination to the short DNA segment (190bp) of the *yaaH* gene using "GS *yaaH* Primer Set 4" presents a biphasic degradation starting at approximately 53,000 copies with a noticeable degradation at the 1-hour decontamination followed by a plateau or refractory effect from 2 hours to 6 hours and then a rapid deterioration at 12 hours of decontamination contact time and ending in about 260 copies. The effects of the decontamination to the long DNA segment (678bp) of the *yaaH* gene using "GS *yaaH* Primer Set 5" presents biphasic mode as well, starting with approximately 3,400 copies with a rapid degradation to the 1-hour decontamination contact time, followed by a plateau or refractory effect in damage from 2 hours to 6 hours, then a noticeable deterioration for the 12 hours decontamination ending in approximately 34 copies.

Table 2-15: Quantification data of the qPCR analysis for DNA damage on the decontamination samples of the G. stearothermophilus spores. Data are presented as the median with interquartile range.

iHP Decontamination Time	Quantification of Short (190bp) DNA segment using "GS *yaaH* Primer Set 4"	Quantification of Long (678bp) DNA segment using "GS *yaaH* Primer Set 5"
Control	53,063	3,473
1 hour	8,826	162
2 hours	7,124	274
6 hours	4,934	145
12 hours	268	34

Figure 2-23: Results of the qPCR analysis to the damage to the yaaH gene of the Geobacillus stearothermophilus spores. Data are presented as the median with interquartile range.

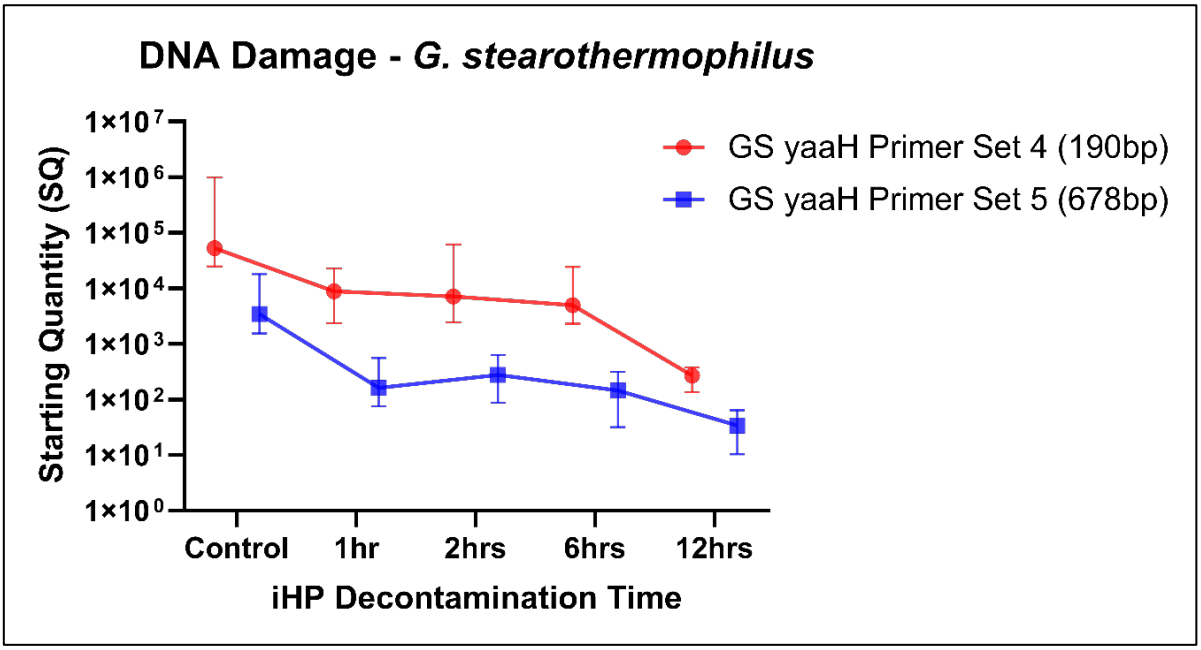

4. Discussion

Typically, DNA extraction from spores required that spores be disrupted to make the DNA available (BELGRADER *et al.*, 1999). Since the purpose of the present study was to analyze the effects, if any, of DNA damage of spores due to the decontamination with ionized hydrogen peroxide (iHP), no mechanical damage could be done to spores in an attempt to improve the fixation for transmission electron microscopy or the extraction of

DNA. Because of any effort to promote either method will affect the real results of this study. The result of this study is significant because they show that ionized hydrogen peroxide inhibits the germination of the spores of both *B. atrophaeus* and *G. stearothermophilus* by damage to the inner membranes of the spore as seen in the TEM micrographs and subsequent damage to the DNA as shown by the qPCR tests results.

Visual effects of the decontamination process can be observed in the micrographs of the *B. atrophaeus* spores in Figure 2-5, Figure 2-6, and Figure 2-7. It is important to note that the longer the exposure time, the better penetration of the fixatives in the spore, and better details of its structure could be observed. This could be a result of the damages that can be seen to the outer layers of the spores that permit the TEM fixatives to have a more effective penetration efficiency. It was observed that visible damages to the spore coat initiated on times after the 1 hour of contact time and most noticeable after 6 hours of contact time. Damage to the inner membrane started at 6 hours of contact time and was more pronounced at the 12 hours contact time.

The results of the qPCR analysis in Figure 2-22 and Figure 2-23, show two initial stages of damage to DNA with very noticeable damage at 12 hrs contact time, which confirms the observations of the micrographs for the *B. atrophaeus* spores. Although qPCR studies could provide excellent results on the effects of the decontamination process on the spores, confirmatory experiments (i.e., TEM analysis) should be performed to elucidate the real impact of the decontamination process.

The use of the *yaaH* gene was selected because, during the spore germination process, the peptidoglycan cortex of the spore is hydrolyzed by specific germination cortex-lytic enzymes. The *yaaH* gene produces the protein that recognizes intact or partially hydrolyzed cortex peptidoglycan structures completing the hydration of the cortex, causing swelling of the spore and the termination of the dormancy period (LAMBERT & POPHAM, 2008; MAKINO & MORIYAMA, 2002). On studies done in spores of *Bacillus subtilis* when treated with a 5% solution of hydrogen peroxide at room temperature, it was observed that cortex degradation was not completed, therefore not allowing swelling and expansion of the core. This effect could be in part by the damage to the cortex-lytic enzymes that are present near the cortex (MELLY *et al.,* 2002). When selecting a gene to analyze for the potential damage of the DNA, the *yaaH* gene was chosen because it resided in the core of the spore and not in the coat since there was the

possibility of extraction of superficial DNA that could be closely associated with the spore coat (BRAUGE *et al.*, 2018).

The methodology used in this study is similar to the protocols used for the evaluation of exposure of DNA and *B. subtilis* spores to a simulated Martian environment developed by Fajardo-Cavazos, et al. (FAJARDO-CAVAZOS *et al.,* 2010). The plasmids generated during this study can be used for determining the capability of ionized hydrogen peroxide and other decontamination technologies to assess the potential deterioration of DNA in surfaces caused by the decontamination process. This test is of utmost importance for determining the possibility of decontaminating laboratories that process DNA samples and for the decontamination of extraterrestrial vehicles in an effort for not contaminating exoplanets. Even though the *B. atrophaeus* and the *G. stearothermophilus* have homologous *rpoB* genes as used in the Fajardo et al. study, it was decided to use another gene (*yaaH*).

Melting curve analysis is a rapid and reliable for the quantification of DNA (AL-ROBAIY *et al.,* 2001). Because all dyes used to detect DNA on a fluorescence-based system can also identify primer-dimers and other products, a melting point analysis was used in this study. The melting point analysis is a function of the GC/AT ratio, length, and sequence. Because of the length differences, non-specific products will have a lower melting temperature than the desired PCR product, and the melting peak identifies the desired product (RIRIE *et al.,* 1997). Also, the sensitivity of the detection of the correct product by using melting point analysis can be up to 10 fold more accurate than agarose gel electrophoresis (BOOT *et al.,* 2013). Furthermore, melting curve analysis can help identify alterations in amplified regions because, when compared to a control sample, it can detect shorter, equivalent, or longer segments such as primer-dimers (BECSAGH *et al.*, 2010).

An unexpected observation in the DNA damage profile was noted during two of the decontamination tests. After a review of the experimental conditions during the decontamination process, a decrease in the initial humidity of the room was observed during these two tests when compared to other experimental trials. No consideration was made to remediate the initial moisture level since water has a lower boiling point than hydrogen peroxide and it was expected that humidity levels were going to rise before the hydrogen peroxide concentration would increase in the room (HULTMAN *et al.,* 2007). This low initial humidity event resulted in a reduction of the DNA damage to the spores as

seen in Figure 2-24, where the two decontamination trials (2hrs and 6 hrs) had substantially lower DNA damage than the results of the other decontaminations with the same contact time (Figure 2-22 and Figure 2-23), even though all biological indicators placed in the room during the decontamination process failed to grow after the inoculation in growth media. After further investigation of this anomaly in the qPCR results, the observations found correlates with a previous study that shows that at low hydrogen peroxide concentrations, the humidity level is essential to achieve inactivation of biological indicators of *G. stearothermophilus* spores (UNGER-BIMCZOK *et al.,* 2008).

Figure 2-24: Effects of Relative Humidity in the damage to DNA in the decontamination process.

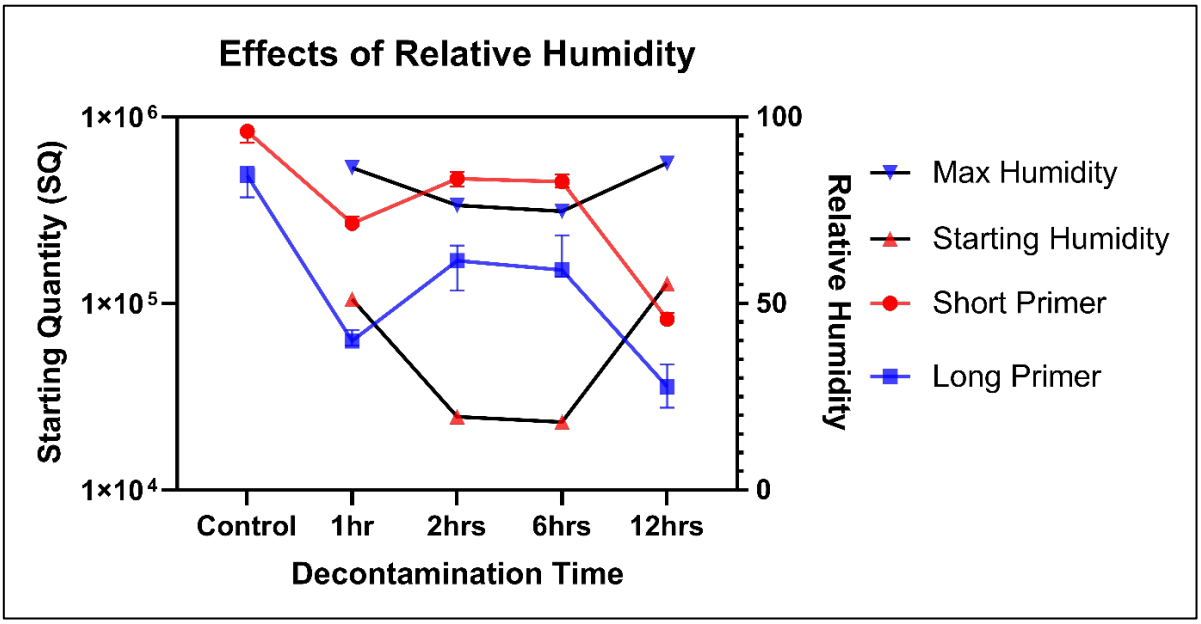

A previous study on the decontamination of biofilms produced by *Chromobacterium violaceum* showed that success was achieved using atmospheric cold plasma generators using carrier gases such as He gas. The generation of reactive particles is similar to the iHP used in this study, but they used an approach of measuring ATP and fluorescence microscopy using a combination of dyes that attached to living or dead cells instead of evaluating DNA damage (JOAQUIN *et al.*, 2009). Another study that utilized a similar methodology as used in this study was the inactivation of adenovirus using low-dose UV/H_2O_2 advanced oxidation. In this study, the authors evaluated inactivation effectiveness by analyzing DNA damages using long-range PCR (BOUNTY *et al.,* 2012).

Although the inactivation of biological agents has always been of utmost importance, recent events have created an increase in public awareness of laboratory research activities

(LAWLER, 2005; MCCARTHY, 2014). These events have moved the research environment towards higher accountability of actions. The inactivation of agents utilized within laboratories will require a quantifiable approach with the use of the agents or their surrogates. The methods presented in this study could be used to evaluate the decontamination effect of different agents by selecting the proper primers and creating the correct plasmids.

The verification of the damages to DNA is a simple, viable alternative to evaluate the decontamination processes. It can be used to evaluate the inactivation of the biological agents that are located in any medium where DNA could be extracted.

5. Future directions

There are several areas that were identified during the course of this study that would be the right avenues for additional research. One would like to evaluate the effects of low humidity in the decontamination process due to an observation made that when the decontamination process started with humidity levels below 20%, the damages to the DNA were reduced.

Also, to experiment on different approaches to increase the yield of DNA extraction without affecting the quality, because to extract DNA from exposed and non-exposed decontamination spore samples was a difficult task since no mechanical procedure could be performed to enhance the extraction of DNA. The overall quantities of DNA extracted were low (less than 50 ng/µl) if compared with DNA extraction of insects, tissues, and from infected cells.

There is also the challenge of obtaining crisp and clear electron microscopy images of spore structures after iHP inactivation and fixation. Additional experiments should be done to evaluate different fixatives to improve the images of the structure for the spores for both *B. atrophaeus* and *G. stearothermophilus*. One such potential fixative is ruthenium red because of the crisp details shown on *B. anthracis* spores TEM micrographs when compared with untreated samples (ZHANG *et al.*, 2007).

6. References

AL-ROBAIY, S.; RUPF, S.; ESCHRICH, K. Rapid competitive PCR using melting curve analysis for DNA quantification. **BioTechniques**, v. 31, n. 6, p. 1382-1386, 1388, Dec 2001.

AUSUBEL, F.; BRENT, R.; KINGSTON, R.; MOORE, D.; SEIDMAN, J.G.; SMITH, J.; STRUHL, K.. **Short protocols in molecular biology**. (3rd Edition), John Wiley & Sons, Inc., New York, 1995.

BECSAGH, P.; VARGA, K.; SZAKACS, O.; KOPPER, L. *et al.* High resolution melting curve analysis of DNA sequence alterations of various sizes. **Pathology & Oncology Research**, v. 16, n. 3, p. 421-426, Sep 2010.

BELGRADER, P.; HANSFORD, D.; KOVACS, G. T. A.; VENKATESWARAN, K. *et al.* A minisonicator to rapidly disrupt bacterial spores for DNA analysis. **Analytical Chemistry**, v. 71, n. 19, p. 4232-4236, 1999.

BERRYMAN, M. A.; RODEWALD, R. D. An enhanced method for post-embedding immunocytochemical staining which preserves cell membranes. **Journal of Histochemistry & Cytochemistry**, v. 38, n. 2, p. 159-170, Feb 1990.

BOOT, M.; RAADSEN, S.; SAVELKOUL, P. H.; VANDENBROUCKE-GRAULS, C. Rapid plasmid replicon typing by real time PCR melting curve analysis. **BMC Microbiology**, v. 13, p. 83, Apr 15 2013.

BOUNTY, S.; RODRIGUEZ, R. A.; LINDEN, K. G. Inactivation of adenovirus using low-dose UV/H2O2 advanced oxidation. **Water Research**, v. 46, n. 19, p. 6273-6278, Dec 2012.

BRAUGE, T.; FAILLE, C.; INGLEBERT, G.; DUBOIS, T. *et al.* Comparative evaluation of DNA extraction methods for amplification by qPCR of superficial vs intracellular DNA from *Bacillus* spores. **International Journal of Food Microbiology**, v. 266, p. 289-294, Feb 2018.

BUSTIN, S.; HUGGETT, J. qPCR primer design revisited. **Biomolecular Detection and Quantification**, v. 14, p. 19-28, Dec 2017.

BUSTIN, S. A.; BENES, V.; GARSON, J. A.; HELLEMANS, J. *et al.* The MIQE guidelines: minimum information for publication of quantitative real-time PCR experiments. **Clinical Chemistry**, v. 55, n. 4, p. 611-622, Apr 2009.

DAS, K.; ROYCHOUDHURY, A. Reactive oxygen species (ROS) and response of antioxidants as ROS-scavengers during environmental stress in plants. **Frontiers in Environmental Science**, v. 2, n. 53, Dec 2014.

FAJARDO-CAVAZOS, P.; SCHUERGER, A. C.; NICHOLSON, W. L. Exposure of DNA and *Bacillus subtilis* spores to simulated martian environments: use of quantitative PCR (qPCR) to measure inactivation rates of DNA to function as a template molecule. **Astrobiology**, v. 10, n. 4, p. 403-411, May 2010.

FOROOTAN, A.; SJOBACK, R.; BJORKMAN, J.; SJOGREEN, B. *et al.* Methods to determine limit of detection and limit of quantification in quantitative real-time PCR (qPCR). **Biomolecular Detection and Quantification**, v. 12, p. 1-6, Jun 2017.

GARIBYAN, L.; AVASHIA, N. Research Techniques Made Simple: Polymerase Chain Reaction (PCR). **The Journal of Investigative Dermatology**, v. 133, n. 3, p. e6, 2013.

GAUNT, L. F.; BEGGS, C. B.; GEORGHIOU, G. E. Bactericidal action of the reactive species produced by gas-discharge nonthermal plasma at atmospheric pressure: a review. **IEEE Transactions on Plasma Science**, v. 34, n. 4, p. 1257-1269, 2006.

HULTMAN, C.; HILL, A.; MCDONNELL, G. The physical chemistry of decontamination with gaseous hydrogen peroxide. **Pharmaceutical Engineering**, v. 27, n. 1, p. 22-32, 2007.

JANSE, I.; HAMIDJAJA, R. A.; BOK, J. M.; VAN ROTTERDAM, B. J. Reliable detection of *Bacillus anthracis*, *Francisella tularensis* and *Yersinia pestis* by using multiplex qPCR including internal controls for nucleic acid extraction and amplification. **BMC Microbiology**, v. 10, p. 314, Dec 2010.

JOAQUIN, J. C.; KWAN, C.; ABRAMZON, N.; VANDERVOORT, K. *et al.* Is gas-discharge plasma a new solution to the old problem of biofilm inactivation? **Microbiology**, v. 155, n. 3, p. 724-732, 2009.

KIM, J. Y.; LEE, I. H.; KIM, D.; KIM, S. H. *et al.* Effects of reactive oxygen species on the biological, structural, and optical properties of *Cordyceps pruinosa* spores. **RSC Advances**, v. 6, n. 36, p. 30699-30709, 2016. 10.1039/C5RA28107E.

LAMBERT, E. A.; POPHAM, D. L. The *Bacillus anthracis* SleL (YaaH) protein is an N-acetylglucosaminidase involved in spore cortex depolymerization. **Journal of Bacteriology**, v. 190, n. 23, p. 7601-7607, Dec 2008.

LAWLER, A. Boston University Under Fire for Pathogen Mishap. **Science**, v. 307, n. 5709, p. 501, 2005.

MAKINO, S.; MORIYAMA, R. Hydrolysis of cortex peptidoglycan during bacterial spore germination. **Medical Science Monitor**, v. 8, n. 6, p. RA119-127, Jun 2002.

MCCARTHY, M. Biosafety lapses prompt US CDC to shut labs and launch review. **British Medical Journal Publishing Group**. v.349:g4615, doi: 10.1136/mbl.g4615, 2014.

MELLY, E.; COWAN, A. E.; SETLOW, P. Studies on the mechanism of killing of *Bacillus subtilis* spores by hydrogen peroxide. **Journal of Applied Microbiology**, v. 93, n. 2, p. 316-325, 2002.

NAKANO, M. Development of a Quantitative PCR assay for thermophilic spore-forming *Geobacillus stearothermophilus* in Canned Food. **Biocontrol Science**, v. 20, n. 3, p. 221-227, 2015.

PRYOR, R. J.; WITTWER, C. T. Real-time polymerase chain reaction and melting curve analysis. **Methods in Molecular Biology, vol. 336: Clinical Applications of PCR**, p. 19-32, Humana Press Inc., 2006.

RAYMAEKERS, M.; SMETS, R.; MAES, B.; CARTUYVELS, R. Checklist for optimization and validation of real-time PCR assays. **Journal of Clinical Laboratory Analysis**, v. 23, n. 3, p. 145-151, 2009.

RIRIE, K. M.; RASMUSSEN, R. P.; WITTWER, C. T. Product differentiation by analysis of DNA melting curves during the polymerase chain reaction. **Analytical Biochemistry**, v. 245, n. 2, p. 154-160, Feb 1997.

ROSE, H. L.; DEWEY, C. A.; ELY, M. S.; WILLOUGHBY, S. L. *et al.* Comparison of eight methods for the extraction of *Bacillus atrophaeus* spore DNA from eleven common interferents and a common swab. **PLoS One**, v. 6, n. 7, p. e22668, Jul 2011.

RUIJTER, J. M.; RUIZ-VILLALBA, A.; VAN DEN HOFF, A. J. J.; GUNST, Q. D. *et al.* Removal of artifact bias from qPCR results using DNA melting curve analysis. **The FASEB Journal**, v. 33, n. 12, p. 14542-14555, Dec 2019.

SARGENT, M. G. A procedure for isolating high quality DNA from spores of *Bacillus subtilis* 168. **Journal of General Microbiology**, v. 116, n. 2, p. 511-514, Feb 1980.

STOKDYK, J. P.; FIRNSTAHL, A. D.; SPENCER, S. K.; BURCH, T. R. *et al.* Determining the 95% limit of detection for waterborne pathogen analyses from primary concentration to qPCR. **Water Research**, v. 96, p. 105-113, Jun 2016.

THORNTON, B.; BASU, C. Rapid and simple method of qPCR primer design. **Methods in Molecular Biology, vol. 1275: PCR Primer Design**, p. 173-179, Springer Science+Business Media, 2015.

UNGER-BIMCZOK, B.; KOTTKE, V.; HERTEL, C.; RAUSCHNABEL, J. The influence of humidity, hydrogen peroxide concentration, and condensation on the inactivation of *Geobacillus stearothermophilus* spores with hydrogen peroxide vapor. **Journal of Pharmaceutical Innovation**, v. 3, n. 2, p. 123-133,Jun 2008.

YE, J.; COULOURIS, G.; ZARETSKAYA, I.; CUTCUTACHE, I. *et al.* Primer-BLAST: a tool to design target-specific primers for polymerase chain reaction. **BMC Bioinformatics**, v. 13, p. 134, Jun 2012.

ZHANG, J.; DALAL, N.; MATTHEWS, M. A.; WALLER, L. N. *et al.* Supercritical carbon dioxide and hydrogen peroxide cause mild changes in spore structures associated with high killing rate of *Bacillus anthracis*. **Journal of Microbiological Methods**, v. 70, n. 3, p. 442-451, Sep 2007.